The Department of Geodesy and Geoinformatics

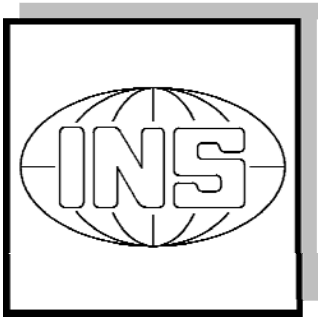

Stuttgart University

2012

editing and layout:
volker walter, friedhelm krumm, helga mehrbrodt, martin metzner

Dear friends and colleagues,

It is our great pleasure to present to you this annual report[1] on the 2012 activities and academic highlights of the Department of Geodesy & Geoinformatics of the University of Stuttgart. The Department consists of the four institutes:

- Institute of Geodesy (GIS),
- Institute of Photogrammetry (ifp),
- Institute of Navigation (INS),
- Institute of Engineering Geodesy (IIGS),

and is part of the Faculty of Aerospace Engineering and Geodesy.

Research

This annual report documents our research contributions in many diverse fields of Geodesy & Geoinformatics: from satellite and physical geodesy through navigation, remote sensing, engineering surveying and telematics to photogrammetry, geographical information systems and location based services. Detailed information on projects and research output can be found in the following individual institutes' sections.

Teaching

Our BSc programme *Geodesy & Geoinformatics* is currently in its fourth year of operation. We were able to welcome close to 42 new BSc students in winter term 2012. The very first BSc students graduated at the end of 2012. The MSc program for Geodesy and Geoinformatics started with the winter term 2012. Currently 12 students are taking part in this Master of Science program. The Diploma programme is slowly being phased out. Total enrolment, in both the BSc and the Diploma programmes, is stable at about 125 students. Please visit our website *www.geodaesie.uni-stuttgart.de* for additional information on the programmes.

In its 7th year of existence, our international MSc programme *Geomatics Engineering* (GEOENGINE) enjoys a gratifying demand. We register an enrolment of 29 students. We attract the GeoEngine student population from such diverse countries as China, Chile, Palestine, Iraq, Iran, Pakistan, Nigeria, India, Netherlands, Turkey, Greece, Egypt, Thailand and Bangladesh. Please visit *www.geoengine.uni-stuttgart.de* for more information.

[1] A version with colour graphics is downloadable from
http://www.ifp.uni-stuttgart.de/publications/jahresberichte/jahresbericht.html

Beyond the transition from the old Diploma programme into the BSc/MSc-system we also put much effort into a general overhaul of the GeoEngine programme. The University of Stuttgart was aiming at a so-called system accreditation. This process necessitated an adaptation of GEOENGINE to conform to the general university's guidelines for MSc programmes. In fact, we stood very much in the spotlight as the accreditation agency selected GEOENGINE as one of only three programmes out of the whole range at the University of Stuttgart to be scrutinized for quality processes. Key elements of our redesign were a change from 3 to 4 semesters, a better spread of credit points over the semesters and the opportunity for more elective courses. The accreditation process was successfully completed in 2012 and now our GEOENGINE program proudly carries the OAQ accreditation seal.

Awards and scholarships

We want to express our gratitude to our friends and sponsors, most notably

- Verein Freunde des Studienganges Geodäsie und Geoinformatik an der Universität Stuttgart e.V. (F2GeoS),
- Microsoft company Vexcel Imaging GmbH,
- Ingenieur-Gesellschaft für Interfaces mbH (IGI),
- DVW Landesverein Baden-Württemberg,

who support our programmes and our students with scholarships, awards and travel support.

Below is the list of the recipients of the 2012 awards and scholarships. The criterion for all prizes is academic performance; for some prizes GPA-based, for other prizes based on thesis work. Congratulations to all recipients!

Award	Recipient	Sponsor	Programme
Karl-Ramsayer Preis	Susanne Haußmann	Department of Geodesy & Geoinformatics	Geodesy & Geoinformatics
Diploma/MSc Thesis Award	Thomas Friederichs	F2GeoS	GEOENGINE
MS Photogrammetry / Vexcel Imaging Scholarship	Hailong FU Wenjian QIN	MS Photogrammetry / Vexcel Imaging	GEOENGINE
IGI Scholarship	Run SHI Jun CHEN	IGI mbH	GEOENGINE
matching funds	Xingyue WIE Ying ZHANG Jinwei ZHANG	DAAD	GEOENGINE

Wolfgang Keller
Associate Dean (Academic)
wolfgang.keller@gis.uni-stuttgart.de

Institute for Engineering Geodesy

Geschwister-Scholl-Str. 24D, D-70174 Stuttgart,
Tel.: +49 711 685 84041, Fax: +49 711 685 84044
e-mail: Sekretariat@ingeo.uni-stuttgart.de or
firstname.secondname@ingeo.uni-stuttgart.de
url: http://www.uni-stuttgart.de/ingeo/

Head of Institute

Prof. Dr.-Ing. habil. Volker Schwieger

Secretary

Elke Rawe

Emeritus

Prof. Dr.-Ing. Dr.sc.techn.h.c. Dr.h.c. Klaus Linkwitz

Scientific Staff

Abdallah Ashraf, M.Sc.(since 01.04.2012)	GNSS Positioning
Bara' Al-Mistarehi, M.Sc.	Construction Process
Dr.-Ing. Alexander Beetz	Machine Guidance
Shenghua Chen, M.Sc.	Kinematic Positioning
Xiaojing Lin, M.Sc.	Machine Guidance
Dr.-Ing. Martin Metzner	Engineering Geodesy
Dipl.-Ing. Annette Scheider	Kinematic Positioning
Rainer Schützle, M.Sc.	Information Quality
Dipl.-Ing. Jürgen Schweitzer (until 31.10.2012)	Construction Process
Dipl.-Ing. Li Zhang	Monitoring
Dipl.-Ing. Bimin Zheng	Monitoring

Technical Staff

Martin Knihs
Lars Plate
Mathias Stange

External teaching staff

Dipl.-Ing. Thomas Meyer - Landratsamt Ludwigsburg - Fachbereich Vermessung

General View

The Institute of Engineering Geodesy (IIGS) is directed by Prof. Dr.-Ing. habil. Volker Schwieger. It is part of the Faculty 6 „Aerospace Engineering and Geodesy“ within the University of Stuttgart. Prof. Schwieger holds the chair in „Engineering Geodesy and Geodetic Measurements“. In 2012 he was elected as Vice Dean of the Faculty 6.

Since 2011 he is full member of the German Geodetic Commission (Deutsche Geodätische Kommission - DGK). Furthermore, Prof. Schwieger is a member of the section „Engineering Geodesy“ within the DGK. He is head of the DVW working group 3 „Measurement Techniques and Systems“ and chairman of the FIG working group 5.4 „Kinematic Measurements“.

In addition to being a member of Faculty 6, Prof. Schwieger is co-opted to the Faculty 2 „Civil and Environmental Engineering“. Furthermore, IIGS is involved in the Center for Transportation Research of the University of Stuttgart (FOVUS). Prof. Schwieger presently acts as speaker of FOVUS. So, IIGS actively continues the close collaboration with all institutes of the transportation field, especially with those belonging to Faculty 2.

The institute’s main tasks in education focus on geodetic and industrial measurement techniques, kinematic positioning and multi-sensor systems, statistics and error theory, engineering geodesy and monitoring, GIS-based data acquisition, and transport telematics. Here, the institute is responsible for the above-mentioned fields within the curricula of „Geodesy and Geoinformatics“ (currently Diploma, Master and Bachelor courses of study) as well as for „GEOENGINE“ (Master for Geomatics Engineering in English language). In addition, the IIGS provides several courses in German language for the curricula of „Aerospace Engineering“ (Master), „Civil Engineering“ (Bachelor and Master), „Transport Engineering“ (Bachelor) and „Technique and Economy of Real Estate“ (Bachelor). Furthermore, lectures are given in English to students within the master course „Infrastructure Planning“. Finally, eLearning modules are applied in different curricula. Also during the year 2012, teaching was still characterized by the conversion of courses from Diploma to Bachelor and Master degree, now with focus on the Master degree. This is going to continue within the next years.

The current research and project work of the institute is expressed in the course contents, thus always presenting the actual state-of-the-art to the students. As a benefit of this, student research projects and theses are often effected in close cooperation with the industry and external research partners. The main research focuses on kinematic and static positioning, analysis of engineering surveying processes and construction processes, machine guidance, monitoring, transport and aviation telematics, process and quality modeling. The daily work is characterized by intensive cooperation with other engineering disciplines, especially with traffic engineering, civil engineering and aerospace engineering.

Research and Development

Center for Transportation Research University of Stuttgart (FOVUS)

In 2012, the main activity within FOVUS was to prepare, organize and host the 6th International Symposium „Networks for Mobility“ which was hold on September 27/28 at the University of Stuttgart. Prof. Sabine Laschat, Vice Rector for Research of the University of Stuttgart, welcomed more than 100 scientists, experts and professionals in transportation research from all over the world who met at the „GENO-Haus“ in Stuttgart. The conference started with an opening lecture during which, among others, Winfried Hermann, the Minister for Transport and Infrastructure of Baden-Württemberg gave a well-recognized speech on his view of „Sustainable Mobility and Climate Protection“ (c.f. Fig. 1).

Fig. 1: Opening lecture of Winfried Hermann, the Minister for Transport and Infrastructure of Baden-Württemberg

Within the course of the conference, more than 40 presentations were given in two plenary and four parallel sessions. The presented topics covered a broad variety of transportation engineering and research. The focus was clearly set on the interdisciplinarity for which the conference is well-known.

Fig. 2: Scientific Committee (left) and rector of the University of Stuttgart, Prof. Ressel (right)

With respect to education, the re-organization of the transportation-related study programs at the University of Stuttgart has been completed. In the winter term 2012/2013, the first students enrolled for the new study program „Transportation Engineering“, in which also the IIGS is involved.

3rd International Conference on Machine Control & Guidance

From 27th March to 29th March 2012 the 3rd International Conference on Machine Control & Guidance took place in GENO-Haus in Stuttgart, Germany. The 103 participants are originated from 13 countries and 4 continents. The conference was organized by the Institute of Engineering Geodesy Stuttgart University and the Institute of Agricultural Engineering Hohenheim University (c.f. Fig. 2). The participations were welcomed by Prof. Ressel, the Rector of the University of Stuttgart. Also Prof. Böttinger, deputy managing director of the Institute of Agricultural Engineering, Mikael Lilje, chair of FIG Commission 5 „Positioning and Measurement“ and Prof. Schwieger gave welcoming speeches.

9 Sessions and 32 presentations extend to many different branches like GNSS-positioning, kinematic measurements, sensor integration, control algorithms, construction and agriculture applications. The organization team was supported by all staff members of the IIGS (c.f. Fig. 3).

Fig. 3: Organizing Team IIGS

Simulation of Quality Parameters in Construction Process

The project EQuiP (Efficiency Optimization and Quality Control of Engineering Geodesy Processes in Civil Engineering), which was funded by the German research foundation (DFG) deals on the part of the IIGS with quality modeling, quality parameter simulation and estimation as well as quality control. In the following the simulation of variances through the sub-process „building of the basement walls“ of a high-rise building is regarded.

To propagate the standard deviation you can use on the one hand an empirical method, the Monte Carlo Method (MCM). This is a numerical method to propagate random variables through a process or a system. A large number m of scattered observations is generated computer-based in a „virtual experiment“ whose impact on the outcome is determined. On the basis of the m results, a statistical analysis can be performed. Important statistical parameters like the expected value μ, the standard deviation σ, confidence interval $[C_l, C_u]$, kurtosis α_4 and skewness α_3 can be determined empirically. On the other hand, the variance covariance propagation law can be used. The basis are a linear or linearised model and normal distributed input variables. The statistical parameters skewness and kurtosis of a probability density function (PDF) of a normal distributed random variable are always zero.

For the named process „building of the basement walls“ two engineering geodetic processes are integrated. The first process „stationing“ describes the free stationing of a total station. The input parameters of the first process are the polar elements (measured with a total station), the coordinates of the control points, and all related standard deviations. The functional model is a free stationing, which is realized by a Helmert Transformation. The second process „align formwork“ describes the alignment of a formwork. The functional model is the simple polar survey. The input parameters are the station coordinates from the first process including variance-covariance information. The output parameters are the coordinates of the formwork corners with the respective statistical information. Finally the distance d from point 1 to point 3 will be the output parameter under investigation. Fig. 4 shows a top view (left) and a side view of the formwork(s) for one floor.

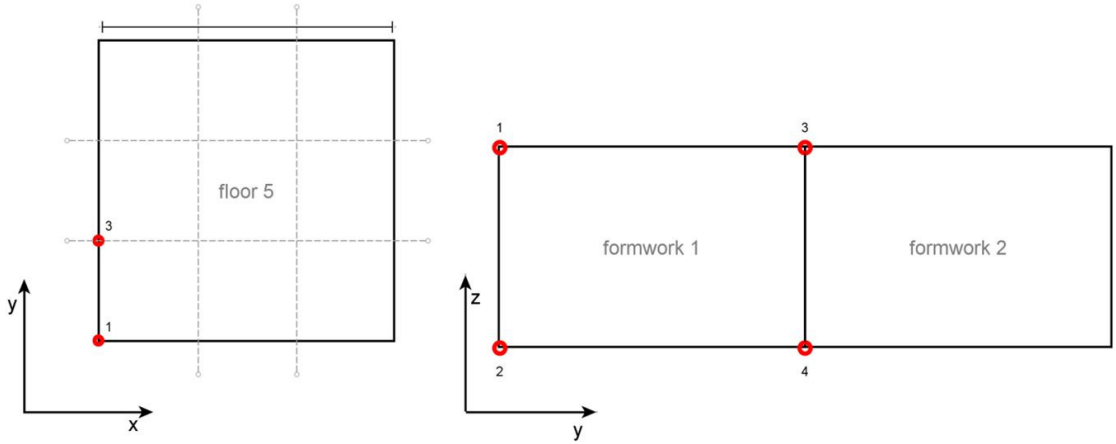

Fig. 4: Top view (left) and side view (right) of formwork for one floor

For the variance-covariance propagation (VCP) the standard procedure assuming linear models can be applied. The empirical Monte Carlo simulation is realized in two variants. The first one is done where all input variables are normal distributed, for the second variant the polar elements are uniform distributed and the coordinates of the control points are normal distributed. There

is no significant difference between the standard deviations σ_d of the distance d_{13} for the three variants. At the second variation of the MCM, the kurtosis of the empirical PDF differs significantly from the other two kurtosises. This can also be seen in Fig. 5 where the PDF of the second Monte Carlo Method variant is plotted together with the normal distribution. It can be seen that the empirical Monte Carlo PDF is narrower. This is due to non-linearity of the model and the non-normal distribution of some input quantities. In this case it has no influence on the standard deviations but on the confidence intervals. The confidence intervals are empirically computed for the Monte Carlo Method. The confidence interval for $\alpha/2 = 0.025$ is shown by the red speckled lines in Fig. 5 in contrast to the confidence interval resulting from VCP shown by the blue lines in the same figure.

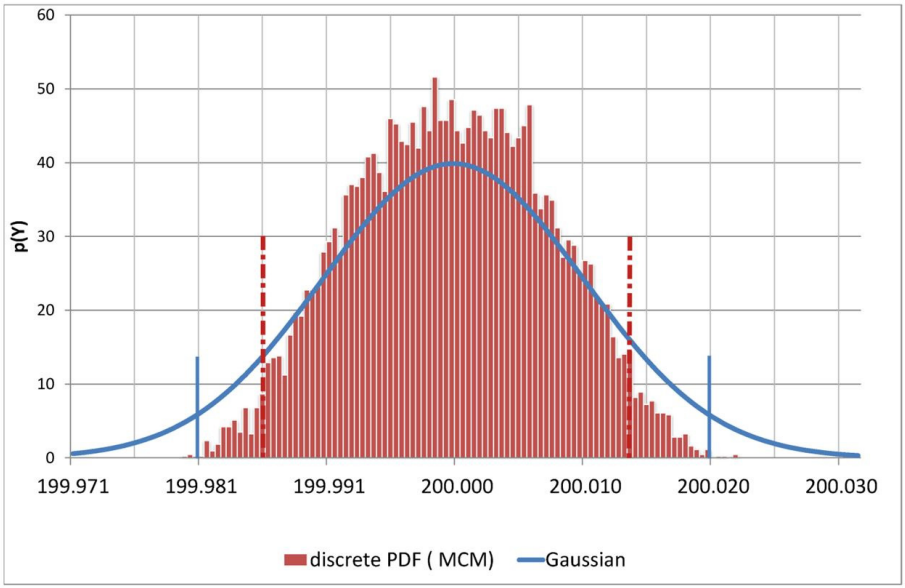

Fig. 5: PDF's with confidence intervals of the distance d13 (VCP blue lines and MCM red speckled lines)

The confidence interval influences the tolerance correctness that gives information about the significant correctness of a result with respect to the given tolerances. The tolerance correctness of the MCM with partly uniform distributed input variables is 4 mm greater than the tolerance correctness of MCM with Gaussian input variables, and 6 mm greater than the VCP result. This leads to more relaxed decisions if the correct knowledge about the distributions is available and non-linearity is taken into account using Monte Carlo simulation. This is essential, because of the high requirements to tolerances in building construction.

iMobility Working Group on Digital Maps (DMWG)

Within its continuous engagement in the iMobility Working Group on Digital Maps (DMWG) and the related eSafety Digital Maps Public Private Partnership Support Action (eMaPS), the IIGS was commissioned to work out a study on „Quality of Service“. Within this study, the IIGS has made use of its scientific expertise in data quality in general and especially in the exchange of traffic information. The eMaPS consortium as the contracting entity, aimed at achieving a dedicated quality model for the road safety attribute data that is exchanged between road authorities and commercial service providers, such as map vendors (i.e. TomTom or Nokia). Since the DMWG also intends to attract more Member States to provide their public road data, the usage and implementation of the developed quality model should be easy.

Thus, a quality model consisting of three levels of service quality was derived, differentiating data that can directly be used by the customer (highest level), data that has to be validated by the customer before using it (intermediate level) and data that does not suffice basic quality requirements (lowest level). In contrast to many other quality management approaches and quality models, the model at hand should be usable by data providers for self-declaration purposes. Hence, only information can be used as quality parameters which is directly available at the road authorities. So, a list of quality parameters describing the data acquisition and maintenance processes such as the used data acquisition method, up-to-dateness, or information about implemented quality assurance was derived. In addition, an easy-to-handle tool was developed, with which the data providers can compute their individual level of quality.

Mobile Positioning Based on Cellular Phone Data

The demand for easier access to data for traffic management and monitoring has driven the efforts to exploit wireless location technology and mobile phone data for mobile terminal positioning. Mobile positioning methods based on cellular phone data have been developed.

One method is to use A data, which mainly records the cells and LAC (Location Area Code) in the wireless communication system. This method takes the traffic road network as assistance to finish the mobile positioning for traffic management. This mobile positioning method consists of: building one traffic network database by integrating digital road map and mobile phone data, and generate vehicles trajectories by selecting the possible traffic road in the road network, refine the result in step two by more constraints, like road attributes, speed limit and road function class.

Another mobile positioning method is developed to use A-bis data, which mainly records the received signal strength in the cells. It uses matching technique between the recorded received signal strength and signal strength map measured before in the same cells. There are still several ways to do the signal strength matching. We use the weighted average method to optimize the matching result, that is to refine the positioning result.

NURBS and Triangulation of Laser Scanning Data for Monitoring

The focus of the research was to compare two mathematical models (Non-uniform rational B-Splines [NURBS] and Triangulation) for surface reconstruction. A bridge model (a beam in K1 basement) was measured by using FARO 3D Focus in two epochs (see Fig. 6). The weight in the middle of the beam was changed to simulate the deformation of 1 cm. A tachymeter TS30 was used to control the measurements.

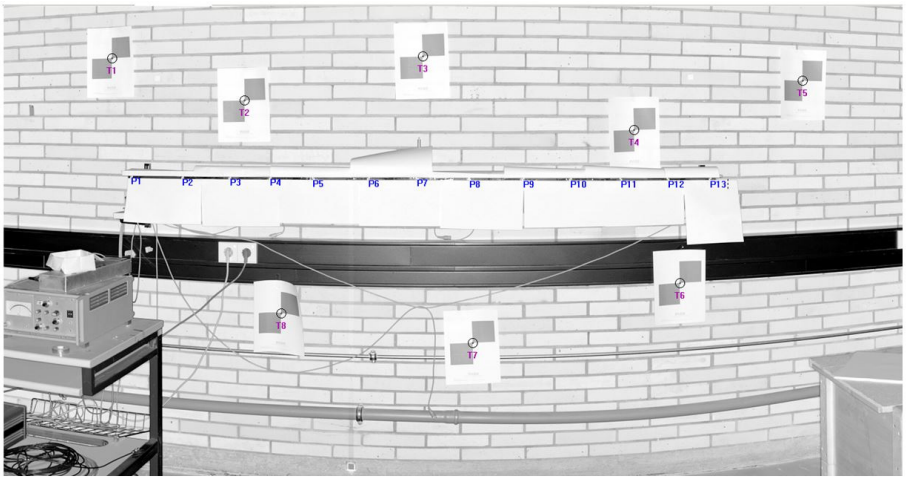

Fig. 6: Bridge model in measurement cellar K1

The object beam as actually deformed and the deformation of the beam can also be vizualized clearly by using a laser scanner. Zooming in to P8 in the middle, it is almost the sharpest deforming place with 1.0 cm deformation.

The point cloud was projected on a surface in Matlab and then imported into Rhinoceros software to apply the NURBS model (see Fig. 7).

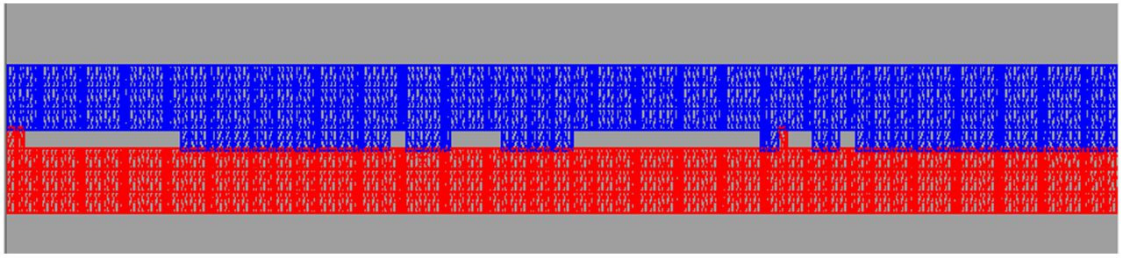

Fig. 7: Result in Rhinoceros

Fig. 8 shows the result of the reconstructed surface in Meshlab. The two point clouds show the difference before and after the deformation. The differences of the TIN before and after deformation were compared.

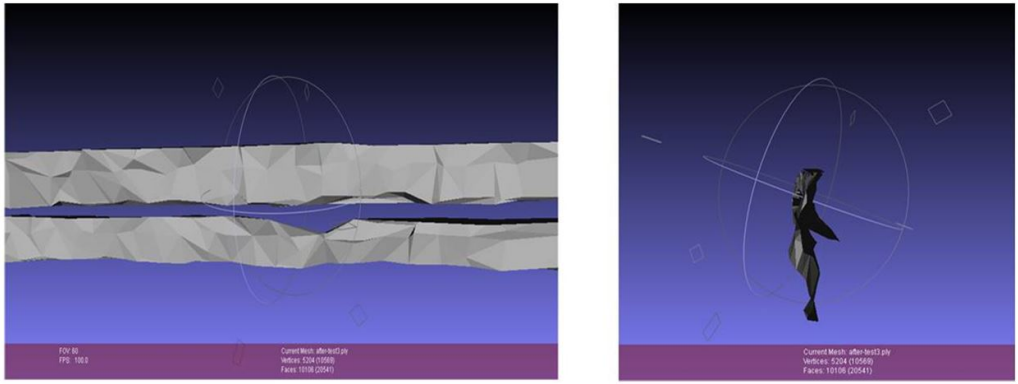

Fig. 8: Result in Meshlab

The comparison was realized in ArcGIS. The resulting TINs shows that the deformation of the object beam is not only decreasing in vertical direction but also tilting. After completing the TIN, the differences were compared by using the model „Surface Difference“ in ArcGIS. The area where the first surface is above the second (reference) surface shows the positive value; and negative values reflect areas where the first surface is below the second. Fig. 9 shows the result of the comparison of the surfaces, the color represents the relative location after the deformation with respect to the reference surface.

In our case the triangulation method shows better results than the NURBS solution. The reason might be as below:

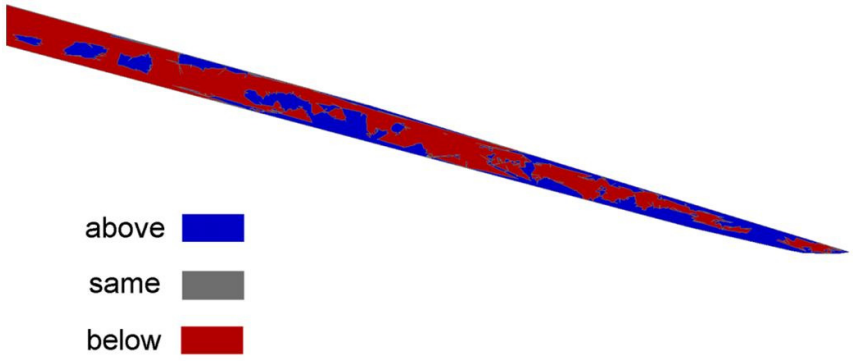

Fig. 9: Result in ArcGIS

Crack Detection for road pavement maintenance

The goal of this work is to develop and implement an algorithm to detect, extract, and classify linear pavement cracks using digital image processing techniques. The method is implemented in four phases. Fig. 10 displays the overall stages for crack detection.

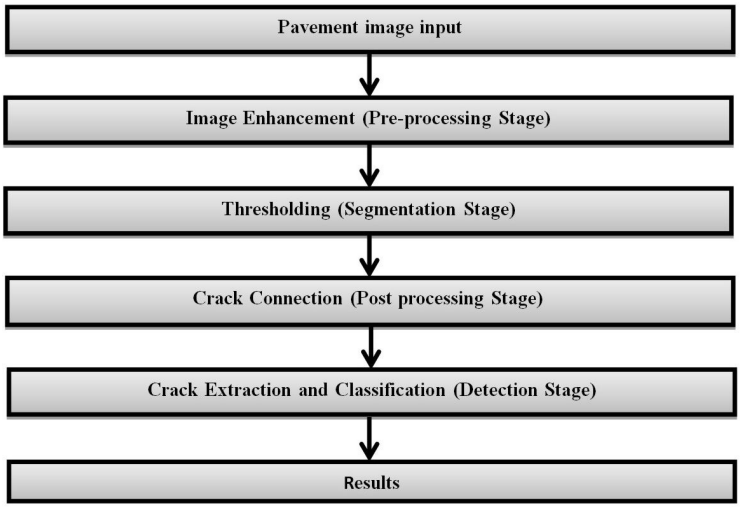

Fig. 10: The overall stages for crack detection

- Image Enhancement (Pre-processing Stage): Pavement images are composed of background, noise, and cracks. The noise on the image, objects on the road, the pavement patterns, and the non-uniform background cause difficulties for crack detection and even fail of the threshold process. In order to recognize distress with fidelity on the road surfaces, an algorithm has been developed to eliminate noise and normalize the background.
- Thresholding (Segmentation Stage): Thresholding is a technique used to separate objects from the background. Since cracks are always darker than the surrounding, the threshold value should be a relatively low intensity value.
- Crack Connection (Post-processing Stage): In this stage, the remaining noise is reduced, all the crack holes are filled, and the discrete linear crack points will be connected using different morphological operation algorithms.
- Crack Extraction and Classification (Detection Stage): Some of the resulting images from post processing stage are still having noise. So the processing in this stage should be able to extract linear cracks alone by setting a threshold to the crack size. Then according to length, width, and orientations, linear cracks are classified into different categories, using the Hough transformed algorithm. Fig. 11 displays the final Hough Transform results.

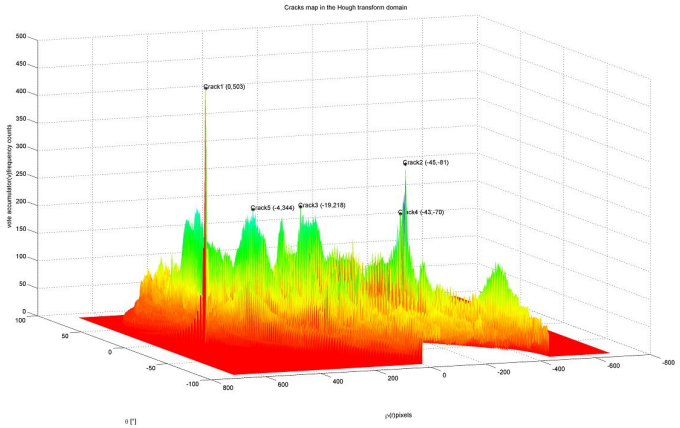

Fig. 11: The Hough transform results

Modular System for Construction Machine Guidance

In the last years the Hardware-in-the-Loop simulator developed by the IIGS has continuously been enhanced. Beside integration of robot tachymeters of the newest generation, several vehicle models have also been integrated. These models are a front-steered wheeled vehicle, a back-steered vehicle model (c.f. Fig. 12) and a tracked vehicle. All these models are remote-controlled and in the scale of 1:14. These remote-controlled vehicles are guided by a control computer on given trajectories with several implemented controllers. The control aim is to guide the vehicle as accurately as possible on a given trajectory.

Fig. 12: Simulator - configuration and back-steered wheeled vehicle

By means of the simulator it is also possible to evaluate different position sensors, filter algorithms and controllers. To describe the achieved control quality, a root mean square (RMS) is computed during a test drive with lateral deviations between the given trajectory and vehicle positions. Due to the achieved position accuracy of the tachymeters (3-10 mm), the RMS of the tachymeter measured positions does not only represent the control quality. A random part is also included which falsifies the result of the control quality. For this reason, a laser tracker was implemented in the system. This means, during the test drives the position of the guided vehicle was measured by the tachymeter and the laser tracker at the same time. Afterwards the two measurements of the trajectory can be compared with each other. The RMS of the lateral deviations between laser tracker trajectory and given trajectory represents the control quality. The RMS of the lateral deviations between tachymeter trajectory and laser tracker trajectory represents the measurement accuracy of the sensor.

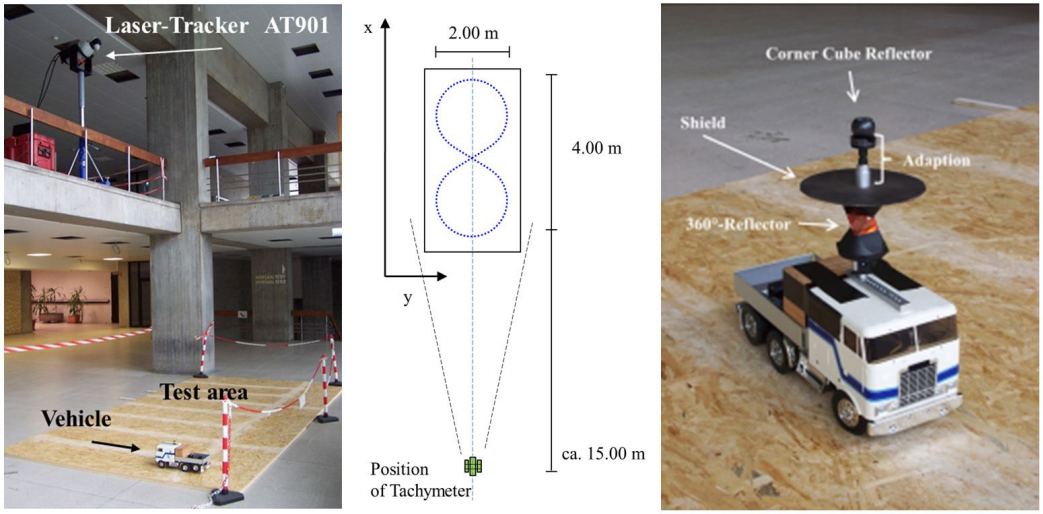

Fig. 13: Test area with laser tracker (left) - Site plan of test area (middle) - Adaption of reflectors on controlled vehicle (right).

In Fig. 13 the test area with the laser tracker (left), the site plan of test area (middle) and the adaption of the two reflectors (right) are shown. The reflector of the laser tracker is called „corner cube reflector“ and is mounted exactly on top of the 360°-prism of the tachymeter. An additional shield has to be fixed between „corner cube reflector“ and 360°-reflector, so that the laser tracker does not aim at the 360°-reflector during measurement.

For further investigations with GNSS-sensors and graveled ground an outdoor simulator has been built (cf. Fig. 14). At the moment, the hardware-in-the-loop simulator will be enhanced in order to use GNSS-sensors. In the future, it is also planned to integrate a new control algorithm on the base of a Fuzzy-controller.

Fig. 14: Outdoor simulator

HydrOs: Optimization of Positioning in Areas of GNSS Shadowing along Inland Waterways

The HydrOs project is dealing with the development of an integrated hydrographic positioning system (German: **Hyd**rographisches **Or**tungs**s**ystem) for areas with insufficient GNSS coverage. The positioning system will be realized as a prototype which is to be installed on a surveying vessel. This project is a cooperation between the Federal Institute of Hydrology (BfG) and the Institute of Engineering Geodesy (IIGS). It has been started in April 2012 and will continue for three years.

To map the waterway bottom, it is necessary to connect the measured data of the depth sounder with the corresponding position of the vessel (cf. Fig. 15). Currently, GNSS-positioning of surveying vessels with accuracy better than 3 dm in the horizontal component and 1 dm in the vertical component can only be realized if there are no barriers around the waterways. In deep valleys, near to vegetation or under bridges the positioning requirements cannot be fulfilled.

Thus, a multi-sensor system should be developed which includes additional sensors like an Inertial Measurement Unit (IMU), the speed sensor Doppler Velocity Log (DVL) or information about the motor output. Another option is to integrate geodetic instruments like total stations or laser scanners into the system.

Processing of the stored measuring data will be realized in the software component of the positioning system. As part of it, a dynamical model is currently developed to describe the 3D position of surveying vessels in real time. By using the measured data and the state vector as input for an adequate filter (e.g. Extended Kalman Filter) the position of the ship will be estimated optimally with an accuracy of better than 1 dm. So, the position of the ship can be predicted in areas without GNSS signal reception.

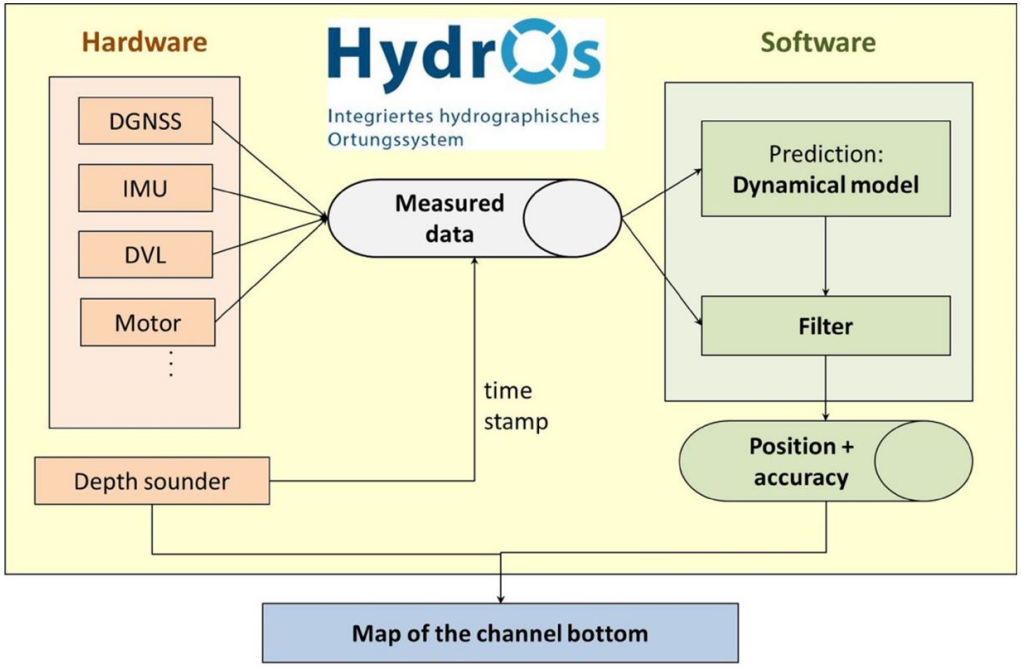

Fig. 15: Data flow of the integrated hydrographic positioning system

Accuracy Analysis of Low-Cost GPS Monitoring System

An automatic low-cost GPS monitoring system is currently being developed in IIGS and is in a testing phase. In the test area Stuttgart-Vaihingen several measurement pillars, which were re-measured in 2012 using total stations and geodetic GNSS receivers, are available. The resulting coordinates are regarded as given coordinates with millimeter accuracy. The aim of the measurements is to evaluate the quality of low-cost system with u-blox GPS receivers combining different low-cost antennas. The three low-cost antennas u-blox ANN-MS, Vimcom 96/1 and Trimble Bullet III (each of them costs less than 100 EUR) were tested in combination with the u-blox LEA-6T receiver. To reduce undesirable multipath effects, the u-blox ANN-MS antenna is shielded with a self-constructed ground plate; Vimcom 96/1 and the Trimble Bullet III antennas are shielded with a self-constructed choke ring (compare Fig. 16).

Two pillars P6 and P7 are chosen for the tests, the length of baselines is 255 m. The reference station P6 and the rover station P7 stand both in a shadowing-free environment. The baseline was measured with the three different antennas. So, there are three sessions in total. The duration of the measurements was about one hour. In order to analyze the accuracy depending on the length of observation time, the observation time interval of one hour was analyzed and then

was divided into several short time intervals: 10, 15, 20 and 30 minutes. All the time intervals have fixed solutions. For quality analysis, the differences between the given and the measured baselines are calculated. Then the mean value and the standard deviation of these differences from the different divided time intervals are estimated. The mean value can be regarded as the reproducibility (absolute) accuracy compared with the true value. The standard deviation can be regarded as the repeatability (relative) accuracy for the stability of the measurements.

Fig. 16: Three antennas

Table 1 shows the results of session 1 to 3 for baseline P6-P7. The small standard deviations (in horizontal position less than 2.5 mm and in the height less than 5 mm) show that the results are very stable. The main reason is that the two stations P6 and P7 are both in shadowing free environment.

The mean values of the differences between the measured and given baselines are less than 1 cm in the horizontal position and less than 1.5 cm in the height. They can be minimized by antenna calibration if the phase center offsets and variations of the antennas differ to such an extent that individual antenna calibrations are necessary. The standard deviations in session 2 (with Vimcom antennas) and session 3 (with Trimble antennas) are similar. They are in the sub-mm range in the horizontal position and almost all less than 1 mm in the height. The standard deviations of the u-blox antenna here are worse compared to the ones of the other two antennas, especially in east direction (less than 3 mm) and height (less than 5 mm). The standard deviations are not decreasing with longer observation time (starting from 15 minutes). In the future, further research on antennas should be realized and on the performance of the system in shading environment.

Session No.	Time Interval	Mean [mm]			Standard Deviation [mm]		
		mΔdN	mΔdE	mΔdh	sΔdN	sΔdE	sΔdh
Session 1 (U-BLOX)	10 min	2.8	-3.0	13.3	0.8	2.1	4.7
	15 min	2.8	-3.1	13.3	0.7	2.3	4.9
	20 min	2.8	-2.9	13.4	0.5	2.2	3.8
	30 min	2.7	-2.0	13.4	0.2	1.1	3.7
	60 min	2.9	-2.3	14.7	-	-	-
Session 2 (Vimcom)	10 min	3.4	-7.4	7.8	0.8	0.8	1.0
	15 min	3.4	-7.4	7.7	0.5	0.6	0.5
	20 min	3.4	-7.4	7.8	0.7	0.9	0.5
	30 min	3.4	-7.4	7.8	0.1	0.5	0.4
	60 min	3.4	-7.4	7.7	-	-	-
Session 3 (Trimble)	10 min	2.8	-5.8	10.9	0.6	0.4	1.2
	15 min	2.8	-5.8	11.0	0.6	0.2	0.9
	20 min	2.8	-5.8	10.9	0.3	0.1	0.7
	30 min	2.8	-5.8	11.0	0.1	0.1	1.1
	60 min	2.7	-5.8	10.8	-	-	-

Table 1: Results of the baseline P6-P7 (session 1-session 3)

PPP and RTK for construction machine guidance

An indoor simulation system has already been developed at the institute and only tachymeters have been used as position sensors up to now. A testing field has been constructed and measured in Stuttgart Vaihingen campus. Now, GNSS receivers can also be integrated to develop the outdoor simulator. A basic precise point positioning software has been developed and it can achieve an accuracy of 1-2 centimeter for static positioning and 10-20 centimeters for kinematic positioning in post processing. The positioning algorithms still have to be improved in the future and real-time positioning will be realized. The RTK solution will be implemented in connection with SAPOS is available. Both real time RTK results and precise point positioning results are put out as real time data stream to the controller. Other sensors, such as IMU, can also be integrated into the outdoor simulator to develop a system than can control and guide the machine autonomously with optimal performance.

Evaluation of PPP-Algorithms

An accuracy assessment study has been prepared to introduce the evaluation of PPP in static and kinematic techniques.

In static mode four stations were observed with an observation time of nearly one hour, using Leica dual frequency antennas. The GNSS data were processed as PDGNSS using a SAPOS reference station as reference solution. GIPSY-OASIS software, CSRS-PPP online service, and

APPS online service were used to get a PPP solution in east, north, and ellipsoidal height directions. GIPSY-OASIS software provided 3D RMS of nearly 4 cm after having excluded some bad satellites data. APPS introduced 3D RMS of 7 cm after excluding the bad satellite data. CSRS online service presented a high efficiency in PPP solution, despite of the cycle slip problem. CSRS provided a RMS of nearly 3 cm in horizontal plane and 4 cm in height. CSRS online service can introduce a code solution with a 3D error of 38 cm. To study the effects of initialization time two stations with 24 hours observation data were processed using GIPSY software and CSRS and APPS online service. GIPSY software and CSRS online service result in a 3D error of 2 cm after 4 hours. This accuracy reached the mm after 4 hours and there is no improvement between 12 and 24 hours. APPS online service provided 3D error of 5 cm after 90 minutes and there is no improvement after that. Fig. 17 shows the layout for the four stations.

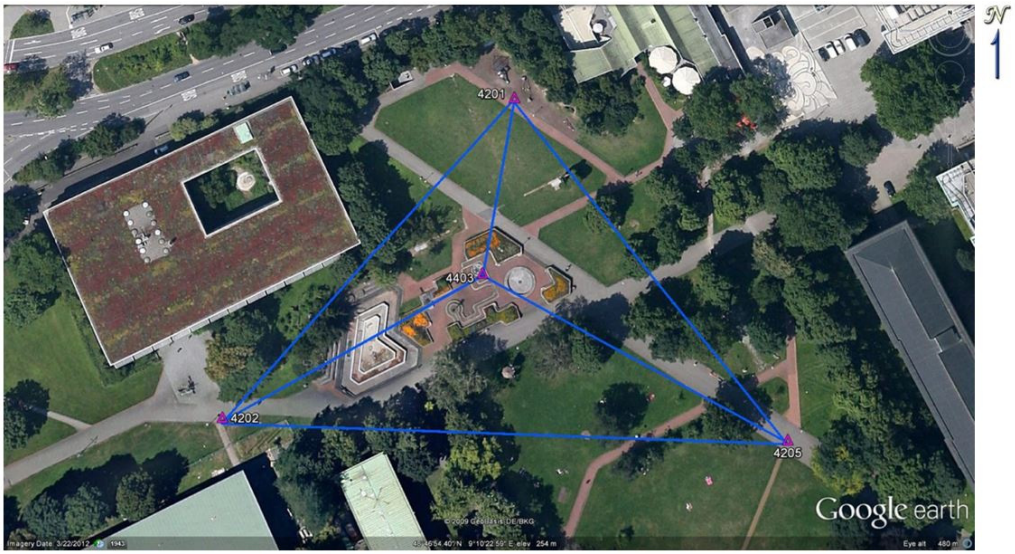

Fig. 17: Layout of Static Surveyed Stations © Google Earth

In kinematic mode a kinematic track was observed in Wasen region in Stuttgart city, the kinematic technique started with one hour static initialization time. The data were processed as a PDGNSS solution with SAPOS reference stations. GIPSY-OASIS software and CSRS-PPP online service were used to get a PPP solution. CSRS-PPP online service reached a good accuracy with 20 minutes initialization; it reached a horizontal RMS between 3 to 12 cm and a height RMS between 10 to 26 cm. In GIPSY-OASIS software the tropospheric modeling is the biggest challenge to solve. It provided unacceptable accuracy using a priori hydrostatic and wet tropospheric delay values. Some trails were done to model the tropospheric delay. The random walk parameters were used to model the wet zenith delay and the tropospheric gradient parameters. These parameters improved the PPP solution using GIPSY software especially for the height component. Initialization

time has no effect on the results in GIPSY processing in case of using dry values from CSRS online service. Using wet tropospheric parameters from CSRS online services provides a 3D error of 14 cm from 10 minutes initialization time. The second kinematic track has a good data quality. CSRS online service introduced a good accuracy for all initialization times. The accuracy reaches 5 cm as 3D RMS. GIPSY software provided an acceptable accuracy from 10 minutes initialization time with the apriori tropospheric model. This accuracy reached 7 cm as 3D RMS and no improvement after 20 minutes initialization time. Fig. 18 shows the kinematic trajectory layout.

Fig. 18: Surveying layout for second kinematic track, Wasen Region © Google Eart

Conferences

In 2012 the IIGS was responsible for the organization of two conferences:

- 27.-29. March 2012 Machine Control & Guidance (see also page 8)
- 27.-28. September 2012 Networks for Mobility (see also page 7).

Publications

Al-Mistarehi, B., Schwieger, V., Obaidat, M.: Cost-Efficient Camera System to Acquire Data for Pavement Maintenance Management System. Proceedings on 3rd International Conference on Machine Control & Guidance, Stuttgart, 27.-29.03.2012.

Beetz, A.: Separation of Control Quality and Measurement Accuracy for Guiding Control Tasks of an Indoor Construction Machine Simulator. Proceedings on 3rd International Conference on Indoor Positioning and Indoor Navigation, Sydney, 13-15th November 2012.

Beetz, A., Schwieger, V.: Automatic Lateral Control of a Dozer. FIG Regional Conference, Montevideo, Uruguay, 26.-29.11.2012.

Scheider, A., Beetz, A., Schwieger, V.: Post-Processed Kinematic Low-Cost GPS. Proceedings on 3rd International Conference on Machine Control & Guidance, Stuttgart, 27.-29.03.2012.

Schützle, R., Metzner, M., Schwieger, V.: Evaluation of Dynamic Location Referencing Algorithms. Proceedings on Networks for Mobility, Stuttgart, 27.-28.09.2012.

Schweitzer, J.: Modular Positioning using Different Motion Models. Proceedings on 3nd International Conference on Machine Control and Guidance, Stuttgart, 27.-29.03.2012

Schweitzer, J., Kochkine, V., Schwieger, V., Berner, F.: Quality Assurance in Building Construction based on Engineering Geodesy Processes. FIG Working Week, Rome, Italy, 06.-10.05.2012.

Schwieger, V.: Challenges of Kinematic Measurements. FIG Working Week, Rome, Italy, 06.-10.05.2012.

Schwieger, V. et al. (Editors): Proceedings on Networks for Mobility, Stuttgart, 27.-28.09.2012.

Schwieger, V., Beetz, A.: Road Construction Machine Guidance: Overview and Hardware-in-the-Loop-Simulator. Proceedings on International Conference on Innovative Technologies for an Efficient Geospatial Management of Earth Resources, Almaty, Kazakhstan, 18.-19.09.2012.

Schwieger, V., Böttinger, S., Zheng, B. (Editors): Proceedings on 3rd International Conference on Machine Control & Guidance, Stuttgart, 27.-29.03.2012.

Schwieger, V., Zhang, L.: Automatisches geodätisches Monitoring mit Low-Cost GNSS. Messtechnik im Bauwesen, Spezial 2012, Verlag Ernst & Sohn, Berlin.

Zhang, L., Stange, M., Schwieger, V.: Reducing the Costs of Geodetic Monitoring. GIM International, September 2012.

Zhang, L., Stange, M., Schwieger, V.: Automatic Low-cost GPS Monitoring System using WLAN Communication. FIG Working Week, Rome, Italy, 06.-10.05.2012.

Presentations

Schwieger, V.: Map Matching Applications. Seminar SE 3.05 „GPS/INS-Integration und Multisensor-Navigation“, Carl-Cranz-Gesellschaft e.V., Oberpfaffenhofen, 14.11.2012.

Schwieger, V.: Geometrische Qualität durch Ingenieurgeodäsie, Geomatik Veranstaltung, ETH Zürich, 15.11.2012

Schwieger, V.: Baumaschinensteuerung - der Beitrag der Ingenieurgeodäsie. Geodätisches Kolloquium der HCU Hamburg, 02.02.2012.

Schwieger, V.: Kinematic GNSS towards Real-Time. Symposium on PPP-RTK & Open Standards, BKG, Frankfurt,12.03.2012.

Schwieger, V.: Automated Geodetic Monitoring by Low-Cost GNSS. Interexpo Geo-Siberia-2012, Novosibirsk, Russia, 17.-19.04.2012.

Zhang, L.: Automatic Low-Cost GPS Monitoring System Using WLAN Communication. FIG Working Week 2012, 6.-10.05.2012, Rom, Italien.

Doctorates

Beetz, Alexander: Ein modulares Simulationskonzept zur Evaluierung von Positionssensoren sowie Filter- und Regelalgorithmen am Beispiel des automatisierten Straßenbaus. Hauptberichter: Prof. Dr.-Ing. habil. V. Schwieger, Mitberichter: Prof. Dr.-Ing. H. Ingensand. Bayerische Akademie der Wissenschaften, Verlag C. H. Beck, DGK, Reihe C, Nr. 688

Diploma Theses and Master Theses

Andries, Elena-Alexandra: Generation of a DTM for the Landslide „Hessigheimer Felsengärten“

Baleanu, Camelia: Allgemeine Nutzenanalyse der OpenStreetMap Daten sowie eine Qualitätsanalyse von OpenStreetMap Daten jeweils mit Hilfe von ArcGis 10

Ding, Chao: Investigation of the Total Stations Leica TS30 and Trimble SPS930

Dünkel, Aldemar: Robuste Ausreißerelimination und Zustandsschätzung für tachymetrische Überwachungsmessungen

Guo, Cheng: Analysis and Integration of Location Referencing Methods for Traffic Information Services

Jiang, Qian: Investigations and Near Real-Time Data Processing of a Low-Cost GPS Monitoring System

Khan, Tanzeel Ur Rehman: Comparison of Different Map Matching Algorithms with Floating Car Data

Li, Ke-Wei: Comparison of two Mathematical Models for the Surface Reconstruction for Deformation Analysis by Using Faro Focus 3D

Nartea, Tiberiu: Qualitätssicherung in der Ingenieurgeodäsie

Wang, Xu: Time Series Analysis for Construction Monitoring - Detailed analysis of High Frequencies

Study Theses and Bachelor Theses

Zhengjie Ren: Die Monte-Carlo-Simulation als Methode für die Fehlerfortpflanzung in geodätischen Anwendungen

Ye Zhou: Zeitreihenanalyse

Johannes Sperr: Adaption und Umsetzung eines Qualitätsmanagementkonzeptes für Prozesse der Geodatenverarbeitung

Education

Diploma Geodesy and Geoinformatics

Engineering Geodesy IV (Schwieger, Beetz)	2/1/0/0
Transport Telematics (in German) (Metzner, Schützle, Scheider)	2/1/0/0

Bachelor Geodesy and Geoinformatics

Basic Geodetic Field Work (Zhang, Stange)	5 days
Engineering Geodesy in Construction Processes (Schwieger, Zheng)	3/1/0/0
Geodetic Measurement Techniques I (Metzner, Zhang)	3/1/0/0
Geodetic Measurement Techniques II (Zhang)	0/1/0/0
Integrated Field Work (Metzner, Zheng)	10 days
Measurement Methods and Estimation Methods in Engineering Geodesy (Schwieger, Zheng)	2/2/0/0
Reorganisation of Rural Regions (Meyer)	1/0/0/0
Statistics and Error Theory (Schwieger, Zhang)	2/2/0/0

Master Geodesy and Geoinformatics

Industrial Metrology (Schwieger, Stange, Zhang)	2/1/0/0
Land Development (Meyer)	1/0/0/0
Monitoring Measurements (Schwieger, Beetz)	1/1/0/0

Master GeoEngine

Integrated Field Work (Metzner, Zheng)	10 days
Kinematic Measurements and Positioning (Schwieger, Beetz)	2/1/0/0
Terrestrial Multisensor Data Acquisition (Schwieger, Beetz)	2/1/0/0
Thematic Cartography (Schützle)	1/1/0/0
Transport Telematics (Metzner, Schützle, Schweitzer)	2/1/0/0

Bachelor „Civil Engineering“

Geodesy in Civil Engineering (Beetz, Scheider)	2/2/0/0

Master „Civil Engineering“

Geoinformationsystems (Metzner, Beetz)	2/1/0/0
Transport Telematics (Metzner, Scheider)	1/1/0/0

Bachelor „Technique and Economy of Real Estate“

Acquisition and Management of Planning Data (Metzner, Stange)	2/1/1/0

Master „Infrastructure Planning“

GIS-based Data Acquisition (Beetz, Schweitzer)	1/1/0/0

Institute of Geodesy

Geschwister-Scholl-Str. 24D, D-70174 Stuttgart,
Tel.: +49 711 685 83390, Fax: +49 711 685 83285
e-mail: gis@gis.uni-stuttgart.de or firstname.secondname@gis.uni-stuttgart.de
url: http://www.uni-stuttgart.de/gi

Head of Institute

SNEEUW NICO, Prof. Dr.-Ing.

Emeritus

GRAFAREND ERIK W, em. Prof. Dr.-Ing. habil. Dr.tech.h.c.mult. Dr.-Ing.E.h.mult.

Academic Staff

KELLER WOLFGANG, Prof. Dr. sc. techn.
KRUMM FRIEDRICH, Dr.-Ing.
REUBELT TILO, Dr.-Ing.
ROTH MATTHIAS, Dipl.-Ing.
WEIGELT MATTHIAS, Dr.-Ing. (until 31.8.)

Research Associates

ABEBINI ABBAS, M.Sc. (since 2.11.)
CAI JIANQING, Dr.-Ing. (until 29.2.)
CHEN QIANG, M.Sc.
DEVARAJU BALAJI, M.Sc.
ELMI OMID, M.Sc. (since 27.9.)
IRAN POUR SIAVASH, M.Sc.
ROOHI SHIRZAD, M.Sc.
TOURIAN MOHAMMAD, M.Sc.
WU GELI, M.Sc.
YE ZHOURUN, M.Sc. (since 2.11.)
ZHAO WEI, M.Sc.

Administrative/Technical Staff

HÖCK MARGARETE, Phys. T.A. (until 31.10.)
SCHLESINGER RON, Dipl.-Ing. (FH)
VOLLMER ANITA, Secretary

Guests

BORKOWSKI A, Prof., Wroclaw/Poland (11.-23.6.)
BRITCHI A, Bukarest/Romania (4.7.-15.8.)
FUJIMOTO M, Prof., Tokyo/Japan (24.5.-17.8.)
GHITAU D, Prof., Bucharest/Rumania (20.7.-24.8.)
LIN Y, Dr., Tongji/China (16.7.-31.8.)
SAFARI A, Ass. Prof., Tehran/Iran (1.8.-30.9.)
SUBRAMANI S, Chennai/India (17.5.-17.7.)
VISHWAKARMA BD, Roorkee/India (1.1.-31.5.)
ZHANG S, Dr., Wuhan/China (until 27.1.)

Additional Lecturers

BOLENZ S, Dipl.-Ing., Stadtmessungsamt, Stuttgart
ENGELS J, PD Dr.-Ing. habil., Stuttgart
HEß D, Dipl.-Ing., Ministerium für Ländlichen Raum und Verbraucherschutz Baden-Württemberg, Stuttgart
SCHÖNHERR H, Präsident Dipl.-Ing., Landesamt für Geoinformation und Landentwicklung Baden-Württemberg, Stuttgart (until 30.9.)
STEUDLE G, Dipl.-Ing., Ministerium für Ländlichen Raum und Verbraucherschutz Baden-Württemberg, Stuttgart

Research

Cyclo-stationary signal covariance models of the temporal variations in the gravity field of the Earth

Signal covariance models have been used in geodesy for a variety of purposes: least squares collocation, least squares prediction, Wiener filtering, Kalman filtering, regularization and other such estimation techniques. The signal covariance models are generally computed from observed datasets, and if the observed phenomenon can be expressed as a spectrum, the signal covariance models can be computed via the auto-covariance function of the spectrum. Gravity field, is a

Laplacian field and hence it is expressed in terms of a spherical harmonic spectrum. The auto-covariance function of the gravity field spectrum follows a power-law ($\kappa_l = 10^a l^b$ where l is the degree of the spectrum, which is the analogue on the sphere to the frequency of the Fourier spectrum), when approximated as the spectrum of a homogeneous isotropic covariance function on the sphere. Power-law based signal covariance models have been widely used in geodesy, and one such model is the well known Kaula-rule for the static gravity field model.

With the launch of the GRACE satellite mission, the temporal variations in the gravity field are being continuously measured for over a decade now, and are being released to the public as monthly snapshots. These monthly snapshots have revealed changes in the gravity field due to the movement and redistribution of mass in the cryosphere, hydrosphere, lithosphere and the atmosphere. For example, the annual cycle of the water storage changes in the large river-basins of the world (Amazon, Ganges, Congo, etc.); ice-mass loss of the Antarctic and Greenland ice-sheets; and glacial isostatic adjustment in North America and Scandinavia. However, the GRACE data is ridden with high-frequency noise, which necessitates filtering (Figure 1).

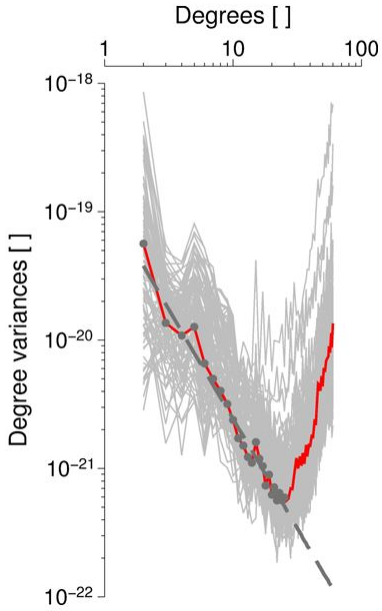

Figure 1: Power spectra of the GRACE monthly snapshots. Notice that higher degrees (> 20) have more power than the lower harmonic degrees, which clearly indicates high noise level. Also illustrated is the choice of the lower harmonics used for computing an approximate power-law-based signal covariance model. The power-law is a straight line in the logarithmic scale.

The computation of the GRACE auto-covariance function is impeded by the high-frequency noise. Nevertheless, the power spectrum of the temporal variations behaves the same way as that of the static gravity field, i.e. the power decreases with increasing degree. Therefore, a power-law-based approximate signal covariance model can be computed by fitting a straight-line to the logarithm of the less noisy low-frequency part of the power spectrum (Figure 1).

The GRACE observations of temporal gravity field variations is dominated by the water storage change signal from the big river basins, and the water storage changes in turn have a dominant annual period. As there is a dominant annual period in the signal we investigated the auto-covariance functions of the individual calendar months if the annual period is expressed in them. In Figure 2, we see the a and b values of the power-law show the 2 cycles per annum, and that is because of the exactly opposite phases of the Northern and Southern summers. If we were to square a once per annum cycle, we would get the same shape as that of the two variables. Thus, the auto-covariance indeed exhibits cyclo-stationarity. However, this is only one side of the story: the spectral side. As aforementioned these approximate degree-dependent power-laws transform into homogeneous isotropic covariance functions on the sphere. The transformed auto-covariance functions (Figure 3) show a dramatic evolution over the complete cycle, where the covariances change from being very local in January to becoming wide-spread in April, again narrowing towards July only to widen in October. Also there are big negative covariances when the covariances are very local, like in January and July. The four extreme months of January, April, July and October in fact coincide with the peak northern winter, onset of northern spring, peak northern summer, and onset of northern autumn, respectively. The local and not so local behaviour is clearly explained by the monthly maps of the gravity field changes expressed in equivalent water height (Figure 4). The month of January shows hardly any changes, while April shows a lot of changes with big signals throughout the globe. This lack of mass redistribution in January and the abundance of the same in April is what is reflected in the narrow and wide covariance functions, respectively. Now that the cyclo-stationarity of the GRACE signal covariance has been established, the effects of their usage in the estimators is what remains to be seen.

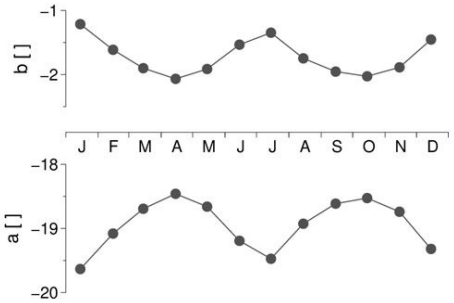

Figure 2: Estimated a and b values of the power-law fits for the individual calendar months, which clearly depict the dominant annual cycle in the temporal variations of the gravity field.

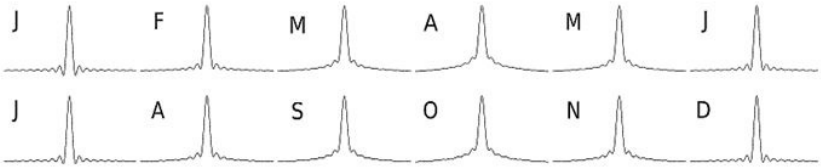

Figure 3: Cross-sections of the covariance functions in the spatial domain for the individual calendar months. Notice the similarity between covariance functions of the months separated by 6 months, and also the widening and narrowing of the functions.

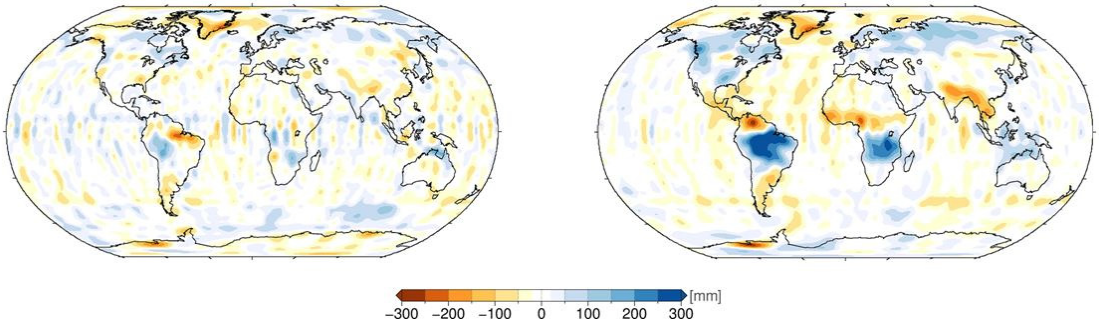

Figure 4: Monthly mass change maps expressed in equivalent water heights. The peak northern winter and peak southern summer in January stabilizes the mass redistribution, while change in the seasons from winter to summer in the North and vice-versa in the South generates an enormous mass redistribution in April.

The global continental water balance using GRACE spaceborne gravimetry and high-resolution consistent geodetic-hydrometeorological data analysis

Fresh water supply is crucial to human life. Surprisingly, human knowledge of the spatial and temporal dynamics of the surface fresh water variations and discharges is limited. Measuring the hydrological cycle is the starting point of fresh water supply studies. However, from the hydrological cycle only few of the major components are measured. Within current hydrological studies, these few measurements are considered to have sufficient accuracy to model the hydrological interactions. Comparison between different models and gauged observation reveals a large modeling error, sometimes greater than 100%. A large difference between the models underlines the necessity of in-situ measurements for improving and validating the models. However, this became problematic as the worldwide number of gauging stations has been decreasing since the 1970s. This emphasizes the demand of independent sensors like space based sensors to observe the hydrological cycle. This demand seems to be more essential in the case of discharge measurement,

as the global publicly available discharge database is limited and tends to decline. Moreover, discharge plays an important role in hydrological studies, being an output for hydrological models and input to many of hydrological interactions. Therefore, during last year we aimed to extract river discharge from satellite altimetry by establishing a rating curve using available discharge measurements and altimetry water level time series. The extraction of discharge is only achievable through having consistent data sets (Figure 5). Data availability and temporal resolution have been recognized as sources of inconsistency between water level time series from altimetry and available discharge measurements. From data availability, different rivers have been categorized into three groups. Group 1: rivers with available in situ discharge simultaneous with altimetry. Group 2: rivers with available in situ discharge non-simultaneous with altimetry. Group 3: rivers with no available discharge measurements at all, which have not been further investigated as it is not possible to establish a rating curve for these rivers.

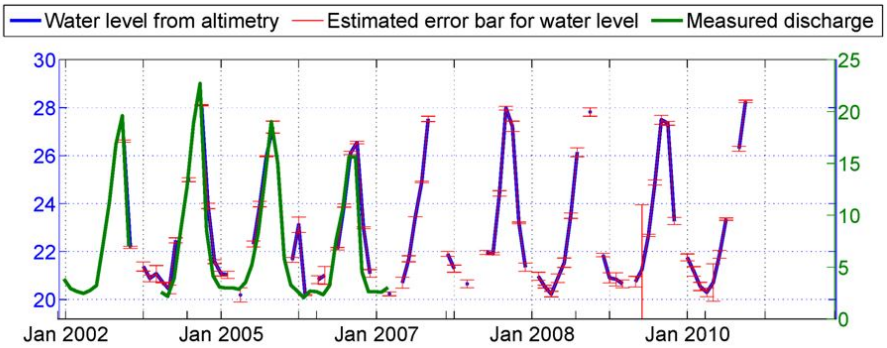

Figure 5: Niger River: Water level time series from ENIVISAT observation over the virtual station at $\varphi = 6.66$, $\lambda = 6.64$ (blue) and estimated error for each observation (red). Discharge time series from in-situ measurement of a gauging station at $\varphi = 7.8$, $\lambda = 6.76$

For rivers in group 1, river discharge can be estimated through a functional relationship that is conventionally established via a rating curve computed using simultaneous data. Yet, having rivers in the group 2 raise the question of how to establish a rating curve without simultaneous data sets. In order to justify the question, we proposed a statistical approach to derive discharge from height through a rating curve based on the quantile functions. This method is based on a scatter diagram of quantile functions, in which the probability-coordinate is eliminated (Figure 6). In contrast, the conventional methods operate directly on time series and eliminate the time-coordinate.

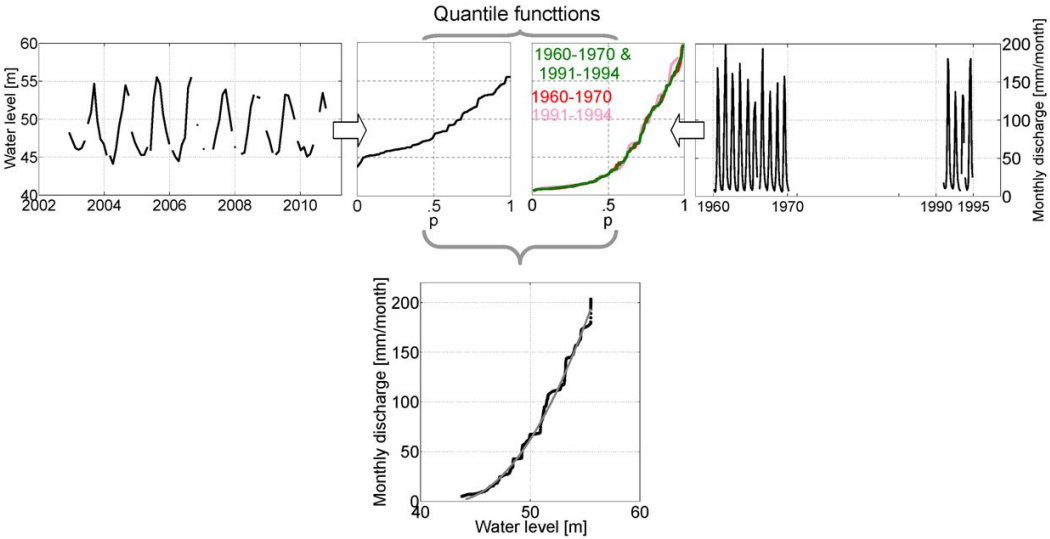

Figure 6: Estimated water level from satellite altimetry and available discharge for the Mekong River are transferred to the quantile functions. From the corresponding probabilities the scatter plot of discharge versus water level is constructed. A smoothened rating curve is then obtained by fitting a quadratic line to the scatter. Note the dissimilar time axes of the two datasets (top).

The method has been validated over five rivers from group 1, where results show that the statistical approach based on the quantile functions of water level and discharge provides the same range of error as the common conventional empirical method (Table 1).

	RMSE [mm/month]		Error
	Empirical	Statistical	
Amazon	8.5	9.1	8%
Niger	1.4	1.6	7%
Danube	4.3	4.4	10%
Amur	2.9	3.5	10%
Ob	4.9	5.1	17%

Table 1: Computed RMSE of estimated discharge from empirical and statistical approach in mm/month for five rivers in group 1

The usefulness of the discharge database generated by satellite altimetry is supported by comparing the estimated discharge from altimetry and available annual cycles. It has been demonstrated that estimated discharge can provide better estimation than the annual cycle. The good performance of the statistical approach supports the usage of altimetry to salvage pre-satellite altimetry

discharge data and turn them into active use for the satellite altimetry time frame. As the number of rivers with this situation is ca. 4680 (ca. 60%) - according to GRDC database - the statistical approach can be used as a tool to augment the discharge database around the world.

In general, the statistical approach based on quantile functions has its own limitations despite the good performance. The main limitation of this approach is that it leads to erroneous discharge when discharge behavior of the river drastically varies over time. This is specially demonstrated where the changes in discharge behavior of e.g. the Amur River over time causes different estimations of discharge from the empirical and statistical methods. On the other hand, similar to the empirical approach, the statistical approach is restricted by performing the model to the correspondent data set. This is highlighted in the Ob River where the noisy ice contaminated water level time series of altimetry close to the gauging station of discharge forces a choice of virtual station far from the gauge leading to an erroneous model out of non correspondent water level and discharge values. Besides that, discharge estimation from the obtained rating curve based on either empirical/statistical method is only possible at the time of altimetry, thus any missing value in altimetry leads to a gap in the estimation. In addition, noisy altimetry causes incorrect estimation of discharge. Therefore, it would be desirable to have an algorithm that covers the missing values and combines all available measurements with their uncertainties to provide an acceptable estimation. Hence, we developed a stochastic process model to cope with this problem and to improve the estimation.

The stochastic process model has been implemented in a way that it benefits from the advantageous cyclo-stationarity discharge. The model has been combined with the estimated discharge from altimetry and available in situ measurements to form a linear dynamic system. This dynamic system helps to estimate the discharge using the available measurements and monthly mean of discharge. The dynamic system has been solved using the Kalman filter that provides an unbiased discharge with minimum variance. The results of the Kalman filter estimation have been then validated against the in situ measurements using a leave-out validation procedure, where average RMSE of 0.97-5.64 mm/month, corresponding to the error of 4-17% are achieved for different rivers (Figure 7). These results indicate comparable range of error with the RMSE from empirical and statistical approaches. As a conclusion, it can be stated that the problems of missing and noisy altimetry values can be tackled by forming the stochastic process model and solving it with the Kalman filter. In general, it can be stated that the estimated river discharge using satellite altimetry would be appropriate for further hydrological investigation if 1) the altimetric water level time series is obtained with sufficient accuracy and 2) the water level variations are appropriately captured by altimetry sampling and 3) the water level time series over the virtual station correspond with in situ discharge measurements in terms of geomorphological situation and 4) river discharge does not vary drastically over time.

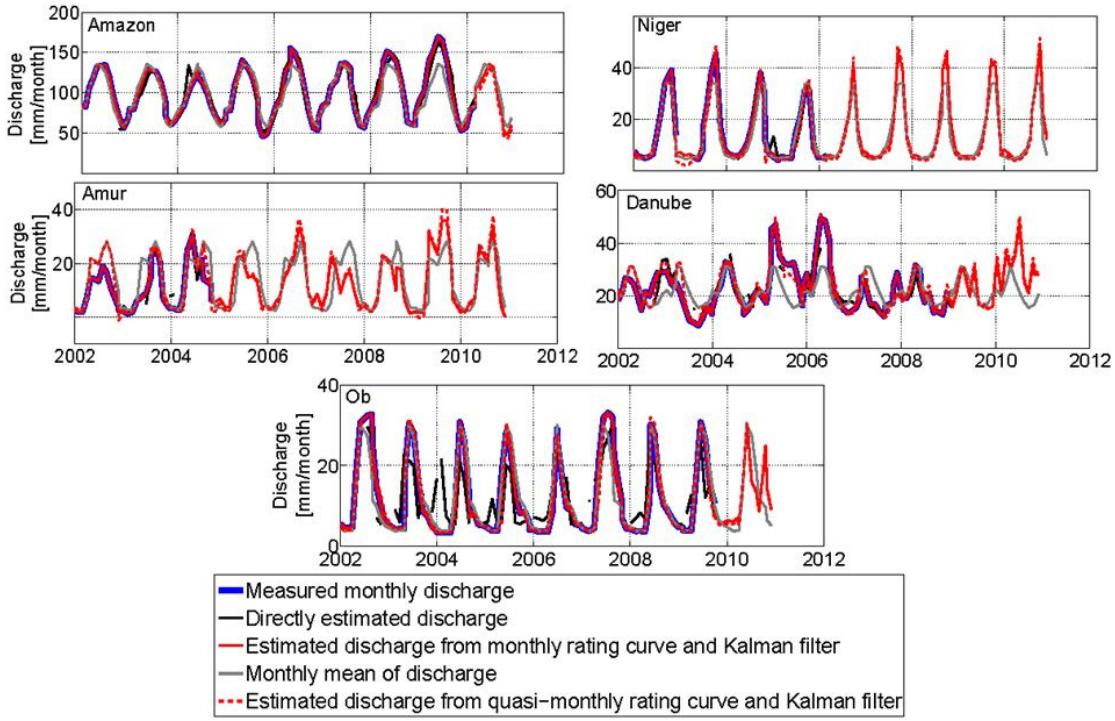

Figure 7: Estimated discharge using Kalman filter over the performed linear dynamic systems for rivers in group 1

Sampling, aliasing and satellite configurations of future gravity satellite missions

Identifying the suitable satellite missions for gravity recovery requires a huge variety of satellite orbits and gravity recoveries simulations. A variety of satellite orbit parameters such as inclination, repeat orbit and altitude of the formation, the inter-satellite distance, the measurement noise level, contribute to the search space for the optimal future gravity formation missions. In order to avoid the time-consuming full-scale gravity recovery simulations, two quick-look tools for fast simulation for sensitivity and gravity recovery analysis of time-variable gravity field from ll-SST (low-low satellite-to-satellite tracking) missions have been employed. The gravity recovery tool for aliasing analysis assumes nominal repeat orbit of the satellite formations within the time interval of the gravity recoveries. The quick-look tool for sensitivity analysis employs error propagation to investigate the influence of the orbital parameter on the retrieval gravity field errors of the formation missions, while the gravity recovery tool is based on the formulation of the equation for range-acceleration for the gravity solution in the time interval of the recovery.

The orbit design of this research project is based on the study of orbit configurations for the single pair inline (GRACE-like) formations with different repeat modes, altitudes and ground-track patterns, mission scenarios of two satellite pairs and alternative formation flights.

The single inline satellite formations are assumed to be near polar. An inline formation together with the alternative formations GRACE Follow-on (GFO), Pendulum, polar-radial Cartwheel, equatorial-radial Cartwheel and Helix have been studied (in order to investigate the effect of formation). Here, GFO is considered as a very conservative pendulum formation with a small opening angle (ρ_y/ρ_x = 10%, where ρ_x is the along-track satellite distance and ρ_y is the maximum cross-track distance).

It has been tried to include a large variety of repeat orbits, mission altitudes, ground-track patterns and time intervals of gravity solutions in design of the mission scenarios. In particular, for dual satellite pairs scenarios, combination of different orbital parameters has been studied. Moreover, the dual mission scenarios with small and large polar gaps and their influence on quality of the gravity recoveries, esp. for low latitudes with more samples, has been considered. Then, the sub-Nyquist time interval recoveries for different single pair inline formation flights as well as for the alternative formations and dual pairs missions have been studied. The effect of measurement white noise on different solutions was also integrated into the work. Different graphics (e.g. Equivalent Water Height (EWH) maps, spherical harmonics triangle plots, geoid height error rms per SH degree and per latitude) have been utilized for comparing the results.

Different formation flights are suggested as potential future scenarios for satellite gravity missions. The suggestions were based on the simulations from the quick-look tools of this research project. Table 2 shows the orbital and formation parameters of the basic missions. Figure 8 illustrates a significant increase in the absolute error level for the laser-missions for the aliasing analysis tool, especially for degrees below 50. It means that the aliasing error is above the laser noise. In contrast, the error curves for GRACE as reference, using K-band ranging and Super-STAR accelerometry, are similar, which indicates that the measurement noise is the dominant error source. Therefore, with the current knowledge of background models used as de-aliasing products, an improvement of the error level of about two orders of magnitude by laser/drag-free systems seems not feasible and is restricted to approximately one order of magnitude.

In addition to quality investigation of full cycle repeat period gravity solutions, a space search for sub-Nyquist gravity recovery, dealing with temporal aliasing, has been targeted. The quality of sub-Nyquist gravity solutions for different single inline pair configurations, alternative formations and dual pairs of inline formations have been investigated.

scenario	orbit parameters	formation parameters	mean Kepler elements (absolute, differential)
GRACE (as reference)	$h \approx 460$ km $\beta/\alpha = 489/32$ $I = 89°$	$\rho = 220$ km	$\Delta a = \Delta e = \Delta i = \Delta\omega = \Delta\Omega = 0$, $\Delta M = 1.8453°$
GRACE-Follow-On	$h \approx 420$ km $\beta/\alpha = 478/31$ $I = 89°$	$\rho_x = 220$ km $\rho_y = 25$ km ($\rho_{avg} = 221$ km)	$\Delta a = \Delta e = \Delta i = \Delta\omega = 0$, $\Delta\Omega = 0.2248°$, $\Delta M = 1.8453°$
pendulum (conservative)	$h \approx 335$ km $\beta/\alpha = 503/32$ $I = 89.5°$	$\rho_x = 96$ km $\rho_y = 43$ km ($\rho_{avg} = 100$ km)	$\Delta a = \Delta e = \Delta i = \Delta\omega = 0$, $\Delta\Omega = 0.3670°$, $\Delta M = 0.8194°$
cartwheel	$h \approx 335$ km $\beta/\alpha = 503/32$ $I = 89.5°$	$\rho_{avg} = 75$ km	$\Delta a = \Delta e = \Delta i = \Delta\Omega = 0$, $\Delta\omega = \Delta M = 180°$ $e_1 = 3.72\text{e-}3$
helix	$h \approx 335$ km $\beta/\alpha = 503/32$ $I = 89.5°$	$\rho_{LISA} = 50$ km $\rho_{x\text{-offset}} = 100$ km ($\rho_{avg} = 100$ km)	$\Delta a = \Delta e = \Delta i = 0$, $\Delta\Omega = 0.3696$, $\Delta\omega = -180.8535°$, $\Delta M = 180°$ $e_1 = 1.862\text{e-}3$, $\omega_1 = 0.4268°$
inline-Bender	$h \approx 335$ km/352 km $\beta/\alpha = (503/32)/(481/31)$ $I = 89.5°/63°$	$\rho = 100$ km	$\Delta a = \Delta e = \Delta i = \Delta\omega = \Delta\Omega = 0$, $\Delta M = 0.8993°$

Table 2: Basic missions and their parameters; mean Kepler elements ($e_1, M_1, \omega_1, \Omega_1$) not mentioned are set to zero

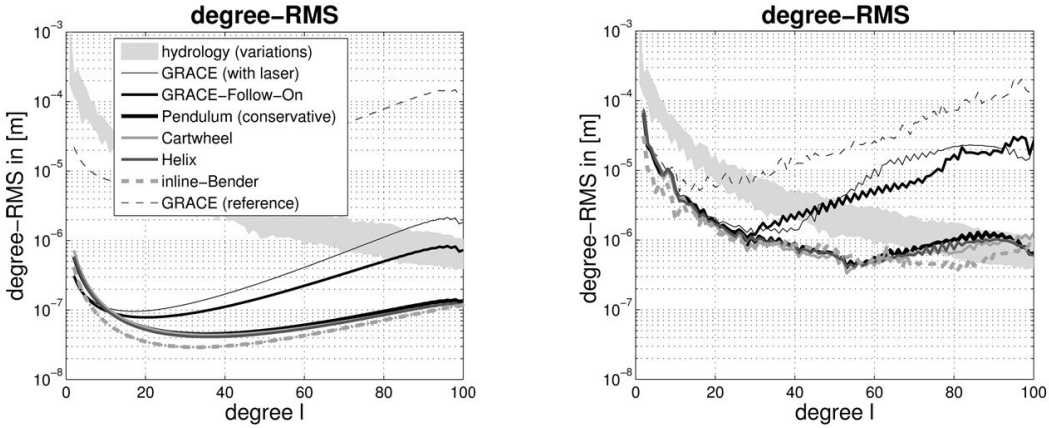

Figure 8: Quick-look analysis of the six basic missions including a GRACE-like scenario using a laser-link, left from sensitivity analysis tool, right from aliasing analysis tool (recovery analysis tool)

It has been showed that the modified Colombo-Nyquist rule ($B \approx L_{max}$) enables higher temporal resolution of gravity recoveries, while poorer spatial resolution can be adjusted by post-processing methods. That means for a single satellite pair we can already achieve gravity recoveries for six days up to maximum degree and order 90 provided that the ground-track coverage is homogeneous enough (Figure 9-left). By employing two satellite pairs, this is even achievable by three days solutions according to an interpretation of the modified CNR for dual formation missions (Figure 9-right). Strictly speaking, the latter solution is actually of higher quality. The reason is that an inclined formation rather increases isotropy significantly by adding East-West measurement components instead of only doubling the amount of samples. Moreover, the three days solution benefits from higher temporal resolution and thus less temporal aliasing, when compared to the six days solution. An important benefit of having sub-Nyquist solutions is that they can be applied as dealiasing products independent from state of the art geophysical models when aiming of time-variable gravity recoveries of longer time spans, e.g. monthly solutions.

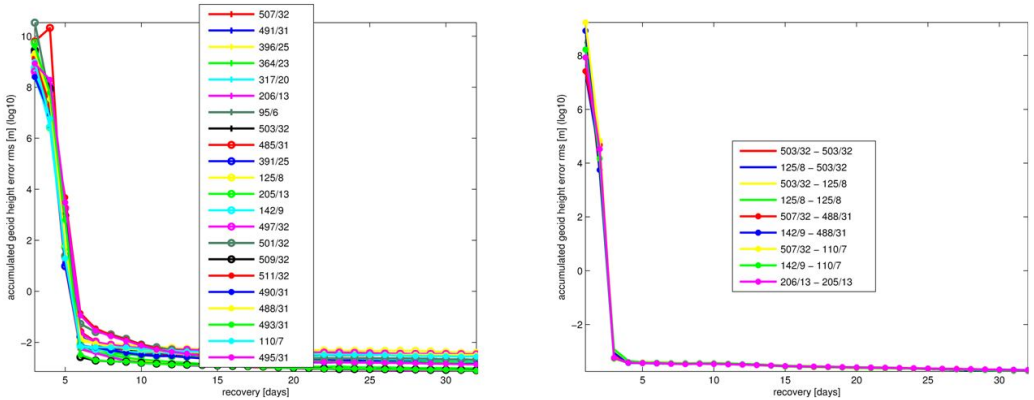

Figure 9: Global geoid height error rms of single inline pair (left) and dual inline formation missions (right) with different repeat orbits for recoveries up to maximum degree/order 90.

It has also been shown that by using alternative formations like Pendulum and Cartwheel, the quality of the gravity recoveries is improved considerably (Figures 10 and 11). However, they are accompanied by severe technical problems and challenges. Those technical problems prevent them to be employed in near future. On the other hand, a very conservative pendulum formation with a small opening angle, GFO, is technically more realistic, and is able to improve the quality of gravity recoveries for single satellite missions for high degrees and low latitudes.

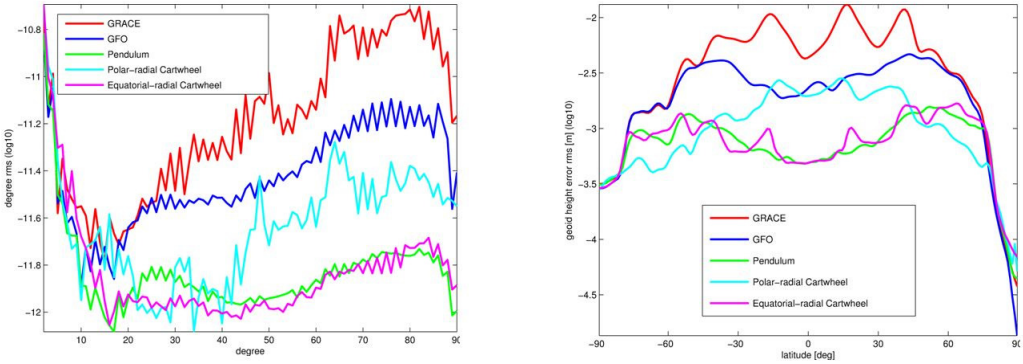

Figure 10: Error degree rms (left) and geoid height error rms per latitude (right) of the 6 days recoveries for the inline and alternative formations for maximum degree/order 90.

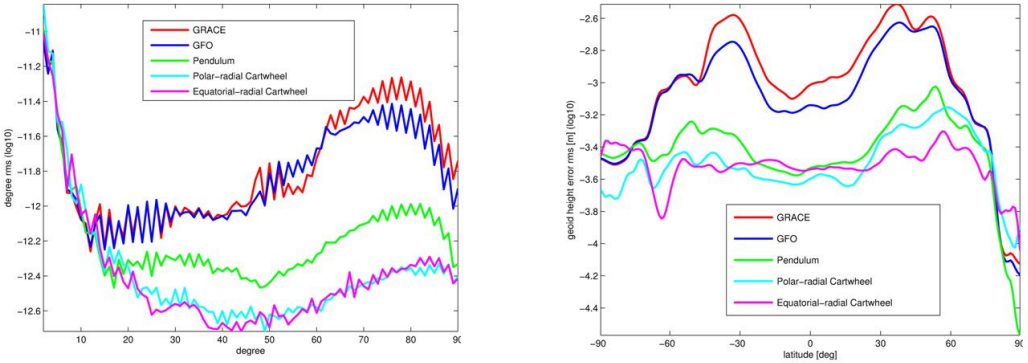

Figure 11: Error degree rms (left) and geoid height error rms per latitude (right) of the 32 days recoveries for the inline and alternative formations for maximum degree/order 90.

The selection of orbital parameters, especially those generating homogeneous and smooth gap evolutions with avoidance of large unobserved gap as they appear for e.g. drifting orbit and the mission altitude play important roles in quality of the gravity recoveries, although they are far less important than the fulfillment of the modified Colombo-Nyquist rule.

For sub-Nyquist gravity recovery, a combination of a near-polar GRACE-like or GFO mission with a 72^{o} inclined inline formation at an altitude of about 300 km is selected as a possible scenario for future gravity missions. It has been shown that the quality of sub-Nyquist recoveries benefit from a low mission altitude, while no significant correlation between the quality of those recoveries of dual missions and the missions' repeat orbits has been found.

Long-wavelength gravity field analysis of GOCE-SST data using the acceleration approach

The GOCE mission, which was launched in March 2009, was designed to recover the Earth's static gravity field up to degree/order 250/250. Therefore it carries a highly sensitive gradiometer instrument on board. However, due to the restricted sensitivity of this instrument for the long wavelength features the data analysis has to be supplemented by orbit analysis from the hl-SST measurements. Within the official state-of-the-art GOCE-only gravity field solutions of ESA (European Space Agency) the orbit analysis is conducted by means of the energy balance approach. As previous studies have shown, this approach is inferior by approximately a factor of $\sqrt{3}$ by using only a 1D-observable compared to other hl-SST or orbit analysis methods. Therefore, within a joint work of the Geodetic Institute and the Space Research Institute (Austrian Academy of Sciences, Graz) it is proposed to apply instead the acceleration approach, which proved to be an efficient tool in CHAMP and GRACE data analysis. This approach evaluates the equation of motion directly. Therefore the kinematic orbits (official GOCE product, delivered by the Astronomical Institute of the University of Bern, AIUB) have to be differentiated twice and reduced from disturbing accelerations. Due to the drag-free system of GOCE the accelerometer measurements are neglected. In contrast to the CHAMP and GRACE analysis, where the orbits were sampled with dt = 30 s, the 1s-sampling of the GOCE orbits lead to severe problems due to strong amplification of high-frequency noise. Different filter and weighting techniques have been tested in order to mitigate this problem.

Finally two successful solution strategies were extracted:

- a) application of an extended differentiation filter (EDF(Δt) with Δt = 30 s) for numerical differentiation and adoption of empirical covariance functions in the orbit frame (or local frame), which have been obtained from residual analysis. Note that extended differentiation with EDF(30s) means that the sampling points for numerical differentiation are chosen 30 s apart whereas the differentiation filter moves along the original 1 s-sampled orbit track, i.e. the whole data-set is exploited.
- b) direct application of the 9-point differentiation filter to the 1 s-sampled orbit (EDF(1s)) and straight-forward error-propagation of the provided orbit variance covariance matrices (VCM). This strategy shows a strong dependence on arc-length and maximum resolution L_{max} compared to method a), but leads to small improvements for certain spherical harmonic degrees. The optimum arc-length is identified as about 8-10 minutes and the optimum maximum resolution as L_{max} = 120.

The results are displayed in Figure 12. It shows that our GIWF (Institute of Geodesy/Space Research Institute) models are of comparable accuracy as an alternative solution obtained by AIUB with the variational equations. Furthermore, it outperforms the INAS solution (applied in official TIM model) estimated by the energy balance approach by approximately a factor of 1.5-2.

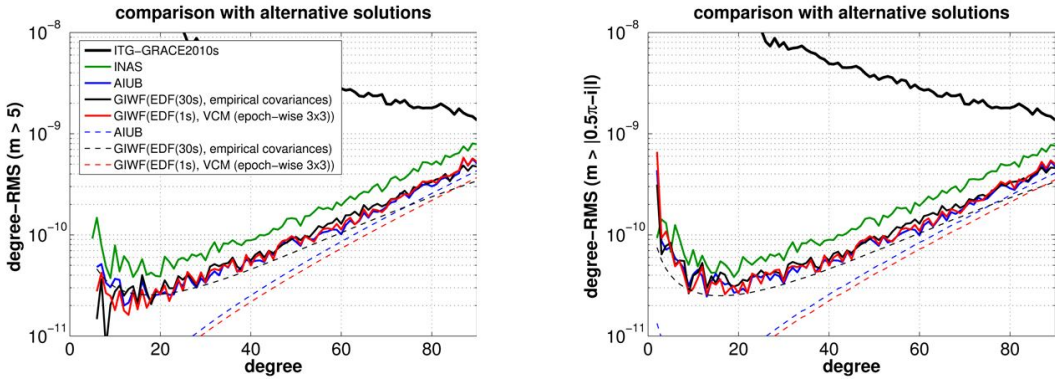

Figure 12: Comparison of the GIWF models ($L_{max} = 120$) obtained from EDF(1s) and EDF(30s) with the solutions of INAS ($L_{max} = 100$) and AIUB ($L_{max} = 120$); left: orders m < 5 omitted; right: orders $m_l \leq |0.5\pi - i|l$ omitted

Recovery of long-wavelength time variable gravity field features from CHAMP

In the event of a termination of the GRACE mission before the launch of GRACE Follow-On (estimated for 2017) high-low satellite-to-satellite tracking (hl-SST) will be the only dedicated observing system with global coverage available to measure the time variable gravity field (TVG) on a monthly basis. Yet, hl-SST TVG observations have been of poor quality and often require augmentation with Satellite Laser Ranging observations. To date, they have been of only very limited usefulness to geophysical or environmental investigations. A thorough reprocessing strategy and a dedicated Kalman filter to CHAMP data have been applied to demonstrate that it is possible to derive the very long wavelength TVG features (approximately degree 8 to 10). A combination of three important procedures enables the recovery of the time-variable gravity field from high-low satellite-to-satellite missions. These procedures include: 1) GPS processing; 2) Gravity field recovery; and 3) Kalman filtering.

Figure 13 shows the trend, the amplitude and phase of the annual signal of four solutions: the CHAMP v2 at the top which is without the Kalman filtering and based on the raw output of the gravity field recovery, in the second row the CHAMP v2 mean model, which is based on a least-squares fit using a bias, trend and annual frequency, the CHAMP v2 Kalman solution in the third row and the GRACE solution at the bottom for comparison. All solutions have been filtered by a Gaussian filter of 1000 km. Due to problems with the sensitivity of CHAMP during 2003 and the switch to the redundant board in October 2008 the time is limited to the period 2004 till October 2008.

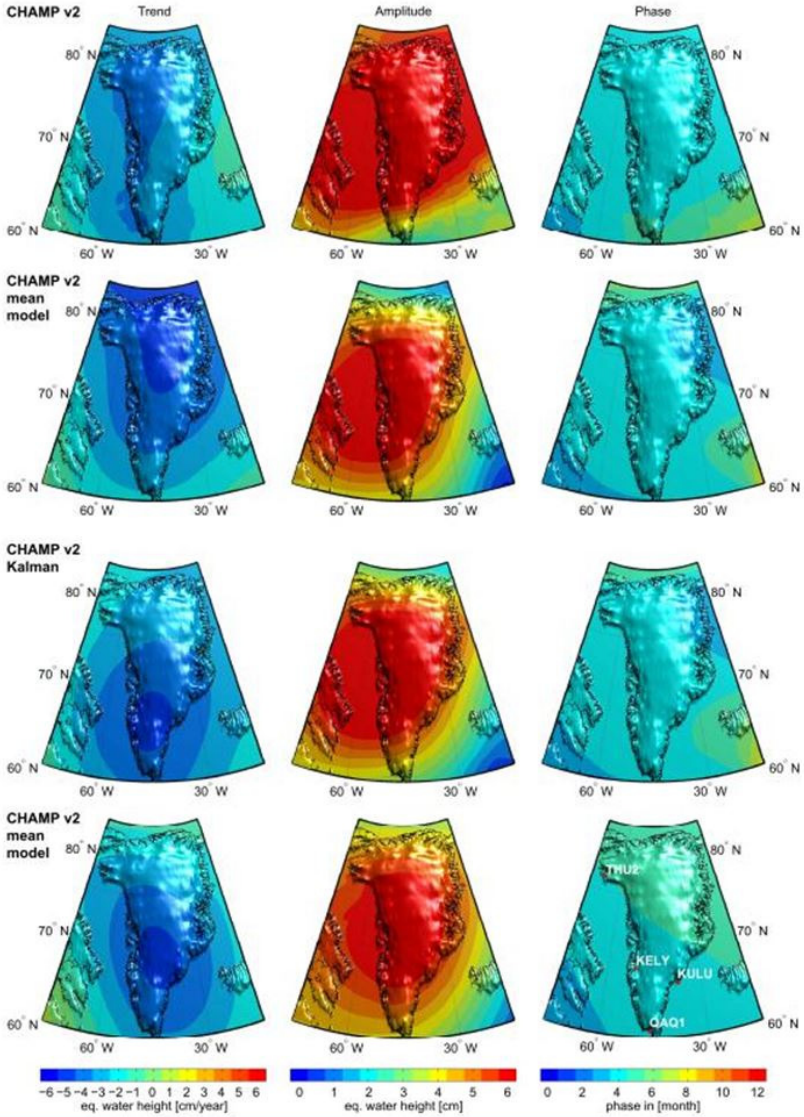

Figure 13: Trend, amplitude and phase for the CHAMP v2 (top panel) solution, the CHAMP v2 mean solution (2nd row), the CHAMP v2 Kalman solution (3rd row) and GRACE (CSR, Rel05, bottom panel) in terms of equivalent water height

As expected and despite the Gaussian filtering, the CHAMP v2 solution performs worst. The dominant noise is preventing to reveal realistic pattern. Only the phase is in good agreement with GRACE. The RMS of the phase shift is only 0.71 month equivalent to ≈20 days. In terms of the RMS, the other two CHAMP solutions do not achieve better results but the visual pattern changes slightly. Most interestingly is certainly the comparison of the CHAMP v2 mean solution vs. the CHAMP v2 Kalman solution. The trend pattern (left column) shows the strongest deviation. The mean solution has a stronger trend in the northern part of Greenland. The overall signal RMS is 2.99 cm/year for CHAMP and 2.78 cm/year for GRACE. The signal RMS is ≈ 23 % higher and also the difference RMS to GRACE is almost a factor 2.5 higher. The peak, i.e. maximum negative trend, is shifted far north.

The comparison to the GRACE solutions shows that the Kalman solution has a superior performance although the pattern is slightly rotated and shifted to the south-west. The magnitude of the peak is -4.36 cm/year in terms of equivalent water height which is just ≈ 0.6% smaller than in case of GRACE. The amplitude pattern in the middle column has for both the CHAMP v2 mean and the CHAMP v2 Kalman solution an almost identical pattern. Only in the utmost north-eastern corner a difference is recognizable. In comparison to GRACE, the pattern is extending further south-west and the peak value is approximately ≈ 8 % higher. The location is nearly identical for both CHAMP solution but shifted relative to GRACE by ≈ 9° to the west. The difference RMS is only slightly better for the CHAMP v2 Kalman solution. This is primarily due to improved phase estimation in the north-east. There, a phase shift of up to two month occurs relative to GRACE which can be reduced by the Kalman approach though not entirely removed.

The time variable pattern is restricted to the very long-wavelength features (≈ degree 8-10) due to the reduced accuracy of the GPS observation w.r.t. the K-Band observation of GRACE but it shows that realistic trends and amplitudes for Greenland can be derived. The research also shows that hl-SST can not only serve as an alternative (at a lower spatial resolution) in case of the termination of GRACE but is also a viable source of information by itself. This is especially interesting in view of the upcoming SWARM mission which promises a higher number of observations due to its three satellites.

Investigations on the capability of SWARM as a gap-filler for estimating time-variable gravity fields and mass variations

Recently, the implementation of the GRACE Follow-On mission has been approved. However, this successor of GRACE is planned to become operational in 2017 at the earliest. In order to fill the impending gap of 3-4 years between GRACE and GRACE-FO, the capability of the magnetic field mission SWARM as a gap filler for time-variable gravity field determination has to be investigated. Since the three SWARM satellites, where two of them fly on a pendulum formation, are equipped with high-quality GPS receivers and accelerometers, orbit analysis from high-low Satellite-to-Satellite Tracking (hl-SST) can be applied for geopotential recovery. As data analysis from CHAMP and GRACE has shown, the detection of annual gravity signals and gravity

trends from hl-SST is possible for long-wavelength features corresponding to a Gaussian radius of 1000 km, although the accuracy of a low-low SST mission like GRACE cannot be reached. However, since SWARM is a three-satellite constellation and might provide GPS data of higher quality compared to previous missions, improved gravity field recovery can be expected.

One of the most important scientific results of GRACE is the estimation of mass trends such as the ice mass loss on Greenland or water accumulation in the Amazon Basin. The potential of SWARM for the continuation of such mass trend time series is investigated. By means of reduced-scale simulations using the acceleration approach and taking into account time-variable background models of atmosphere, ocean, hydrology, ice, solid Earth and ocean tides as well as measurement noise a first simulation cycle based on monthly solutions (up to degree 60) was investigated.

In order to improve the data quality and extract the time variable signals, a Kalman-based filter approach is employed. The Kalman-filter consists of two steps: a prediction step and an update step. In order to avoid contamination with a priori information the model used for prediction is derived directly from the time series of each coefficient separately. The prediction model consists of the mean, a trend and a sine/cosine function with the main frequency at 1 cycles per year. Process noise is added to the predicted model which is eventually updated with the coefficient time series. The Kalman-filtered time series show a clear improvement in both the temporal and spectral domain without smoothing the signals of interest significantly.

In a second step mass trends are estimated by fitting a regression line together with annual/semi-annual signals to (residual) mass-variation time-series. Figure 14 displays the mass trends for smoothing radii of R = 750 km. As it can be seen, the trend-lines and LS-fits for the Kalman-filtered and unfiltered noise simulation as well as from the „true“ models match quite well. Figure 14 demonstrates furthermore that the effect of Kalman-filtering on the trend estimates is almost negligible, although LS-fit residuals are reduced by a factor of ≈ 4 and the time-series (without regression) fits better to the one of the „true“ models. The results show the possible capability of SWARM for long-wavelength time-variable gravity recovery and motivates further investigations.

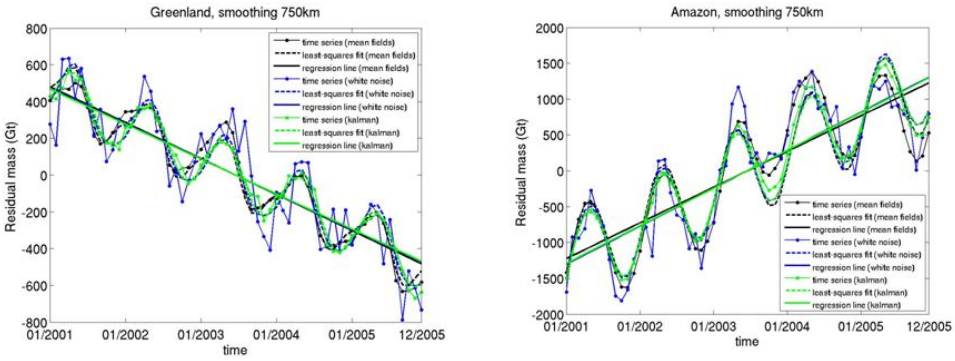

Figure 14: Mass trend estimates from simulated 5 years SWARM time series; left: Greenland, right: Amazon Basin; Gaussian smoothing with radius R = 750 km applied.

Geometry analysis of SWOT satellite mission

A careful repeat orbit design plays important role in sampling the earth from the space by satellites and choice the optimized repeat orbit is a key element for successful establishment of a mission. Achieving the mission goal without a proper orbital geometry is not possible. If satellite mission interests in hydrological applications, it must be able to monitor water bodies such as lakes and rivers with sufficient spatial and temporal resolution. Current satellite altimetry con not cover well some parts of the world like arctic region while this area includes many water bodies. A part of this deficiency goes back to the orbital geometry configuration of previous missions. Therefore the repeat orbit design of future missions involves with new requirements. Surface Water and Ocean Topography (SWOT) mission addressed the deficiency of current satellite altimetry missions in monitoring small water bodies. This mission tries to provide globally coverage with enough spatial and temporal resolution even in higher latitude area. For example an arbitrary point located in the latitude 70^{o} can be monitored 13 and 18 times for the inclination angle 74^{o} and 78^{o} respectively during one repeat orbit period with 23 nodal days. that can be an important factor to study lakes and rivers dynamic behavior. In this research we analyze the orbital geometry to find an optimized repeat orbit for SWOT mission. This analysis was performed at the presence of J2, the second degree zonal term of geopotential, via analytical solution. For all possible orbits with a height 750km to 1000km and a repeat period less than 25 nodal days we compared the ground track density, homogeneity and gap graph evolution as well as spatial-temporal resolution. Based on this comparison some repeat modes such as those that highlighted in Figure 18 can be candidates orbit. But some of them are better options that shown in Table 3 and Table 4.

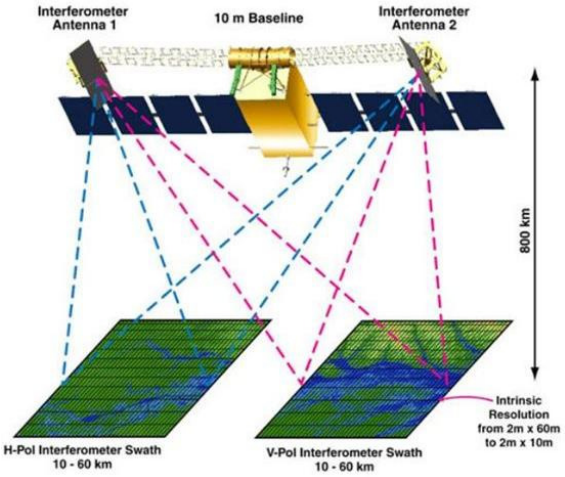

Figure 15: SWOT satellite configuration

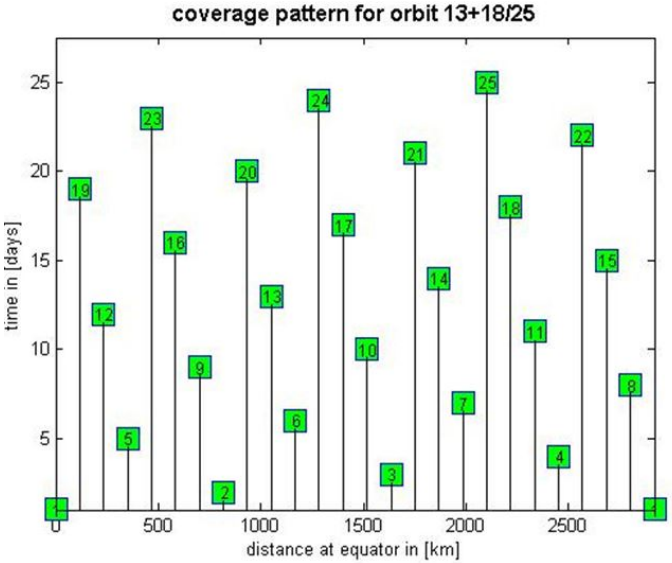

Figure 16: Coverage pattern for skipping orbit of SWOT satellite mission

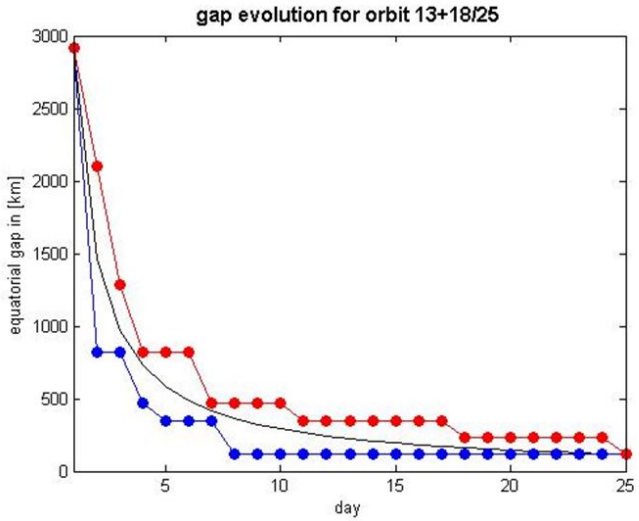

Figure 17: Gap evolution graph for a skipping orbit

α [day]	β	Subcycle [day]	Pass break [°]	Pass break [km]	Orbit height [km]
20	277	7	1.2996	144.67	910.38
21	286	8	1.2587	140.12	993.35
22	303	9	1.1881	132.26	937.89
23	315	10	1.1428	127.22	965.57
24	329	7	1.0942	121.81	961
25	343	7	1.0496	116.83	956.8

Table 3: Candidate orbits for nominal phase of SWOT satellite mission

α [day]	β	Subcycle [day]	Pass break [°]	Pass break [km]	Orbit height [km]
3	41	1	8.7805	977.44	976.05
4	55	1	6.5455	728.64	946.02
5	69	1	5.2174	580.80	928.15

Table 4: Candidate orbits for fast phase of SWOT satellite mission

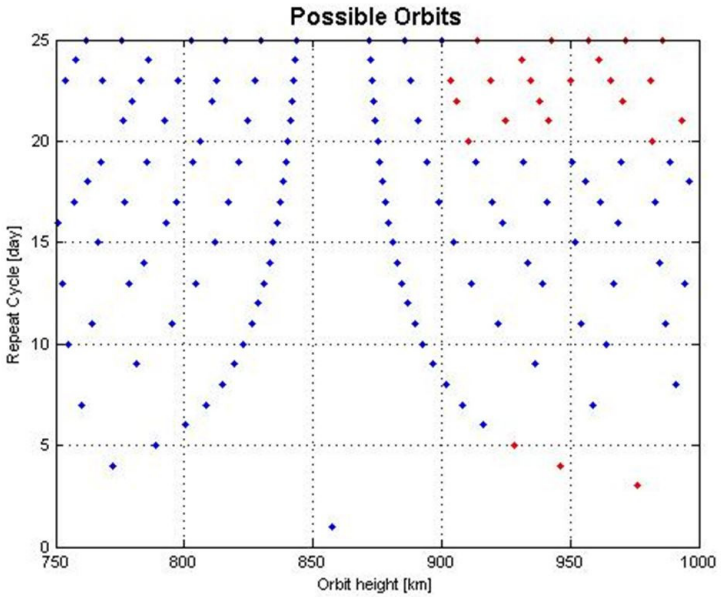

Figure 18: Candidate orbits

Euler deconvolution

Euler deconvolution is a semi-automated method to estimate possible locations of magnetic field or gravity field sources. Based on Euler's homogeneous function theorem, development on Euler deconvolution started already in the 1960s for magnetic gradient data. However, the lack of powerful computers stalled development until the 1980s when Thompson (1982) developed a computer program to solve the Euler deconvolution for a small amount of magnetic data. Thus, Euler deconvolution became of interest to prospecting companies, what gave also some increase in development speed. Since the 1990s, this method was extended to be used with gridded data (before: only lines) and also became applied to gravity data.

However, only ship-borne or air-borne measurements of gravity gradients within relatively small areas (around 3000 km^2 at maximum) were done so far.

Now, the satellite mission GOCE (Gravity field and steady-state Ocean Circulation Explorer) provides for the first time gravity gradient data of a near global coverage.

We investigate the benefit of Euler deconvolution to geodesy, e.g. to retrieve global gravity models. We are still in preparatory stage (mainly, theoretical work, data preprocessing, developing structures for data storage, functionality testing, etc.). Here, we present a part of the theoretical work. For standard Euler deconvolution, we reformulate the functional model

$$(x - x_0)\delta V_{xz} + (y - y_0)\delta V_{yz} + (z - z_0)\delta V_{zz} + N(\Delta\delta V_z + B_z) = 0$$

in the Gauss-Markov model

$$\boldsymbol{\eta} = \mathbf{A}\boldsymbol{\xi} + \boldsymbol{e},$$

which leads to

$$\begin{pmatrix} \delta V_{xz,1} & \delta V_{yz,1} & \delta V_{zz,1} & -N \\ \vdots & \vdots & \vdots & \vdots \\ \delta V_{xz,m} & \delta V_{yz,m} & \delta V_{zz,m} & -N \end{pmatrix} \begin{pmatrix} x_0 \\ y_0 \\ z_0 \\ B_z \end{pmatrix} = \begin{pmatrix} x_1\,\delta V_{xz,1} & y_1\,\delta V_{yz,1} & z_1\,\delta V_{zz,1} & -N\,\delta V_{z,1} \\ \vdots & \vdots & \vdots & \vdots \\ x_m\,\delta V_{xz,m} & y_m\,\delta V_{yz,m} & z_m\,\delta V_{zz,m} & -N\,\delta V_{z,m} \end{pmatrix}.$$

Here the δV_{ij} represent disturbing gravity gradients, δV_z the gravity disturbance in z-direction, (x, y, z) the measurement position, (x_0, y_0, z_0) the location of the mass anomaly and $-N$ the degree of homogeneity.

A window is slid over the data and for each window such a linear system of equations is solved to obtain the unknown parameters (x_0, y_0, z_0, B_z) . However, the fact is disregarded, that measured quantities are never error-free. As the design matrix consists mainly of such measured quantities, the included errors lead to an inaccurate estimation of the unknowns.

In such a case the Gauß-Helmert model is the better choice in terms of estimation precision as also the measured quantities' errors can be considered. However, the drawback is that matrices get several times bigger due to the additional conditions. We also want to retrieve variance-covariance information, hence we need one inversion of a matrix per window. For the standard Euler deconvolution the size of that matrix depends only on the amount of unknown parameters, i.e. matrix size is 4 x 4. The matrix size of the extended Euler deconvolution depends also on m (the amount of observations in each window), i.e. the matrix size increases to 4m + 4 x 4m + 4. This leads to an increase of computing time increase by a factor of 60.

Measured - and as such stochastic - quantities are $x, y, z, \delta V_{ij}, \Delta\delta V_i$; unknown quantities are $x_0, y_0, z_0, B_i (i, j = x, y, z)$. Exemplarily, we examine one equation, while taking into account the stochastic quantities (e.g. x becomes now $x + e_x$, etc.)

$$\begin{aligned}(x + e_x - x_0)\left(\delta V_{xz} + e_{\delta V_{xz}}\right) + \left(y + e_y - y_0\right)\left(\delta V_{yz} + e_{\delta V_{yz}}\right) + (z + e_z - z_0)\left(\delta V_{zz} + e_{\delta V_{yz}}\right) \\ + N\left(\Delta\delta V_z + e_{\delta V_z} + B_z\right) = 0.\end{aligned}$$

This equation is not linear, hence, linearization becomes necessary. Additionally, we can assume that the errors of (x, y, z) are very small (the position of GOCE is known from GPS positioning with high accuracy, i.e. we set $e_x = e_y = e_z = 0$). Rewritten in matrix-vector notation, we get

$$\begin{aligned}&\begin{bmatrix}-\left(\delta V_{xz} + \check{e}_{\delta V_{xz}}\right) & -\left(\delta V_{yz} + \check{e}_{\delta V_{yz}}\right) & -\left(\delta V_{zz} + \check{e}_{\delta V_{zz}}\right) & N\end{bmatrix}\begin{bmatrix}\Delta y_0 \\ \Delta z_0 \\ \Delta B_z\end{bmatrix} \\ &+ \begin{bmatrix}(x + \check{e}_x - \check{x}_0) & \left(y + \check{e}_y - \check{y}_0\right) & (z + \check{e}_z - \check{z}_0) & N\end{bmatrix}\begin{bmatrix}e_{\delta V_{xz}} \\ e_{\delta V_{yz}} \\ e_{\delta V_{zz}} \\ e_{\Delta\delta V_z}\end{bmatrix} + (x - \check{x}_0)\delta V_{xz} \\ &+ (y - \check{y}_0)\delta V_{yz} + (z - \check{z}_0)\delta V_{zz} + N\left(\Delta\delta V_z + \check{B}_z\right) = 0.\end{aligned}$$

Here, $\check{}$ on top of a variable indicates that this variable is evaluated at the Taylor point. The equation is nearly in the form of the Gauß-Helmert model, so we can write

$$\mathbf{A}\Delta\boldsymbol{\xi} + \mathbf{B}^{\mathrm{T}}\boldsymbol{e} + \boldsymbol{w} = 0.$$

Minimizing the Lagrange function

$$\mathcal{L}(\Delta\boldsymbol{\xi}, \boldsymbol{e}, \boldsymbol{\lambda}) = \frac{1}{2}\boldsymbol{e}^{\mathrm{T}}\boldsymbol{e} + \boldsymbol{\lambda}^{\mathrm{T}}(\mathbf{A}\Delta\boldsymbol{\xi} + \mathbf{B}^{\mathrm{T}}\boldsymbol{e} + \boldsymbol{w}) \longrightarrow \min_{\Delta\boldsymbol{\xi}, \boldsymbol{e}, \boldsymbol{\lambda}}$$

leads us to the linear system of equations

$$\begin{bmatrix} 0 & 0 & \mathbf{A}^{\mathrm{T}} \\ 0 & \mathbf{I} & \mathbf{B} \\ \mathbf{A} & \mathbf{B}^{\mathrm{T}} & 0 \end{bmatrix} \begin{bmatrix} \widehat{\Delta\boldsymbol{\xi}} \\ \hat{\boldsymbol{e}} \\ \hat{\boldsymbol{\lambda}} \end{bmatrix}$$

whose solution is refined iteratively, until the vector of increments $\Delta\xi$ becomes small enough to meet the accuracy threshold. The initial values of the variables evaluated at the Taylor point are obtained by a preceding standard Euler deconvolution.

So far, in this project we reformulated the adjustment process to introduce the consideration of measurement errors to Euler deconvolution. First tests with a small amount of data looks promising, but the result is not interpretable (hence, not shown here). The conclusion is that a much bigger amount of data is needed for Euler deconvolution to succeed.

Hence, we are preprocessing all the available GOCE gravity gradiometry data. This preparatory step is nearly completed.

Theses

Diploma/Master Theses

(http://www.uni-stuttgart.de/gi/education/MSC/master_theses.de.html)

CAO Z: Analysis of earthquake signals by spaceborne gravimetry

QIN W: GRAIL Lunar gravity field recovery simulations based on short-arc analysis

TOURIAN MJ: Controls on satellite altimetry over inland water surfaces for hydrological purposes

VISHWAKARMA BD: The GRACE event calendar

ZHAO W: Local gravity field modeling by gradiometry

Study Theses

(http://www.uni-stuttgart.de/gi/education/BSC/study_reports.en.html)

CAO W: Literature Analysis of SWOT Mission from Geodetic Perspective (Literaturanalyse der SWOT-Mission aus Geodätischer Sicht)

WU B: Comparison of different ocean tide models especially with respect to the GRACE satellite mission (Vergleich verschiedener Meeresgezeitenmodelle insbesondere unter Berücksichtigung der GRACE-Satellitenmission)

Publications

(http://www.uni-stuttgart.de/gi/research/index.en.html)

Refereed Journal Publications

BAUR O, T REUBELT, M WEIGELT, M ROTH AND N SNEEUW: GOCE orbit analysis: Long-wavelength gravity field determination using the acceleration approach. Advances in Space Research 50, pp 385-396, DOI 10.1016/j.asr.2012.04.022

FERSCH B, H KUNSTMANN, A BÁRDOSSY, B DEVARAJU AND N SNEEUW: Continental-scale basin water storage variation from global and dynamically downscaled atmospheric water budgets in comparison with GRACE-derived observations, Journal of Hydrometeorology 13, pp 1589-1603, DOI 10.1175/JHM-D-11-0143.1

KELLER W AND A BORKOWSKI: Wavelet based buildings segmentation in airborne laser scanning data sets. Geodesy and Cartography 60, pp 99-121

MOGHTASED-AZAR K, F TAVAKOLI, HR NANKOLI AND E GRAFAREND: Multivariate statistical analysis of deformation tensors: independent vs. correlated tensor observations. Stud. Geophys. Geod. 56, pp 977-992, DOI 10.1007/s11200-011-9024-6

RIEGGER J, M TOURIAN, B DEVARAJU AND N SNEEUW: Analysis of GRACE uncertainties by hydrological and hydro-meteorological observations. Journal of Geodynamics 59-60, pp 16-27, DOI 10.1016/j.jog.2012.02.001

ROESE-KOERNER L, B DEVARAJU, N SNEEUW AND W-D SCHUH: A stochastic framework for inequality constrained estimation. Journal of Geodesy 86, pp 1005-1018, DOI 10.1007/s00190-012-0560-9

VARGA P, F KRUMM, C DOGLIONI, E. GRAFAREND, GF PANZA, F RIGUZZI, AA SCHREIDER AND N SNEEUW: Did a change in tectonic regime occur between the Phanerozoic and earlier Epochs ? Rendiconti Lincei Scienze Fisoche e Naturali 23, pp 139-148, DOI 10.1007/s12210-012-0172-6

VARGA P, F KRUMM, F RIGUZZI, C DOGLIONI, B SÜLE, K WANG AND GF PANZA: Global pattern of earthquakes and seismic energy distributions: Insights for the mechanisms of plate tectonics. Tectonophysics 530-531, pp 80-86, DOI 10.1016/j.tecto.2011.10.014

WEIGELT M, N SNEEUW, E SCHRAMA AND P VISSER: An improved sampling rule for mapping geopotential functions of a planet from a near polar orbit. Journal of Geodesy (2012) online-first, DOI 10.1007/s00190-012-0585-0

Other Refereed Contributions

DEVARAJU B AND N SNEEUW: Performance Analysis of Isotropic Spherical Harmonic Spectral Windows. In: Sneeuw N, P Novák, M Crespi and F Sansò (Eds.): Proceedings VII Hotine-Marussi Symposium on Mathematical Geodesy, IAG Symposia 137, pp 105-110, Springer.

VII Hotine-Marussi Symposium, 6.-10.6.2009, Rome, Italy, DOI 10.1007/978-3-642-22078-4-16

GRAFAREND E: The MARUSSI Legacy: The Anholonomity Problem, Geodetic examples. In: Sneeuw N, P Novák, M Crespi and F Sansò (Eds.): Proceedings VII Hotine-Marussi Symposium on Mathematical Geodesy, IAG Symposia 137, pp 5-15, Springer. VII Hotine-Marussi Symposium, 6.-10.6.2009, Rome, Italy, DOI 10.1007/978-3-642-22078-4

IRAN POUR S AND N SNEEUW: Properties and Applications of EOF-Based Filtering of GRACE Solutions, In: Sneeuw N, P Novák, M Crespi and F Sansò (Eds.): Proceedings VII Hotine-Marussi Symposium on Mathematical Geodesy, IAG Symposia 137, pp 273-278, Springer. VII Hotine-Marussi Symposium, 6.-10.6.2009, Rome, Italy, DOI 10.1007/978-3-642-22078-4-41

REUBELT T, N SNEEUW AND E GRAFAREND: Comparison of kinematic orbit analysis methods for gravity field recovery. In: Sneeuw N, P Novák, M Crespi and F Sansò (Eds.): Proceedings VII Hotine-Marussi Symposium on Mathematical Geodesy, IAG Symposia 137, pp 259-265, Springer. VII Hotine-Marussi Symposium, 6.-10.6.2009, Rome, Italy, DOI 10.1007/978-3-642-22078-4_39

RIEGGER J AND M TOURIAN: Characterization of water storage dynamics in arid areas by satellite. In: Rausch R, C. Schüth and T. Himmelsbach (Eds.): Proceedings Conference „Hydrogeology of Arid Environments“, Hannover, Germany (14.-17.12.), ISBN 978-3-443-01070-6

ROTH M, O BAUR AND W KELLER: „Brute-force“ solution of large-scale systems of equations in a MPI-PBLAS-ScaLAPACK environment. In: Nagel WE, DB Kröner and MM Resch (Eds.): High Performance Computing in Science and Engineering ’11, Springer-Verlag Berlin Heidelberg, pp 581-594

SNEEUW N: Inclination Functions: Orthogonality and Other Properties, In: Sneeuw N, P Novák, M Crespi and F Sansò (Eds.): Proceedings VII Hotine Marussi Symposium on Mathematical Geodesy, IAG Symposium 137, pp 267-271, Springer. VII Hotine-Marussi Symposium, 6.-10.6.2009, Rome, Italy, DOI 10.1007/978-3-642-22078-4-40

TOURIAN M, N SNEEUW, J RIEGGER AND A BÁRDOSSY: A new method to derive river discharge from satellite altimetry (ENVISAT). Geoscience and Remote Sensing Symposium (IGARSS, 22.27.7.), IEEE Conference Publications 2012, pp 5250-5253, doi: 10.1109/IGARSS.2012.6352425

VISSER PNAM, EJO SCHRAMA, N SNEEUW AND M WEIGELT: Dependency of Resolvable Gravitational Spatial Resolution on Space-Borne Observation Techniques, In: Kenyon S, M Pacino and U Marti (Eds.): Geodesy for Planet Earth, IAG Symposium 136, pp 373-379, Springer Verlag. Geodesy for Planet Earth, 31.8.-4.9.2009, Buenos Aires, Argentina, DOI 10.1007/978-3-642-20338-1 45

WEIGELT M, W KELLER AND M ANTONI: On the comparison of radial base functions and single layer density representations in local gravity field modeling from simulated satellite observations. In: Sneeuw N, P Novák, M Crespi and F Sansò (Eds.): VII Hotine-Marussi Symposium on Mathematical Geodesy, Proceedings of the Symposium in Rome, 6.-10.6.2009, IAG Symposia, Vol.137, pp 199-204, Springer, DOI 10.1007/978-3-642-22078-4

Non-refereed Contributions

GRAFAREND E: Von A. Einstein über H. Weyl und E. Cartan zur Quanten-Gravitation. Sitzungsberichte der Leibniz-Sozietät der Wissenschaften 113, pp 13-21

Poster Presentations

CHEN Q, T VAN DAM, N SNEEUW, X COLLILIEUX AND P REBISCHUNG: Extracting seasonal signals from continuous GPS time series with modern statistical methods. EGU General Assembly, Vienna, Austria (22.-27.4.)

IRAN POUR S, T REUBELT, M ELLMER AND N SNEEUW: Quality assessment of sub-Nyquist recovery from future gravity satellite missions. EGU General Assembly, Vienna, Austria (22.-27.4.)

NOVÁK P, O BAUR, Z MARTINEC, N SNEEUW, D TSOULIS, B VERMEERSEN, W VAN DER WAL, M ROTH, J SEBERA, M VALKO AND E HOECK: Towards a better understanding of the Earth's interior and geophysical exploration research „GOCE-GDC". EGU General Assembly, Vienna, Austria (22.-27.4.)

REUBELT T, O BAUR, M WEIGELT AND N SNEEUW: On the capability of SWARM for estimating time-variable gravity fields and mass variations. International Symposium on Gravity, Geoid and Height Systems GGHS 2012, Venice, Italy, (9.-12.10.)

REUBELT T, O BAUR, M WEIGELT, M ROTH AND N SNEEUW: GOCE long-wavelength gravity field recovery from high-low satellite-to-satellite-tracking using the acceleration approach. EGU General Assembly, Vienna, Austria, (22.-27.4.)

ROTH M: Euler deconvolution in satellite geodesy. EGU General Assembly, Vienna, Austria (22.-27.4.)

ROTH M: GOCEXML2ASCII - an XML to ASCII converter for GOCE level 2 EGG_NOM and SST_PSO data. First International GOCE Solid Earth Workshop, Enschede, The Netherlands, (16.-17.10.)

ROTH M, N SNEEUW AND W KELLER: Euler deconvolution of GOCE gravity gradiometry data. The 15th Results and Review Workshop, HLRS Stuttgart, (10.-11.10.)

WEIGELT M AND W KELLER: Refinement of the differential gravimetry approach for future inter-satellite observations. EGU General Assembly, Vienna, Austria (22.-27.4.)

Conference Presentations

ANTONI M AND W KELLER: Local improvement of GRACE gravity field solutions using SO(3) representations. Joint American Mathematics Meeting, Boston (MA), (10.-14.1.)

CHEN Q AND N SNEEUW: GPS time series analysis with Monte-Carlo singular spectrum analysis. Geodätische Woche Hannover (9.-11.10.)

CHEN Q, T VAN DAM, N SNEEUW AND X COLLILIEUX: Separation of modulated seasonal signals from GPS time series with singular spectrum analysis. International Symposium on Space Geodesy and Earth System, Shanghai, China (18.-21.8.)

DEVARAJU B AND N SNEEUW: Anisotropic low-pass filters on the sphere: Design and performance analysis. Geodätische Woche Hannover (9.-11.10.)

DEVARAJU B AND N SNEEUW: Design and analysis of anisotropic low-pass filters on the sphere. EGU General Assembly, Vienna, Austria (22.-27.4.)

DEVARAJU B, C LORENZ, M TOURIAN AND N SNEEUW: Estimating hydrological mass changes from GRACE level-2 data: filtering and data assimilation. DFG SPP-1257 Workshop on GRACE hydrology, Bonn, Germany (13.-14.2.)

DEVARAJU B, C LORENZ, M TOURIAN AND N SNEEUW: Estimating runoff from the assimilation of GRACE data and hydro-meteorological models. International Symposium on Gravity, Geoid and Height Systems GGHS 2012, Venice, Italy (9.-12.10.)

DEVARAJU B, C LORENZ, M TOURIAN AND N SNEEUW: On the cyclo-stationarity of the time-variable Kaula rule. EGU General Assembly, Vienna, Austria (22.-27.4.)

DEVARAJU B, C LORENZ, M TOURIAN, J RIEGGER AND N SNEEUW: Estimating runoff from GRACE, hydrological data and hydro-meteorological models - a Kalman filtering approach. International Symposium on Gravity, Geoid and Height Systems GGHS 2012, Venice, Italy (9.-12.10.)

IRAN POUR S, T REUBELT AND N SNEEUW: How do the different satellite orbit configurations sample the gravity field? Geodätische Woche Hannover (9.-11.10.)

KELLER W: Wavelet compression of geodetic integral operators. EGU General Assembly, Vienna, Austria (22.-27.4.)

REUBELT T, O BAUR, M WEIGELT, M ROTH AND N SNEEUW: GOCE long-wavelength gravity field recovery from high-low satellite-to-satellite-tracking using the acceleration approach. International Symposium on Gravity, Geoid and Height Systems GGHS 2012, Venice, Italy (9.-12.10.)

RIEGGER J AND M TOURIAN: Characterization of water storage dynamics in arid areas by satellite gravimetry. Hydrogeology of Arid Environments, Hannover, Germany (14.-17.3)

SNEEUW N AND B DEVARAJU: Analysing the performance of linear low-pass spectral filters on the sphere. Geodätische Woche Hannover (9.-11.10.)

SNEEUW N, J MÜLLER, W FICHTER AND T REUBELT: Future Gravity Missions - Status Report. Final Seminar GEOTECHNOLOGIEN „Observation of the System Earth from Space III", Deutsches GeoForschungsZentrum, Helmholtz-Zentrum, Potsdam (24.5.)

SNEEUW N AND M TOURIAN: Application of altimetric and gravimetric space geodetic sensors to hydrology. Asia Oceania Geosceinces Society AOGS Joint Assembly, Singapore (13.-17.8.)

TOURIAN M, J RIEGGER AND N SNEEUW: Satellite altimetry for river discharge. DFG SPP-1257 Workshop on GRACE hydrology, Bonn, Germany (13.-14.2.)

TOURIAN M, N SNEEUW, J RIEGGER AND A BÁRDOSSY: A new method to derive river discharge from satellite altimetry (ENVISAT). International Geoscience and Remote Sensing Symposium IGARSS 2012, Munich, Germany (22.-27.7.)

WEIGELT M, A JÄGGI, L PRANGE, Q CHEN, W KELLER AND N SNEEUW: Time variability from high-low SST - filling the gap between GRACE and GFO. International Symposium on Gravity, Geoid and Height Systems GGHS 2012, Venice, Italy (9.-12.10.)

WEIGELT M, T VAN DAM, A JÄGGI, L PRANGE, N SNEEUW AND W KELLER: Large scale time variability from high-low SST - filling the gap between GRACE and GFO. GRACE Science Team Meeting GSTM 2012, Potsdam, Germany (16.-21.9.)

Books

GRAFAREND E AND J AWANGE: Applications of Linear and Nonlinear Models: Fixed Effects, Random Effects and Total Least Squares. 1016 pages, Springer, Berlin, Heidelberg, New York

SNEEUW N, P NOVÁK, M CRESPI AND F SANSÒ: VII Hotine-Marussi Symposium in Rome, 6.-10.6.2009, IAG Symposium 137 Proceedings of the Symposium in Rome, 407 pages, Springer, Berlin Heidelberg (2012), DOI 10.1007/978-3-642-22078-4

Guest Lectures and Lectures on special occasions

BOSCH W (Deutsches Geodätisches Forschungsinstitut, München): Höhenmessung aus dem Weltraum - wie die Geodäsie hilft, das System Erde zu verstehen (13.1.)

GHITAU D (Bucharest/Rumania): Evolution of Reference Coordinate Systems in Romania (2.8.)

SUBRAMANI S (Anna University Chennai, India): Exploratory analysis of catchment areas with GRACE data (12.7.)

VISHWAKARMA, BD (Roorkee/India): GRACE event calendar (10.5.)

ZHANG, S (Wuhan/China): GPS zero-difference ambiguity fixing for PPP (26.1.)

Lectures at other universities

KELLER W: Geostatistics in a Nutshell. Seminar series, Chen Jung University Tainan, Taiwan

SNEEUW N: Satellite Gravimetry and its Application in Earth Science, Shaanxi Province Society for Geodesy, Photogrammetry and Cartography, Xian, PR China (2.7.)

Research Stays

GRAFAREND E:
National Chung Kung University, Department of Geomatics, Tainan, Taiwan (13.-28.4.)
Finnish Geodetic Institute, Masala/Helsinki, Finland (15.8.-2.9.)

KELLER W
Landwirtschaftliche Universität Wroclaw, Poland (3.-17.10.)
Staatliche Chen Jung Universität Tainan, Taiwan (12.8.-25.9.)

Lecture Notes

(http://www.uni-stuttgart.de/gi/education/BSC/lecturenotes.en.html,
http://www.uni-stuttgart.de/gi/education/MSC/lecturenotes.en.html,
http://www.uni-stuttgart.de/gi/geoengine/lecturenotes.html)

GRAFAREND E AND F KRUMM
Kartenprojektionen (Map Projections), 238 pages

KELLER W
Foundations of Satellite Geodesy, 51 pages
Foundations of Satellite Geodesy (Viewgraphs), 281 pages
Observation Techniques in Satellite Geodesy, 211 pages

KRUMM F AND SNEEUW N
Adjustment Theory, 140 pages

KRUMM F
Map Projections and Geodetic Coordinate Systems, 172 pages
Mathematical Geodesy (Landesvermessung), 156 pages
Reference Systems (Referenzsysteme), 172 pages
Statistical Inference, 166 pages

SNEEUW N
Geodesy and Geoinformatics, Part Geodesy, 31 pages
History of Geodesy, 38 pages
Physical Geodesy (Measurement Techniques of Physical Geodesy, Modeling and Data Analysis in the Field of Physical Geodesy), 137 pages

WOLF D
Continuum Mechanics in Geophysics and Geodesy: Fundamental Principles, 100 pages

Participation in Conferences, Meetings and Workshops

IRAN POUR S

Final Seminar GEOTECHNOLOGIEN „Observation of the System Earth from Space III“, Deutsches GeoForschungsZentrum, Helmholtz-Zentrum Potsdam (24.5.)

Project meeting 6 of „Zukunftskonzepte für Schwerefeld-Satellitenmissionen“ (Geotechnologies - Observation of the System Earth from Space III), Albert Einstein Institute, Leibniz University, Hannover (29.2.-1.3.)

REUBELT T

Project meeting 6 of „Zukunftskonzepte für Schwerefeld-Satellitenmissionen“ (Geotechnologies - Observation of the System Earth from Space III), Albert Einstein Institute, Leibniz University, Hannover (29.2.-1.3.)

Final Seminar GEOTECHNOLOGIEN „Observation of the System Earth from Space III“, Deutsches GeoForschungsZentrum, Helmholtz-Zentrum Potsdam (24.5.)

EGU General Assembly, Vienna, Austria (22.-27.4.)

International IAG Symposium on Gravity, Geoid and Height Systems GGHS 2012, Venice, Italy (9.-12.10.)

ROTH M

GOCE GDC 1st Project Meeting, hosted at University of West Bohemia, Pilsen, Czech Republic (27.-28.2.)

EGU General Assembly, Wien, Austria (22.-27.4.)

The 15th Results and Review Workshop, HLRS, Stuttgart (10.-11.10.)

1st International GOCE Solid Earth Workshop, ESA, hosted at ITC, Enschede, The Netherlands (16.-17.10.)

Joint Science Meeting GOCE GeoExplore and GOCE GDC, hosted at ITC, Enschede, The Netherlands (18.10.)

Mid-term Meeting GOCE GDC, hosted at ITC, Enschede, Netherlands (19.10.)

SNEEUW N

SPP1257 Workshop, Bonn, Germany (13.2.)

European Geosciences Union (EGU), General Assembly 2012, Vienna, Austria (22.-27.4.)

Symposium „Dragon 2 Final Results and Dragon 3 Kick-Off“, Beijing, China (28.-29.6.)

AOGS Joint Assembly (Asia Oceania Geosciences Society), Singapore (13.-17.8.)

Abschlusskolloquium DFG-Schwerpunktprogramm „Massentransporte“, SPP1257 - GRACE Hydrology, Potsdam, Germany (17.-19.9.)

Sealevel-Symposium, Potsdam, Germany (20.9.)

Geodetic Week, Hannover, Germany (9.-11.10.)

GOCE Solid Earth Workshop, Enschede, Netherlands (16.-19.10.)

TOURIAN M

Abschlusskolloquium DFG-Schwerpunktprogramm „Massentransporte“, SPP1257 - GRACE Hydrology, Potsdam, Germany (17.-19.9.)

WEIGELT M

Workshop on Regional Gravity and Geomagnetic Field Modelling. Bavarian Academy of Sciences and Humanities, Munich, Germany (23.-24.2.)
European Geosciences Union (EGU), General Assembly 2012, Vienna, Austria (22.-27.4.)

University Service

Grafarend E

Member Faculty of Aerospace Engineering and Geodesy
Member Faculty of Civil- and Environmental Engineering
Member Faculty of Mathematics and Physics

KELLER W

Associate Dean (Academic) Geodäsie & Geoinformatik and GeoEngine, Stuttgart (since 14.11.)

ROTH M

Member/chairman of the PR-committee of the study course Geodesy & Geoinformatics

Sneeuw N

Associate Dean (Academic) Geodäsie & Geoinformatik and GeoEngine, Stuttgart (until 14.11.)
Stand-by Member Senate Committee for Structural Development and Research, Stuttgart
Vice-Chair Examining Board of the Faculty of Aerospace Engineering and Geodesy, Stuttgart (until 17.10.)

Professional Service (National)

GRAFAREND E

Emeritus Member German Geodetic Commission (DGK)

SNEEUW N

Search Committe Geodätische Erdsystemforschung, TU Dresden
Full Member Deutsche Geodätische Kommission (DGK)
Chair DGK section „Erdmessung“
Member Scientific Board of DGK
Member Scientific Advisory Committee of DGFI
Chair AK7 (Working Group 7), „Experimentelle, Angewandte und Theoretische Geodäsie“, within DVW (Gesellschaft für Geodäsie, GeoInformation und LandManagement)

Professional Service (International)

GRAFAREND E

Elected Member of the Finnish Academy of Sciences and Letters, Finland
Elected Member of the Hungarian Academy of Sciences, Hungary
Member Royal Astronomical Society, Great Britain
Corresponding Member Österreichische Geodätische Kommission (ÖGK)
Member Flat Earth Society
Elected Member Leibniz-Sozietät, Berlin
Fellow International Association of Geodesy (IAG)

SNEEUW N

Member Editorial board of Studia Geophysica et Geodaetica
Member Editorial board of Journal of Geodesy and Geoinformation
Präsident IAG InterCommission Committee on Theory (ICCT)
Member of IAG GGOS Working Group Satellite Missions
Fellow International Association of Geodesy (IAG)

WEIGELT M

Chair of the study group JSG0.6: Applicability of current GRACE solution strategies to the next generation of inter-satellite range observations, (InterCommission Committee on Theory, IAG)
Member of study group JSG0.3: Methodology of Regional Gravity Field Modeling (Inter-Commission Committee on Theory, IAG)
Member InterCommission Working Group (IC-WG2): „Evaluation of Global Earth Gravity Models“ (IAG)

Courses - Lecture/Lab/Seminar

Adjustment I, II (Krumm, Roth)	4/2/0
Advanced Mathematics (Keller, Weigelt)	3/2/0
Analytic Orbit Computation of Artificial Satellites (Sneeuw, Reubel)	2/1/0
Dynamic Satellite Geodesy (Keller)	1/1/0
Foundations of Satellite Geodesy (Keller)	1/1/0
Geodesy and Geoinformatics (Sneeuw)	1/1/0
Geodetic Reference Systems (ICRS-ITRS) for Satellite Geodesy and Aerospace (Weigelt)	2/1/0
Geodetic Seminar II (Krumm, Sneeuw)	0/0/2
Gravity Field Modelling (Keller)	2/1/0
Integrated Field Work Geodesy and Geoinformatics (Keller, Sneeuw)	10 days
Map Projections and Geodetic Coordinate Systems (Krumm, Roth)	2/1/0
Mathematical Geodesy(Krumm, Roth)	2/2/0
Modelling and Data Analysis in the Field of Physical Geodesy (Engels, Reubelt)	2/1/0

Observation Techniques and Evaluation Procedures of Satellite Geodes (Keller, Weigelt)	1/1/0
Official Surveying and Real Estate Regulation (Schönherr)	2/0/0
Orbit Deteremination and Analysis of Artificial Satellites (Sneuww, Reubelt)	2/1/0
Physical Geodesy (Sneeuw, Reubelt)	4/3/0
Real-Estate/Property Valuation II (Haug)	1/1/0
Property Valuation (Bolenz)	2/0/0
Reference Systems (Krumm, Roth)	2/2/0
Satellite Geodesy Observation Techniques (Weigelt)	1/1/0
Satellite Geodesy (Keller)	3/2/0
Statistical Inference (Krumm, Roth)	2/1/0

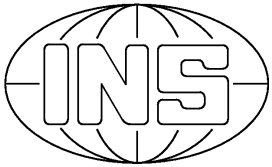

Institute of Navigation

Breitscheidstrasse 2, D-70174 Stuttgart,
Tel.: +49 711 685 83400, Fax: +49 711 685 82755
e-mail: ins@nav.uni-stuttgart.de
homepage: http://www.nav.uni-stuttgart.de

Head of Institute

Prof. Dr.-Ing. A. K l e u s b e r g

Deputy: Dr.-Ing. Aloysius W e h r
Secretary: Helga M e h r b r o d t
Emeritus: Prof. em. Dr.-Ing. Ph. H a r t l

Staff

Dipl.-Ing. Doris B e c k e r	Navigation Systems
Dipl.-Ing. Michael G ä b	Navigation Systems
Dipl.-Geogr. Thomas Gauger	GIS Modelling and Mapping
Dipl.-Ing. René P a s t e r n a k	Remote Sensing
Dipl.-Ing. Bernhardt S c h ä f e r	Navigation Systems
M. Sc. Hendy S u h a n d r i	Navigation Systems
Dipl.-Ing. (FH) Martin T h o m a s	Laser Systems
Dr.-Ing. Aloysius W e h r	Laser Systems
Dr. Ing. Franziska W i l d - P f e i f f e r	Navigation Systems

EDP and Networking

Regine S c h l o t h a n

Laboratory and Technical Shop (ZLW)

Dr.-Ing. Aloysius W e h r (Head of ZLW)
Technician Peter S e l i g - E d e r
Electrician Sebastian S c h n e i d e r
Mechanician Master Michael P f e i f f e r

External teaching staff

Hon. Prof. Dr.-Ing. Volker L i e b i g - Directorate ESA
Hon. Prof. Dr.-Ing. B r a u n - RST Raumfahrt Systemtechnik AG, St.Gallen

Research Projects

3D-Pilot

The 3D-Pilot is a device comprised of a position and orientation system (POS), a display and sophisticated software which should support pilots of small and medium sized airplanes in general- and business aviation during approach and landing on airports not equipped with a ground-based instrument approach system, e.g. instrument landing system (ILS). The device should be designed so that it can be mounted by the pilot in the cockpit like the navigation system in a car. This 3D-landing aid will display the pilot the instantaneous orientation and position and the optimum flight path. A key element of this landing aid is the POS which has been developed and realized by INS: It is built-up with a μblox-GPS/EGNOS receiver, an inertial measurement unit (IMU) in MEMS technology which comprises three axis digital accelerometers and three axis digital gyroscopes, and a software Kalman filter which is run in the central unit, a PC compatible computer board (s. Figure 1). A first flight test with the Diamond DA-40-V1 airplane of the Institut für Luftfahrtsysteme (s. Figure 2) as a carrier was carried out in the year 2012. A typical flight trajectory measured by the 3D-pilot is shown in Figure 3. Further flight tests will be performed in 2013 to optimize the Kalman filter parameters.

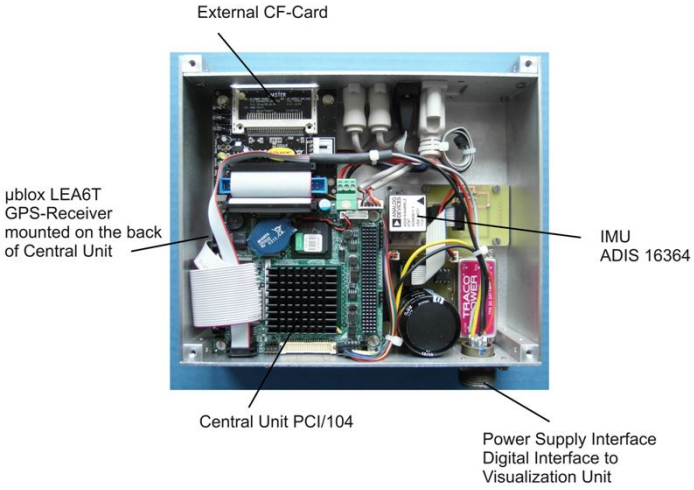

Figure 1: Hardware of the 3D-Pilot

Figure 2: Airplane used for Flight Tests

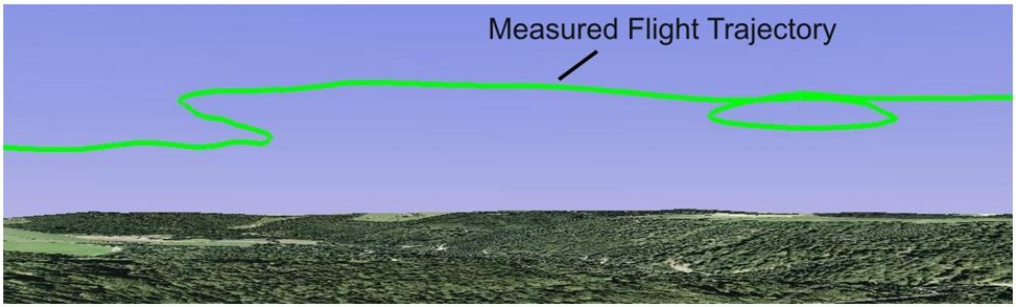

Figure 3: Flight Trajectory measured by 3D-Pilot

Development of GPS-Transponders using CDMA-Signals for the ICARUS initiative

The initiative „International Cooperation for Animal Research Using Space“ (ICARUS) has the objective to study globally the migration behavior of animals by using GNSS and radio measurement technology in combination with digital coding schemes. Using advanced digital electronic components extreme small transceivers will be developed, which will be fixed on animals e.g. birds. The signals of the transceiver will be received by the International Space Station (ISS), which distributed the gathered information to ground stations. The transceivers mounted on the animals will be equipped with a GNSS receiver and a transmitter which transmits the stored and the actual positions since the last contact with the ISS. This transceiver is called TAG. Due to the small size of the TAG the available transmitting power is limited and very efficient coding schemes are required to assure a robust data link to the ISS.

By order of the Max Planck Institute for Ornithology the INS developed TAGs to study CDMA-Coding schemes and carried out field tests to demonstrate the feasibility and the possibility of multiple access. The TAGs comprises a GPS-receiver and transmitter, which transmits the instantaneous position with a 433 MHz carrier modulated with a spread spectrum signal. The PN-coded spread spectrum signal is generated by an FPGA. Therefore, different CDMA-Codes can be tested by programming the FPGA. Figure 1 shows the TAG. First tests with the TAGs were performed on the vicinity of the campus (Figure 2) and in Stuttgart (Figure 3). In Figure 2 a Hertzian dipole was applied in the receiver. Figure 4 shows that a stable link was established over a range of 1.7 km (s. Figure 3) having a transmitting power of 4 dBm and using a Yagi receiving antenna with 9 dBi gain.

As the TAGs were built for feasibility test and were realized with commercially available FPGA evaluation boards, the size of the TAGs is too big for birds. However, the used electronic components have only a mass of less than 6 g without power supply and can be housed in a box of less than a cubic centimeter. A smaller TAG version including energy harvesting techniques will be developed as soon as the studies concerning the optimum broadcasting technique will be completed.

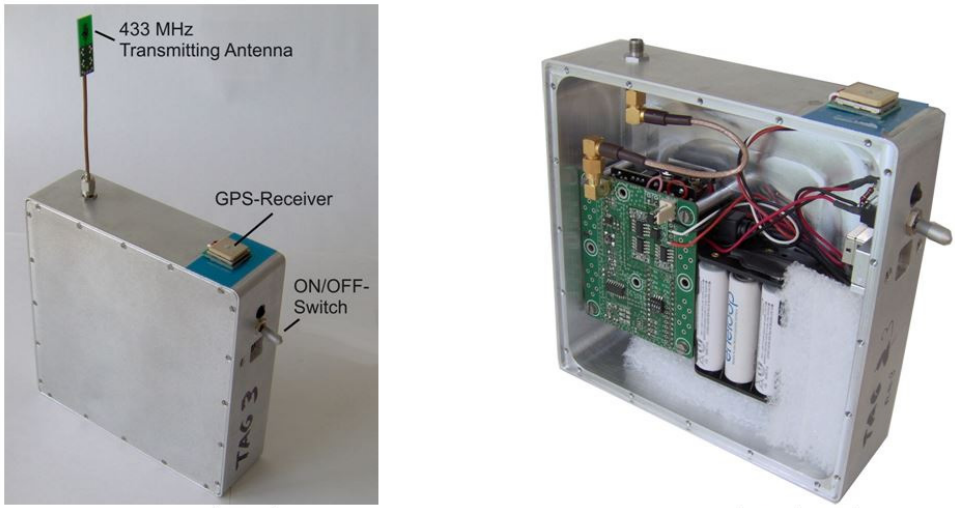

Figure 1: TAG

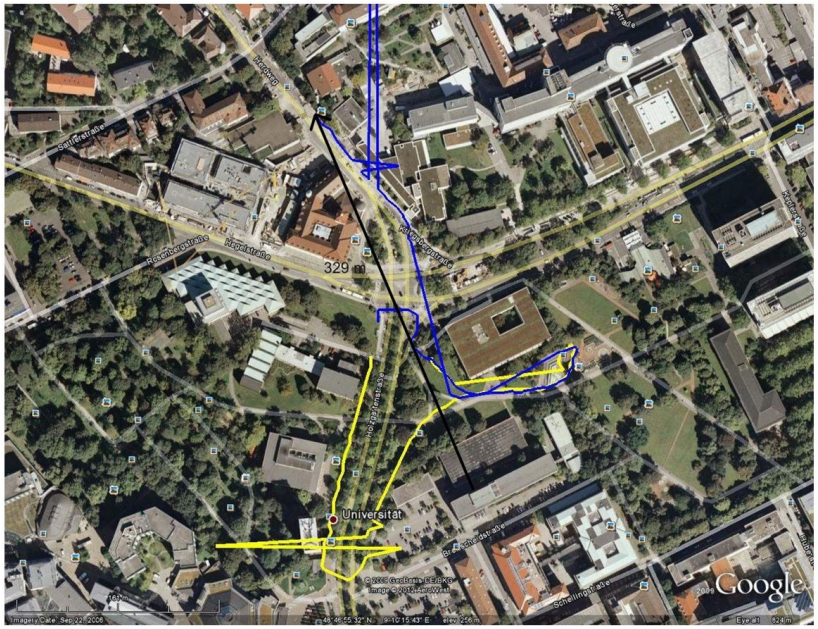

Figure 2: Field test with two TAGs moving around (maximum range 320 m)

Figure 3: Established data link (range 1,7 km)

Evaluation of inertial sensor range for their body mounted usage

Two products of the company Xsens were reviewed for their usability for pedestrian navigation with body mounted inertial sensors, namely MT9-B-28A23G95 and MTi-G-28A53G35. With the sensor ranges of their accelerometers and gyroscopes stated in the documentation they are not immediately the first choice for such high dynamic applications, but experiments promise that they perform different than specified. For the experiment both devices were attached to each other, so their x-axes were parallel and their y- and z-axes were antiparallel respectively. Both devices were then moved by hand, which can cause inertial observations in the same range as for foot-mounted devices. The synchronized turn rate measurements from the x-axis gyroscopes are exemplary visualized in Fig. 1 with the specified maximum range indicated by dashed horizontal lines at $\pm$300 deg/s for the MTi-G and at $\pm$900 deg/s for the MT9-B respectively. The true maximum sensor range for the MTi-G in the experiment was $\pm$400 deg/s and for the MT9-B it was approximately $\pm$1450 deg/s. This result concludes to not use the MTi-G for pedestrian navigation, because the turn rates will be easily out of the sensor range and the orientation cannot determined correctly. The true sensor range leads to a different sensor resolution for the MTi-G of 0.012 deg/s/LSB compared to 0.009 deg/s/LSB calculated from the values in the datasheet. Therefore another inertial sensor will be used for pedestrian navigation, which meets the requirements in terms of sensor range. The MPU6xxx series from Invensense offers up to $\pm$2000 deg/s and $\pm$18g. Fig. 2 shows a prototype configuration incorporating the MPU6050 on a soldered protoboard. This setup will be further developed in terms of size and firmware handling the data retrieval.

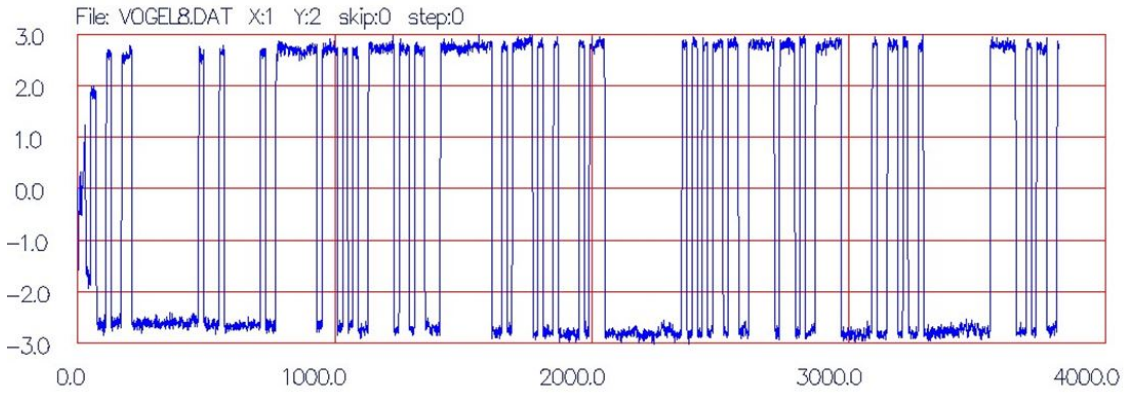

Figure 4: Received data signal

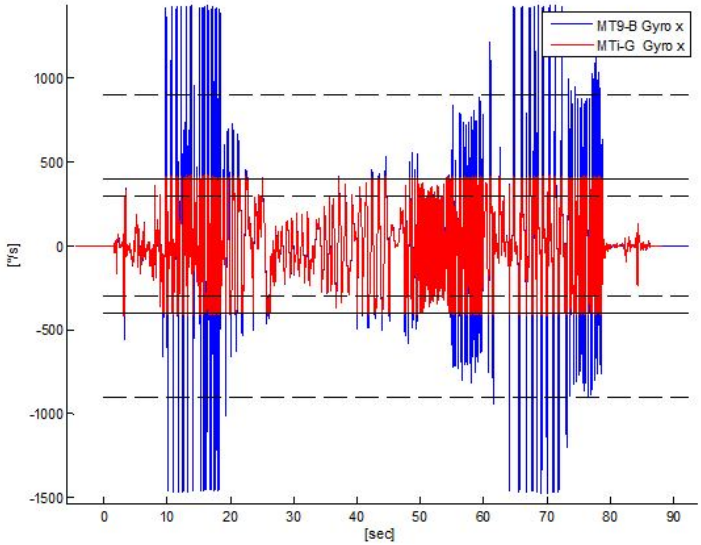

Figure 1: Synchronized turn rate measurements of MTi-G and MT9-B.

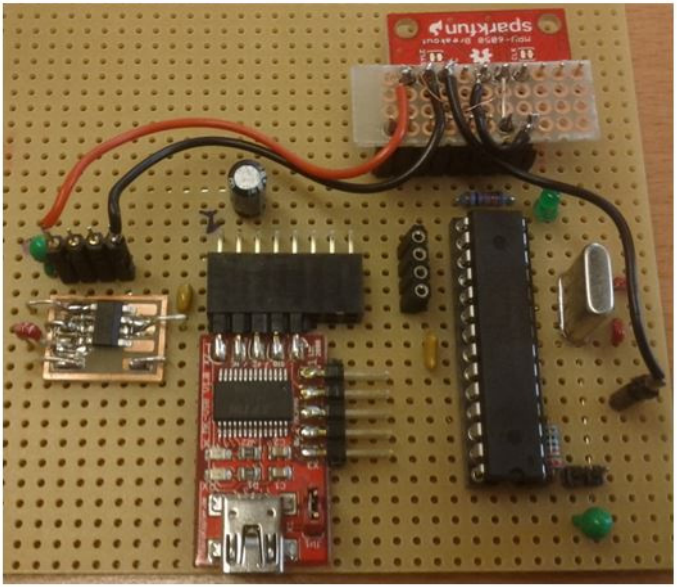

Figure 2: Prototype configuration incorporating MPU6050 on a protoboard.

Development of Software GNSS Receiver

The software GNSS receiver is based on a low-cost L1-frequency patch antenna, a low-cost front-end and a powerful notebook. An overview of these components is shown in Figure 1.

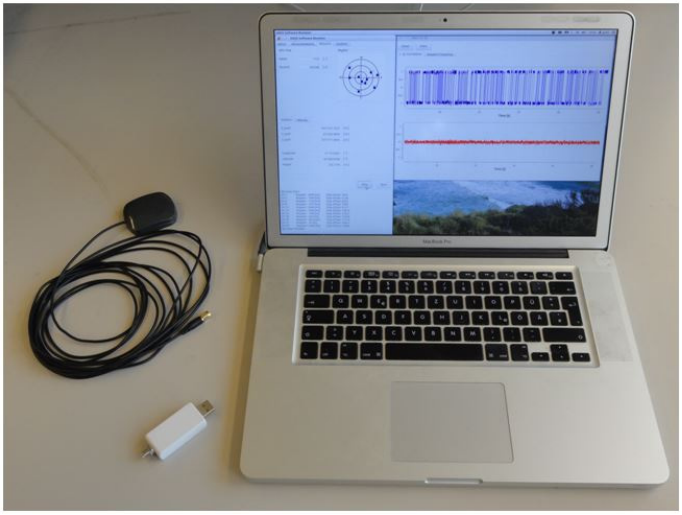

Figure 1: Software GNSS Receiver

The front end converses down the received GNSS signals on L1-Frequency to an intermediate frequency and digitalizes it. An example of real obtained samples is shown in Figure 2 and its power spectrum is shown in Figure 3.

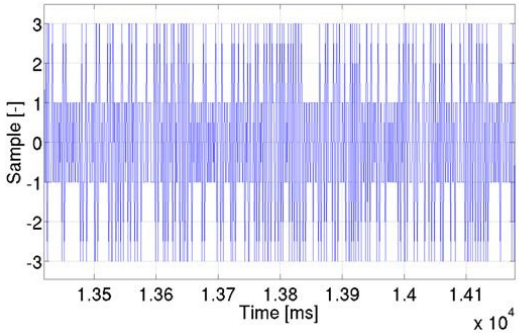

Figure 2: Samples from Front End

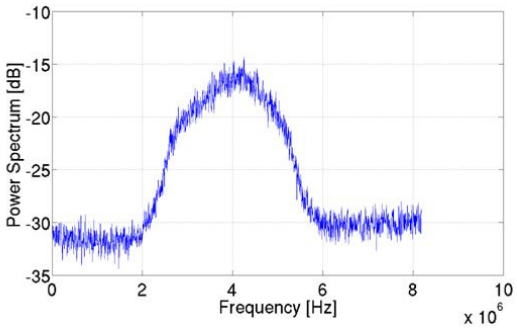

Figure 3: Power Spectrum of Samples

The intermediate frequency of the down converted signal is 4.096 MHz and the sampling frequency is 16.368 MHz. Each sample has a resolution of 3 bits (-3, -1, +1, +3). The power spectrum shows the intern filter bandwidth of 2.5 MHz and a peak by ≈4.096 MHz. This curve is slightly moved because the Doppler shift in each received signal.

The completely signal processing is realized with software and is based on the civil GPS C/A-Code. The software is written with c/c++ and runs in Linux operating system because of the high effort of calculation. All algorithms for signal processing and calculation of the position are based on the official documentation IS-GPS 200F and Kai Borre (2007). A user interface of the software is shown in Figure 4.

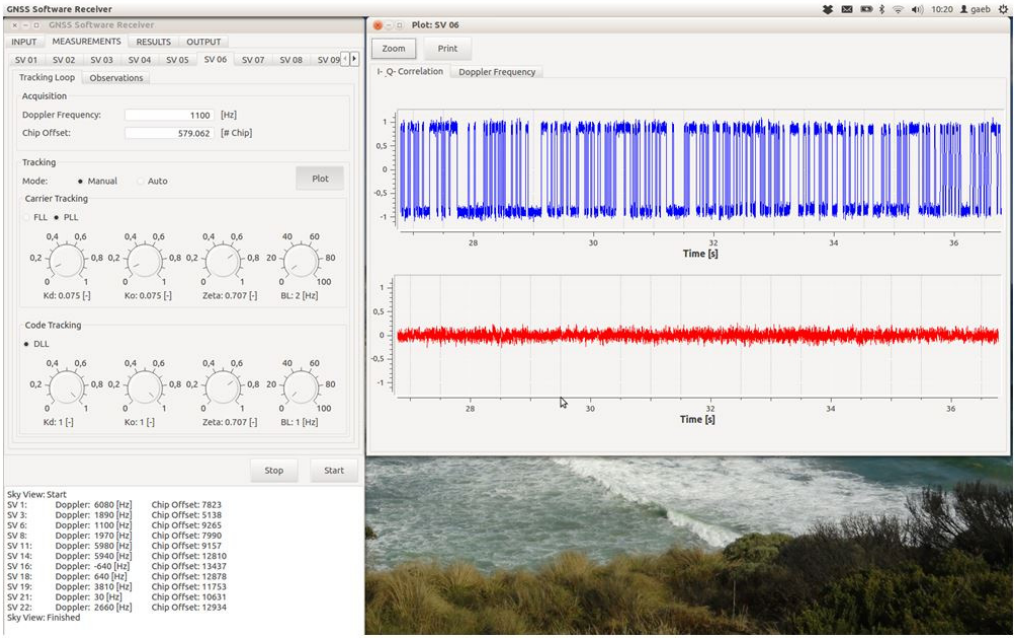

Figure 4: User Interface of the Software

For analysis purposes of the tracking properties controllers were implemented. The controllers can change the parameters of the tracking loop during the running process. The calculation of position and velocity is calculated with a frequency of 1 KHz. At the moment the research focuses are finding the optimal loop parameter by dynamic application and optimizing the algorithms.

Kai Borre (2007); „A Software-Defined GPS and GALILEO Receiver, A Single-Frequency Approach“ Birkhäuser 2007

Data sets of Nitrogen Deposition at Forest Plots in the Free State of Saxony Derived from Modelled Data for 2004 to 2007

On behalf and on the account of the Free State of Saxony, the results of the research project „Assessment, Prognosis, and Review of Deposition Loads and Effects in Germany“ (BMU/UBA FE-No 3707 64 200), finalised in 2011, are compiled for forest ecosystem stands in Saxony. The modelled data of the previous BMU/UBA modelling and mapping project are of interest for the federate states of Germany, because these data are supporting EU and national regulations on air pollution control and emission abatement (EU NEC directive, BImSchG, TA-Luft), which have to be implemented on the sub-national level. Moreover scientific interest is supported by these data, e.g. when setting up flux assessment studies for certain ecosystems.

Within the project national maps of deposition loads are used to derive forest ecosystem specific nitrogen deposition fluxes at the locations of interest for forest soil survey studies in the Free State of Saxony (see Figure 1). The resulting data are as well delivered as data base for further calculation, and as graphical representation (maps).

From data of modelled high resolution maps of different deposition fluxes nitrogen loads for several forest stands are calculated using GIS technique. The dose, in terms of deposition loads of air pollutants causing acidification and eutrophication efffects in forest ecosystems can be compared to ecosystem sensitivity given as modelled critical loads in order to provide an impact assessment for these ecosystems of interest. The trend of air pollutant input over time into the respective receptors on the regional, and local scale can be identified.

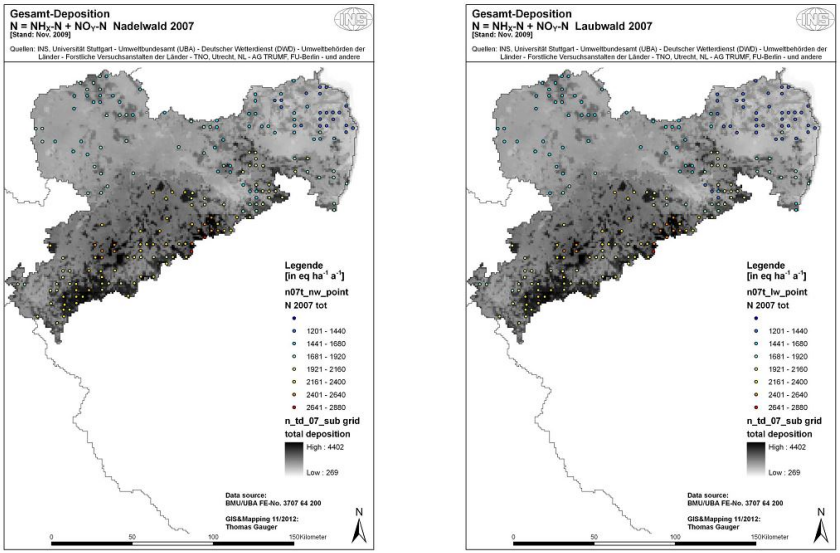

Fig. 1: Total deposition of nitrogen at coniferous and deciduous forest plots in Saxony 2007

Publications and Presentations:

SCHÄFER, B.: „Exchange semester in Brazil - A retrospective view“; Mayer, M.; Krueger, C. P.; Heck, B. (eds.): Highly Precise Positioning and Height Determination using GPS: Results of a PROBRAL project by Universidade Federal do Paraná (UFPR, Curitiba, Brazil) and Karlsruhe Institut für Technologie (KIT, Karlsruhe, Germany). (KIT Scientific Reports; 7604), KIT Scientific Publishing, Karlsruhe, 2012, S 75-78

MIRALIAKBARI, A.; SCHÄFER, B.; HAHN, M.: „A brief Note on a GPS-aided IMU Drive through Stuttgart“; Behr, F.-J.; Rahman, A. A.; Zimmermann, M.; Pradeepkumar, A. P. (eds.): Geoinformation - Catalyst for planning, development and good governance. Applied Geoinformatics for Society and Environment, Vol. 1 (2012), Karlsruhe, Germany, pp. 17-24, ISBN 978-3-943321-06-7

PETER, M.; FRITSCH, D.; SCHÄFER, B.; KLEUSBERG, A.; BITSCH LINK, J. A.; WEHRLE, K.: „Versatile Geo-referenced Maps for Indoor Navigation of Pedestrians“; 2012 INTERNATIONAL CONFERENCE ON INDOOR POSITIONING AND INDOOR NAVIGATION, 13-15TH NOVEMBER 2012, Sydney, Australia

SCHÄFER, B.; MIRALIAKBARI, A.; HAHN, M.: „Vergleich von geschätzten und gerechneten Genauigkeiten verschiedener INS Systeme“, Poster, Geodätische Woche 2012, 09.-11.10.2012, Hannover

Janák, J., Wild-Pfeiffer, F., Heck, B.: „Smoothing the gradiometric observations using different topographic-isostatic models: A regional case study“, In: Sneeuw, N., Novák, P., Crespi, M., Sansò, F. (eds.): VII Hotine-Marussi Symposium on Mathematical Geodesy, Rome, 6 - 10 July, 2009, Vol. 137 (2012), Springer-Verlag, S. 245-250.

Knöpfler, A, Mayer, M., Wild-Pfeiffer, F.: „Brazilian experiences - An insight into German perceptions“, In: Mayer, M; Krueger C.P.; Heck, B. (Hrsg.): Highly Precise Positioning and Height Determination using GPS - Results of a PROBRAL project by Universidade Federal do Paraná (UFPR, Curitiba, Brazil) and Karlsruhe Institut für Technologie (KIT, Karlsruhe, Germany), Karlsruhe Institute of Technology, KIT Scientific Reports 7604, 67-73.

M. Wikelski, Ph. Hartl und A. Wehr: „Tiere auf Wanderschaft“, Biotelemetrie; Thema: Mobilität, Akademie Aktuell, Heft 3 - Ausg. Nr. 42, pp. 18-21, Herausg. Bayrische Akademie der Wissenschaften, 2012.

Study Thesis

Carmona, Juan: „Evaluation of a low cost and a survey grade Integrated Navigation System“; Diplomarbeit, Institute of Navigation; University of Stuttgart; Feb 2012; (Schäfer).

Oware, Stephen: „ Comparison and Evaluation of Civil GPS Signals“; Master Thesis, Institute of Navigation; University of Stuttgart; Aug 2012; (Schäfer).

Lu, Y.: „Orientierungsbestimmung mit Xsens MT9“ (Xue, Wild-Pfeiffer)

Cheng, P.: „Untersuchung der Rauscheigenschaften von low-cost MEMS Sensoren“ (Xue, Wild-Pfeiffer)

Zhang, J.: „Skalierung bei MEMS-Sensoren“ (Wild-Pfeiffer)

Participation in Conferences, Meetings and Workshops:

Wild-Pfeiffer, F.
Gyro Symposium, Karlsruhe, 18.-19.09.2012
Intergeo, Hannover, 09.-11.10.2012

Schäfer B.:
UPINLBS 2012 Helsinki
Geodetic Week 2012 Hannover
IPIN 2012 Sydney

Guest Lectures

Bitsch Link, J.A. (Communication and Distributed Systems, RWTH Aachen): „Wikipedia für Karten und Navigation - OpenStreetMap“, 07.02.2012.

Weidner, U. (Institute of Photogrammetry and Remote Sensing, Karlsruhe Institute of Remote Sensing): „Hyperspectral Remote Sensing“, 09.05.2012.

Activities in National and International Organizations

Alfred Kleusberg
Fellow of the International Association of the Geodesy
Member of the Institute of Navigation (U.S.)
Member of the Royal Institute of Navigation
Member of the German Institute of Navigation

Education (Lecture / Practice / Training / Seminar)

Introduction of Geodesy and Geoinformatic (BSc) (Kleusberg, Schäfer)	2/2/0/0
Electronics and Electrical Engineering (Wehr)	2/1/0/0
Satellite Measurement Engineering (Wehr)	2/1/0/0
Parameter Estimation in Dynamic Systems (Kleusberg)	2/1/0/0
Navigation I (Kleusberg, Gäb)	2/2/0/0
Inertial Navigation (Kleusberg,Schäfer)	2/2/0/0
Remote Sensing I (Wild-Pfeiffer, Pasternak)	2/2/0/0

Remote Sensing I (BSc) (Wild-Pfeiffer, Pasternak)	2/1/0/0
Remote Sensing II (Wild-Pfeiffer, Pasternak)	1/1/0/0
Satellite Programs in Remote Sensing, Communication and Navigation I (Liebig)	2/0/0/0
Satellite Programs in Remote Sensing, Communication and Navigation II (Liebig)	2/0/0/0
Radar Measurement Methods I (Braun)	2/0/0/0
Radar Measurement Methods II (Braun)	2/1/0/0
Dynamic System Estimation (Kleusberg, Suhandri)	2/1/0/0
Integrated Positioning and Navigation (Kleusberg, Suhandri)	2/1/0/0
Satellite Navigation (Kleusberg, Suhandri)	2/1/0/0
Interplanetary Trajectories (Becker)	1/1/0/0
Geodetic Seminar I, II (Fritsch, Sneeuw, Keller, Kleusberg, Möhlenbrink)	0/0/0/4
Integrated Fieldwork (Schäfer) (SS 2012)	

Institute for Photogrammetry

Geschwister-Scholl-Str. 24D, D-70174 Stuttgart
Tel.: +49 711 685 83386, Fax: +49 711 685 83297
e-mail: firstname.secondname@ifp.uni-stuttgart.de
url: http://www.ifp.uni-stuttgart.de

Head of Institute

Director: Prof. Dr.-Ing. Dieter Fritsch
Deputy: apl. Prof. Dr.-Ing. Norbert Haala
Personal Assistant: Martina Kroma

Emeritus Professor: Prof. i.R. Dr. mult. Fritz Ackermann

Research Groups at the ifp:

Geoinformatics

Chair: Prof. Dr.-Ing. Dieter Fritsch	
Deputy: Dr.-Ing. Volker Walter	GIS and Remote Sensing
Dr.-Ing. Susanne Becker	Point Cloud Interpretation and Hybrid GIS

Photogrammetry and Computer Vision

Chair: Prof. Dr.-Ing. Dieter Fritsch	
Deputy: Dr.-Ing. Michael Cramer	Digital Airborne Sensors
Dipl.-Ing. Alessandro Cefalu	Photogrammetric Calibration and Object Recognition
Dipl.-Ing.(FH) Markus Englich	Sensor Laboratory
M.Sc. Eng. Ali Mohammed Khosravani	Indoor Modeling and Positioning
M.Sc. Eng. Wassim Moussa	Sensor Fusion
M.Sc. Eng. Mohammed Othman	Image Orientation
Dipl.-Ing. Michael Peter	Indoor Positioning
M.Sc. Eng. Rongfu Tang	Bundle Block Adjustment Extension
Dipl.-Ing. Konrad Wenzel	Dense Image Matching in Close Range Applications

Photogrammetric Image Processing

Chair: apl. Prof. Dr.-Ing. Norbert Haala	
Dipl.-Ing. Mathias Rothermel	Semi-Global Matching

External Teaching Staff

Dipl.-Ing. Stefan Dvorak, Amt für Stadtentwicklung und Vermessung, Reutlingen
Dipl.-Ing. Sabine Urbanke, Landesvermessungsamt Baden-Württemberg

Research Projects

Geoinformatics

Results of the EuroSDR Survey: 3D Data Management in European National Mapping and Cadastral Agencies

In the last years, substantial technological progress in managing 3D geospatial data could be observed. New technologies for the collection of 3D data (in particular airborne and terrestrial laser scanning) as well as an increasing performance of CPUs and GPUs allow for 3D data collection and processing on standard PCs. However, 3D Geographical Information Systems (GIS) are often not fully capable to meet the requirements of managing 3D data. One problem is that 3D data management and 3D analysis are in a state where 2D GIS was 10 to 15 years ago. The other problem is that in many cases no integrated IMAP (Input, Management, Analysis and Presentation) solutions are available, but different software systems are needed to process 3D data.

In order to investigate this situation in more detail and to find solutions for the future, we conducted on behalf of EuroSDR a survey to identify the state-of-the-art of 3D data management, the future requirements as well as existing problems. The EuroSDR (European Spatial Data Research Network) is a non-profit organisation linking national mapping and cadastral agencies (NMCAs) with research institutes and universities for the purpose of applied research in spatial data provision, management and delivery. Our main target group of this survey were NMCAs. However, we decided to open the survey also to other public and private institutions in order to get a full overview of the situation. We are very pleased that 32 institutions all over Europe participated in this survey.

The questionnaire consisted of two parts. The first part contained fourteen questions about the market and the state-of-art of 3D data management. These questions could be answered by selecting one or more predefined answers. Optionally it was possible to add free-text for additional information or comments. The second part provided six general questions about 3D data management. These questions could be answered with free-text.

A total of 32 institutions have participated in the survey, most of them (25) are public institutions. Those public institutions can be subdivided into: National Mapping and Cadastral Agencies (10), Regional Mapping and Cadastral Agencies (8) and City Surveying Offices (7).

The following list summarizes the main important results of this study:

- The evaluation of the answers showed, that the participants have very different views about the definition of a 3D GIS. The three definitions with the highest consensus are *A 3D GIS can handle 2D and 3D spatial data* (87.5%), *A 3D GIS must provide functionalities for the interactive input/modelling of new 3D data* (81.3%) and *A 3D GIS must provide functionalities for the interactive editing of already collected 3D data* (78.1%). The three definitions with the lowest consensus are *A 3D GIS can handle only 3D spatial data* (6.3%), *A 3D GIS should be one single software system* (18.8%) and *The realisation and implementation of a 3D GIS must be independent from the application* (34.4%).
- It is expected that 3D GIS will be an important key technology in the near future. Most of the participants think that 3D GIS has the potential to become a key technology (84.4%). No one of the participants believes that 3D GIS will never be a key technology, but 21.9% have the opinion that 3D GIS is already a key technology. Some participants selected both *3D GIS is already a key technology* and *3D GIS has the potential to become a key technology*. Therefore, the sum of both answers is higher than 100%.
- The participants expect that the 3D geospatial market will grow in the next years. *Hardware* is the market segment with the lowest growth expectations. However, no more than 3.1% of the participants think that this market segment will shrink and only 6.3% think that it will stagnate. All others expect that this market segment will grow. The market segment *Software* is seen by most of the participants as medium growing. No one of the participants expect that this segment will shrink. The segments *Data and Services* are seen as strong segments: 34.4% of the participants think that these segments will grow fast in the future.
- The main customers of 3D geospatial data are currently public institutions (96.9%). Private companies represent at the moment only a small market segment, but it is expected that this segment will grow in the future. Private persons are at the moment and presumably in the near future not an important clientele.
- The application areas of 3D geospatial data are manifold. Nearly all areas, where 2D geospatial data are used, are also potentially working areas of 3D geospatial data. The simple reason for that is, that our world is three-dimensional and therefore people want to work with three-dimensional representations.
- Even though, only 32 institutions participated in this study, 40 different software systems are used. The software market for processing 3D geospatial data is at the moment very heterogeneous. Different software products are in use and very often one specific product is only used by one or two institutions. This leads to problems, because the different systems are often not interoperable. The same situation holds true for the standardisation of 3D geospatial data: 26 different 3D data standards are used by the participants.
- Most of the participants have difficulties to process 3D geospatial data. The existing tools and algorithms are not yet matured and powerful enough. The programs are difficult to understand and can be used by experts only.

Modeling concepts for consistency analyses of heterogeneous and multiply represented 3D geodata

In a dynamic world, where the steadily increasing demand for up-to-date geodata drives the continuous acquisition of 3D data, appropriate systems for managing and analyzing the resulting data become more and more important. Efficient solutions for handling multiple representations and data heterogeneity are of special significance. The concept we developed for the integrated management of heterogeneous and multiply represented geodata is hybrid with respect to data given in different data models, dimensions and quality levels. Through the combination of various object representations to one „feature“ and the definition of „hybrid identities“ the pure geometric modeling is enriched by information on semantic entities, i.e., knowledge about the relations between different object representations is introduced. Based on the example of a multiply represented 2D line object illustrated in Figure 1a, Figure 1b-d demonstrates a small selection of the many possibilities to define hybrid identities. Such explicitly modeled knowledge about geometric correspondences provides the basis for consistency analyses.

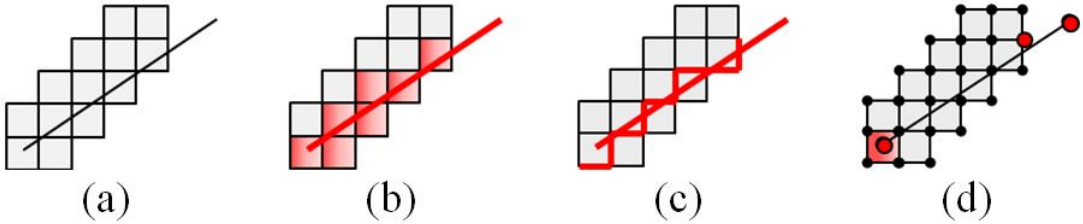

Figure 1: Possibilities to define hybrid identities for a multiply represented 2D line object.

Integrated in our hybrid data model, consistency can now be evaluated and quantified even for highly heterogeneous object representations that stem from different data models and have different dimensions and quality levels. The traditional understanding of consistency as the lack of contradiction within a single data set or between two structurally homogeneous data sets consequently has to be extended to a so-called „hybrid consistency“. The definition of the term „hybrid consistency“ is closely related to our hybrid data model and directly refers to the modeling concepts proposed for multiple representations and hybrid identities. Thus, it is possible to determine the degree of hybrid consistency between different object representations which describe the same real world object either entirely or partially. These can be data sets showing real world objects of the same type as for example two partially overlapping street networks from different providers. Beyond this, the object representations can also show different object types, e.g. an indoor model of a building on the one hand whose entrance is connected to a street network on the other hand. In both cases, the determination of hybrid consistency is restricted to those entities which are represented in both data descriptions.

The basis for evaluating hybrid consistency for partially overlapping or adjacent object representations is given by the possibility to explicitly model geometric correspondences as hybrid identities.

As an example for partially overlapping data sets, we extend the geometric configurations illustrated in Figure 1 to a scenario of two different network representations. As indicated in Figure 2 by the geometries highlighted in red (bold), data sets may be connected through more than one hybrid identity. One possibility to get an overall consistency value is to compute a weighted mean out of the consistency values determined for all individual hybrid identities. The weight of a hybrid identity either can be estimated from the accuracy of the geometries involved or may result from the ratio of the spatial extension of its geometries compared to the spatial extension of the geometries of all other hybrid identities.

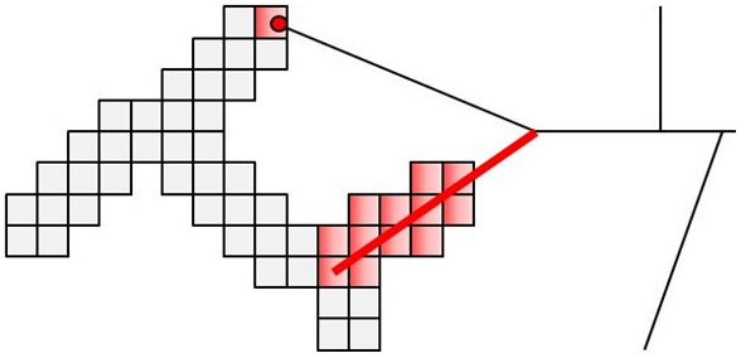

Figure 2: Consistency analysis for partially overlapping object representations.

Photogrammetry and Computer Vision

Reconstruction and Refinement of Building Interiors

In the past year, our previously presented approach for the automatic reconstruction of building interiors by means of analyzing photographed evacuation plans has been extended in two different ways. Firstly, the approach was generalized in order to enable the analysis of plans with an arbitrary layout. Secondly, the possibility of the refinement of the derived coarse indoor models employing user position traces and user interaction was investigated.

While in the previous approach, working on the well-known layout of our institute building's plans, we used cross-correlation template matching in order to detect symbols. The generalization of the approach to arbitrary plan layouts relies on the colors found in evacuation plans. Thus, after binarizing the image, we use color segmentation for the detection of the most common signal colors which represent the sought-after symbol areas, which will be removed from the binary image. In order to distinguish rooms from stairs, detect door openings and to deliver the final model in metric coordinates, the transformation parameters between image coordinates and world coordinates have to be computed by matching the floor plan's outer contour to an available external

model (e.g. from OpenStreetMap). Due to the differences concerning scale and level-of-detail, this matching step is carried out on a generalized version of both polygons. Starting from the symbol areas which previously occluded parts of the image, the final 2D model is derived in a completion and vectorization step. A 2.5D model can be inferred using an approximate room height computed using the number of detected stairs in the model.

For the refinement of the coarse models, the user's initial position and orientation are extracted from the same photograph and are put to use in a foot-mounted MEMS IMU positioning approach. By analyzing the user tracks derived employing this positioning approach in the context of the coarse model, they may not only be corrected by map-matching, but also the possibility of a fully automated derivation of door positions has been shown. Additionally, the user's positions may be used to geo-reference semantic information collected by user interaction. As an example, we have investigated the derivation of room numbers and people assigned to a room from photographed door plates using Optical Character Recognition (OCR).

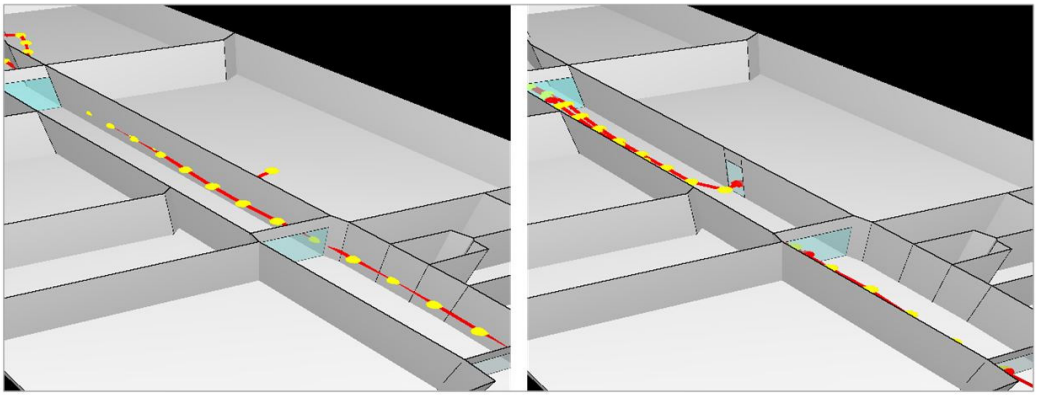

Figure 3: Coarse model derived from evacuation plan before (left) and after automated door reconstruction using tracks from foot-mounted MEMS IMU positioning (corrected by map-matching, right).

Image based 3D surface reconstruction in close range applications

Dense image matching methods enable efficient 3D data acquisition. Digital cameras are available at high resolution, high geometric and radiometric quality and high image repetition rate. They can be used to collect imagery for photogrammetric purposes in short time. Accuracy and resolution can be chosen freely with the selection of the camera and the image stations.

Photogrammetric image processing methods today deliver 3D information automatically. For example, *Structure from Motion* reconstruction methods can be used to derive orientations and sparse surface information. In order to retrieve complete surfaces with high density, *dense image matching methods* can be applied subsequently.

Figure 4: Depth estimation by dense image matching for a church tower in Rottenburg/Neckar, Germany. An unmanned aerial vehicle (UAS) was used to acquire multiple views of the façade. Left: image, right: point cloud from dense image matching with depth coded coloring.

At the Institute for Photogrammetry, software for dense image matching using a modified Semi-Global Matching [Heiko Hirschmüller, DLR, 2005] algorithm was implemented. The modification of the *Semi-Global Matching* stereo method enables processing of imagery with large depth variations on common computers at short processing time. Furthermore, the stereo method was embedded into a *Multi-Stereo-Framework* that is capable of processing complex image networks. The resulting redundancy due to multiple depth estimations for each pixel is used for outlier rejection and noise reduction.

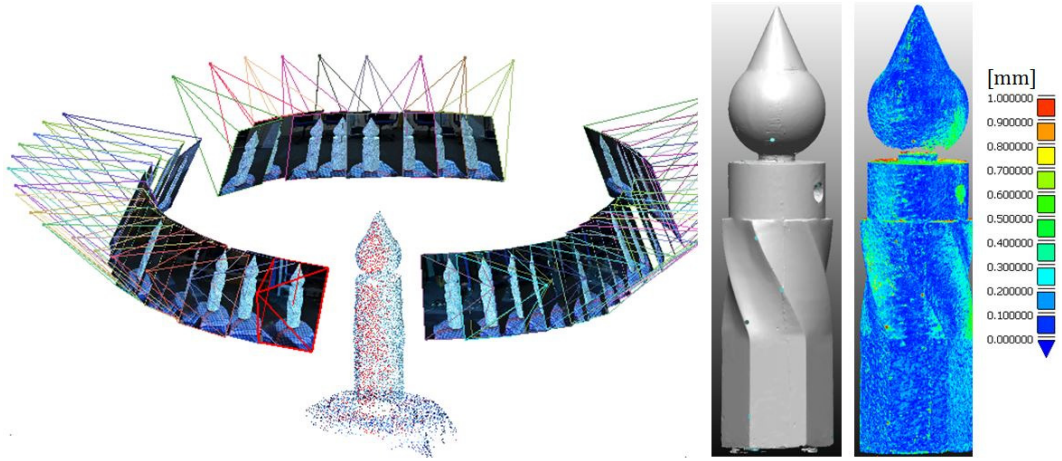

Figure 5: Automatic image based surface reconstruction for a test object. The 35cm high test object „Testy“, developed by Martin Misgaiski and Ralf Reulke from the HU Berlin, has been captured with a Nikon D7000 DSLR camera.

At the Institute for Photogrammetry two solutions for dense image matching were developed. While one was particular used for aerial imagery (developed by Mathias Rothermel), the other was used for close range applications (developed by Konrad Wenzel). In fall 2012, both solutions reached the required flexibility to process both kinds of imagery. Thus, a joint development of a solution has been started, which is called *SURE*, for photogrammetric SUrface REcontruction.

Several applications of using dense surface reconstruction have been investigated. For example, images have been acquired for the test object „Testy“, as shown in Figure 5. Since the object is white and free of texture, 3 video projectors have been used to ensure artificial texture for automatic image registration and dense surface reconstruction. The 48 images were automatically oriented using the software *VisualSFM*. The resulting orientations were used within the dense surface reconstruction step with the ifp software *SURE*. The resulting surface was compared to a reference acquired with a structured light system with 10μm precision, by using the *Iterative Closest Point* algorithm for registration. The standard deviation to the reference amounted to 0.2mm.

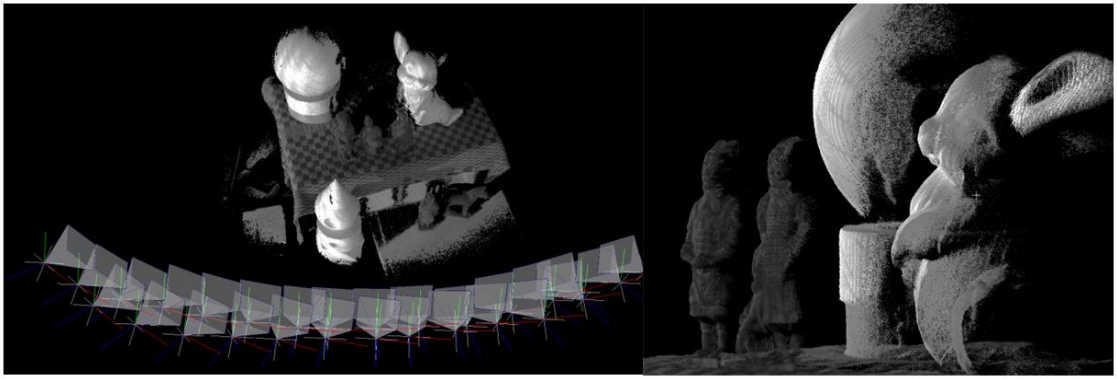

Figure 6: Dense surface reconstruction from images of a multi-camera rig using artificially projected texture. The sphere has a diameter of 15cm.

Reconstruction of the St. Martin Dome-tower

As an initial step most cultural heritage preservation actions include a documentation of the current state of the object of interest. In case of façade restoration actions, standard surveying methods are usually chosen to observe the façade's geometric appearance. Enough points need to be measured to allow a mapping of each single stone and other details important for the restoration task. From these measurements 2D CAD drawings are derived, which again enable civil or structural engineers and architects to map damages, plan corresponding counter measures and estimate costs.

Photogrammetry provides fast on-site acquisition. When used in a highly automated manner, incorporating techniques as structure-from-motion and dense image matching, it can provide results comparable to laser scanning to a much lower price of hardware. Our institute promotes the introduction of modern image processing strategies into the branch of heritage preservation through practical application of internal and external developments. Within the presented project, which aims at the restoration of the facades of the tower of the St. Martin dome in Rottenburg am Neckar, we took over the task of status-quo-documentation.

Figure 7: Left: View at the dome from a market square west of the dome; Right: The octocopter capturing images of the south façade.

For better object coverage an octocopter was used to capture the imagery. Unfortunately, disadvantageous wind conditions and a defect rotor caused it to crash after a short time. Due to time limits, the rest of the imagery was collected terrestrially and combined with laser scans.

The imagery was oriented by means of structure-from-motion using our internal implementation and cross-checked with the free software VisualSFM. The results were passed to our dense image matching framework, resulting in a large amount of point cloud data. These were co-registered with the laser scanning point clouds and further processed into orthographic projections of the facades. From these, 2D CAD drawings were derived in a last step.

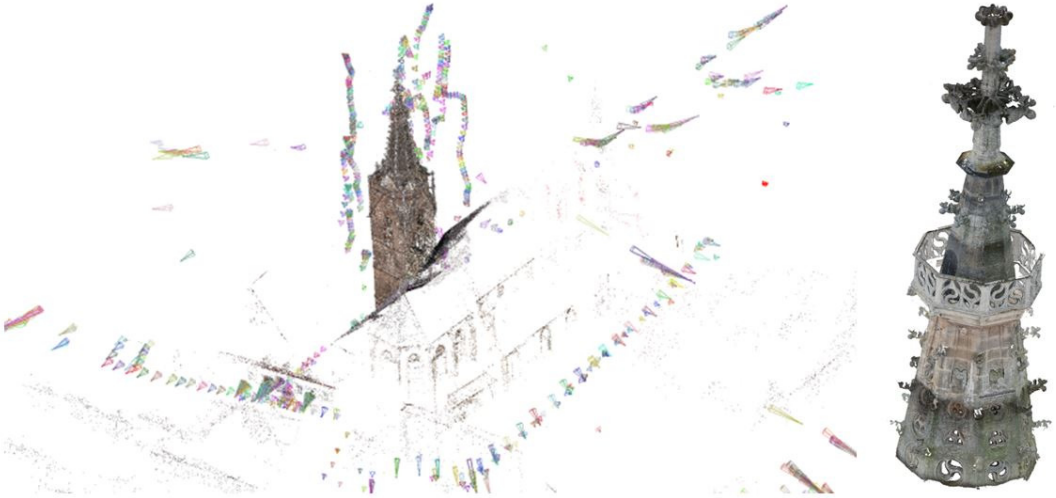

Figure 8: Left: Sparse point cloud and camera stations after structure-from-motion (VisualSFM output); Right: Dense point cloud derived for the uppermost part of the tower.

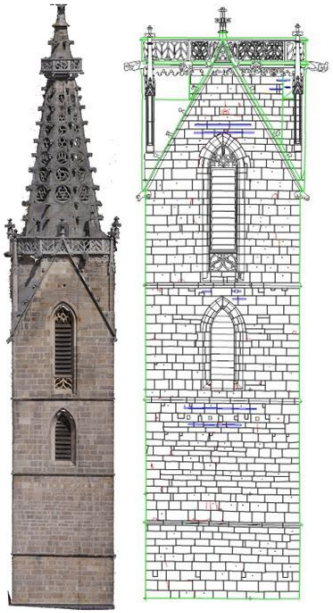

Figure 9: Left: Orthographic projection of the southern façade's point cloud; Right: Corresponding CAD drawing.

Co-Registration of Kinect Point Clouds Based on Image and Object Space Observations

The Kinect system is a RGB-D sensor that collects RGB images along with per-pixel depth information. We evaluated two approaches for the alignment of the Kinect point clouds, based on image and object space observations. In the first approach, sensor poses are incrementally estimated using Structure from Motion methods and bundle adjustment, based on image features extracted and matched in the corresponding RGB images. In the second approach, the range data are used within the software KinectFusion, which estimates surfaces by volumetric range image integration and determines the sensor pose by the Iterative Closest Point algorithm (ICP). The accuracy of the pose estimation using the first method highly depends on the distribution of enough visual features, whereas the second method relies on the existence of enough geometrical information. Therefore, a combination of the two methods is going to be implemented in future.

The Kinect pose estimation enabled an efficient solution for the acquisition of accurate and high density point clouds. In this application, the Kinect sensor pose is used in combination with two additional cameras in order to retrieve high density point clouds by means of dense image matching. Figure 10 shows the system configuration.

The sensor system consists of two high resolution monochrome CCD cameras (5 Megapixels) for the dense image matching and a Kinect for providing artificial texture by the speckle pattern and tracking the sensor pose by the KinectFusion. Therefore, it enables data acquisition and image matching in low light conditions or for featureless objects.

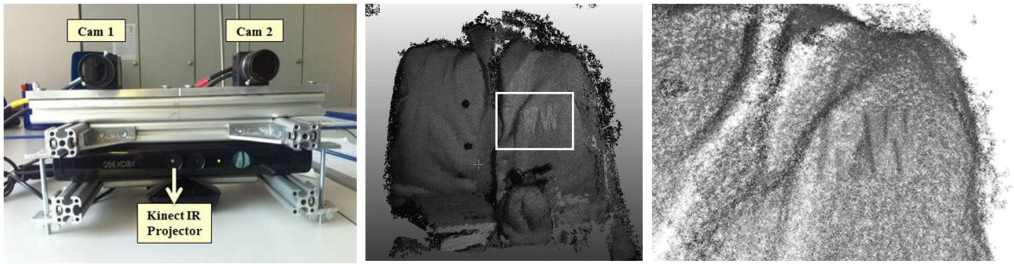

Figure 10: System configuration and results.

Automatic Fusion of Digital Images and Laser Scanner

Automatic procedures for combining digital images and laser scanner data serve photogrammetric close range applications such as 3D digital preservation and documentation of cultural heritages by generating comprehensive virtual reality models. Our method is based on a bundle block adjustment for the orientation estimation of generated images from laser data and camera images by means of an optimized Structure from Motion (SfM) reconstruction method. This results in having target-free registration of multiple laser scans and absolute image orientations. The proposed

pipeline was tested on a real case study and experimental results are shown to demonstrate the effectiveness of the presented approach.

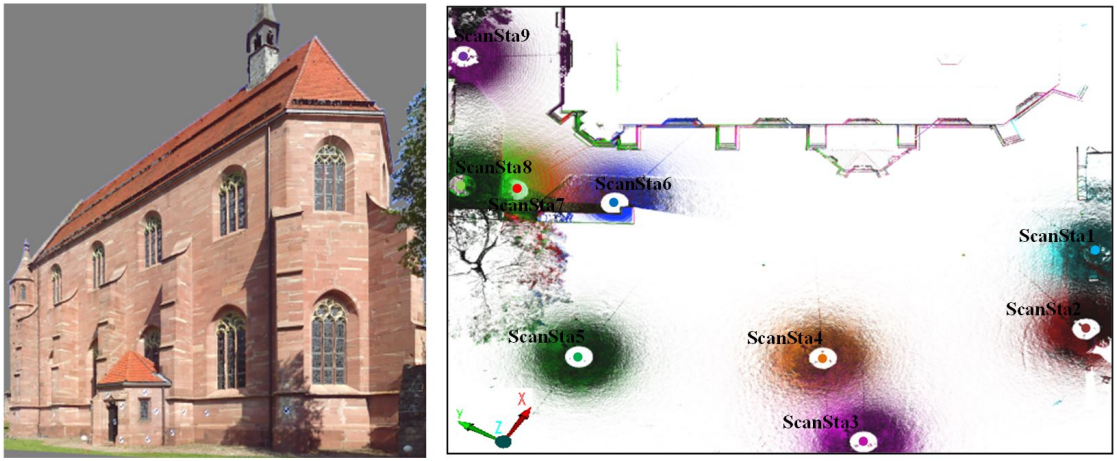

Figure 11: Left: A generated RGB image from laser scan Nr. 2. Right: Overview of the aligned scans, with all 9 TLS stations, depicted in different colors in order to show its corresponding scan coverage area.

The developed procedure was applied to the dataset of the Lady Chapel of the Hirsau Abbey ruins, which was acquired using the Faro Focus^{3D} with 9 scans; see Figure 11 right. The angular resolution selected for the dataset in both the horizontal and the vertical directions is a quarter of the full resolution given by the scanner manufacturer (at approximate point distance 6 mm/10m). A generated image from laser data is shown in Figure 11 left. It was processed based on 97 camera images in one bundle block adjustment after calculating the initial orientation values by our SfM approach. The results are shown in Figure 12 left with an accuracy (root mean square error of the reprojection error) less than one pixel. It can be seen, that the sparse point cloud delivered by the imagery fits correctly to the laser point cloud.

After the estimation of the transformation parameters, the absolute orientations of the camera images are known. These orientations can be used as input for dense image matching algorithms. This results in reconstructing a geo-referenced dense image point cloud, which is directly aligned together with the laser scanner data to form a complete detailed representation of the scene. Figure 13 depicts that the dense image point cloud fits correctly to the laser point cloud because of the accurate images alignment to laser scaner data. Moreover, gaps resulted from the weak reflectivity of the window's material (glass) in the laser point cloud are filled better by the dense matching approch.

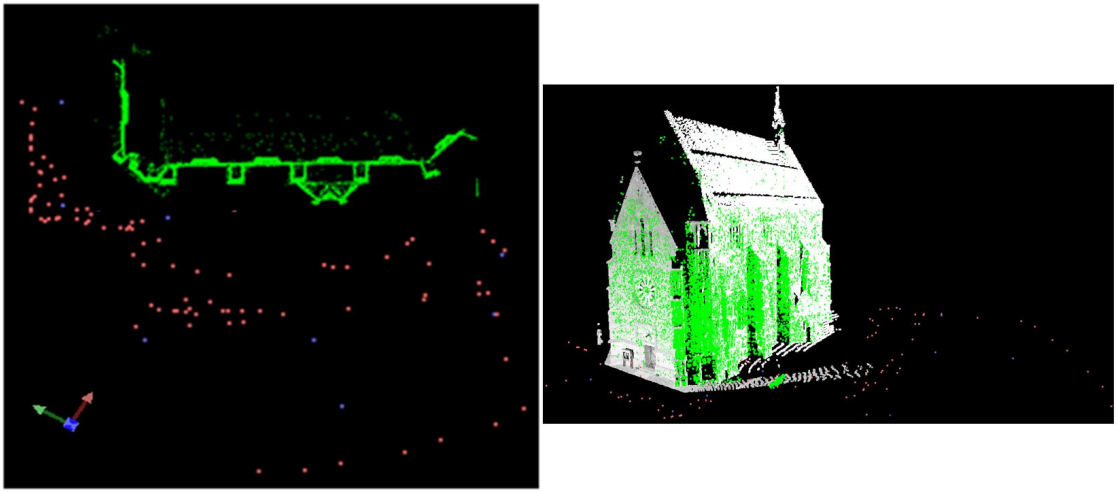

Figure 12: SfM output. Left: an ortho view of sparse point cloud (green), 97 camera positions (red dots), 9 laser scanner stations (blue dots). Right: sfm output aligned automatically in one coordinate system with laser point clouds from two scan stations (Nr. 2 and 9).

Mathematical methods for camera self-calibration in photogrammetry

Camera self-calibration is an essential topic in photogrammetry. In aerial photogrammetry, many self-calibration additional parameters (APs) are used increasingly without evident mathematical or physical foundations, and they may be highly correlated with other correction parameters. We point out that photogrammetric self-calibration (or building photogrammetric self-calibration models) can - to a large extent - be considered as a *function approximation* problem in mathematics. The unknown function of distortion can be approximated by a linear combination of specific mathematical basis functions.

After examining a number of mathematical basis functions, the Fourier series are suggested to be the theoretically optimal basis functions to build the self-calibration model in photogrammetry. A family of Fourier self-calibration model is developed, whose mathematical foundations are the Laplace's equation and the Fourier theorem. By considering the advantages and disvantages of the physical and the mathematical self-calibration models, it is recommended that the Fourier model should be combined with the radial distortion parameters in many calibration applications. This combination can find applications in calibrating airborne as well as close range cameras.

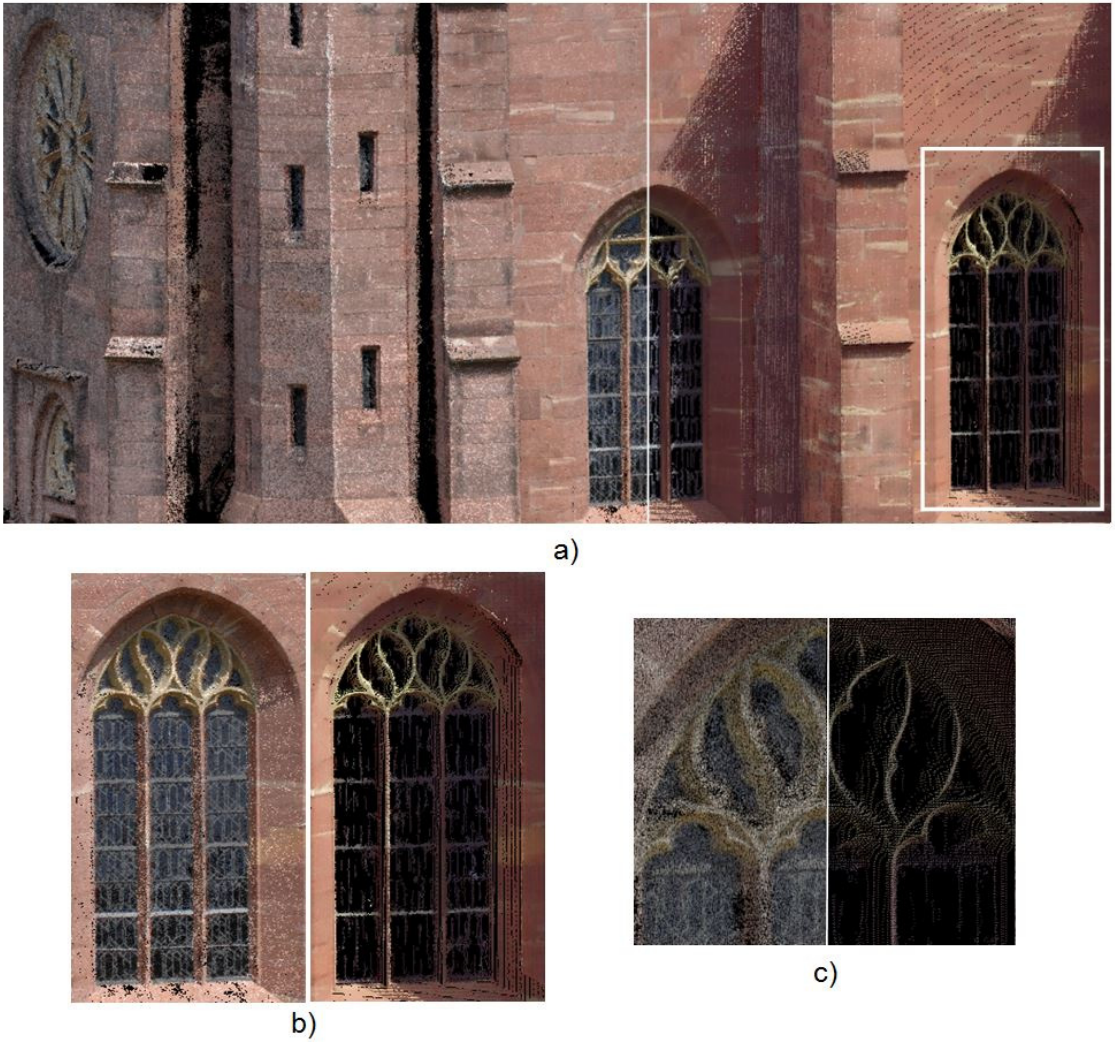

Figure 13: The Lady Chapel dataset: (a) Point cloud derived by dense image matching from direct registered imagery (left) and laser scanner point clouds from 6 scans with resolution of 7 mm/10m (right). (b) A close-up view for a window area depicted in (a), in image point cloud and laser point cloud respectively. (c) A detailed view for the window's decoration in image point cloud and laser point cloud respectively.

A number of simulation and empirical tests were performed on the new self-calibration models. The airborne camera tests demonstrate, that the Fourier self-calibration model is rigorous, flexible, generic and effecitive to calibrate the distortion of digital frame airbonre cameras of large-, medium- and small-formats, mounted in single- and multi-head systems (including the DMC, DMC II, UltraCamX, UltraCamXp, DigiCAM cameras and so on). The advantages of the Fourier model are that they usually need fewer APs and obtain more reliable distortion calibration.

An example which is illustrated in Figure 14 shows the advantages of the Fourier model in calibrating a DMC airborne camera in different block configurations.

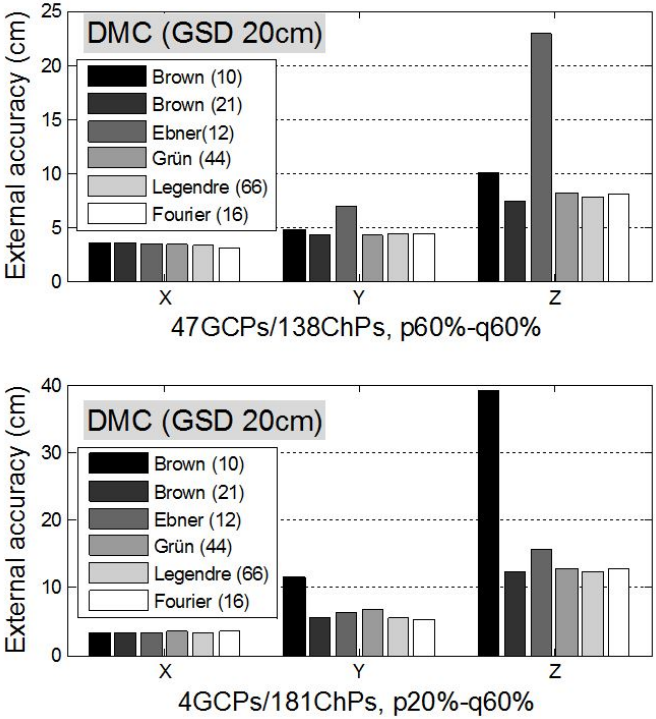

Figure 14: Accuracy comparisons of different APs in the DMC (GSD 20 cm) block of two scenarios: the in-situ calibration (above) and the operational project (below).

Photogrammetric Image Processing

Image based 3D surface reconstruction for UAS Imagery

UASs are establishing as serious alternative for traditional photogrammetric data capture. Since these systems can be completely built-up at very reasonable prices, photogrammetric data collection can be very cost effective. This is especially true while aiming at large scale aerial mapping of areas at limited extent. In principle, the photogrammetric evaluation of UAS-based imagery is feasible by off-the-shelf commercial software products. Thus, standard steps like aerial triangulation, the generation of Digital Surface Models and orthoimage computation can be performed effectively. However, this processing pipeline can be hindered due to the limited quality of UAS data. This is especially true if low-cost sensor components are applied.

Tools for DSM generation by automatic stereo image matching are available for more than two decades. However, the revival of image based 3D data collection was triggered only recently due to important hardware and software developments. One example is the success of algorithms like the Semi-Global Matching (SGM) stereo method. This approach, used for our investigations on dense multiple stereo matching of highly overlapping UAS imagery approximates a global approach by minimizing matching costs, which are aggregated along a certain number of 1D path directions through the image. By these means, the pixel-wise SGM approach provides a dense point distribution, while the global approximation on paths enables a reasonable runtime on large imagery. The potential of the SGM algorithm was already demonstrated for different applications and data sets. This was our motivation to implement and use SGM for dense image matching, which already provided a considerable improvement compared to standard commercial tools while using standard aerial imagery. These investigations also showed the benefits of combining multiple image information during surface reconstruction and 3D point cloud generation.

Beside the worse signal-to-noise ratio of the sensors used for UAS data collection, block configurations are rather unstructured (Figure 16). This is a result of the sensitivity of UAS platforms with respect to wind. Moreover, the comparable low image scale in combination with undulating terrain results in non-rectangular footprints. For the dense image matching process suitable sets of stereo pairs have to be selected. This selection is mainly based on the overlaps of the images. In order to determine the actual overlaps an additional pre-processing step was implemented. All images were downscaled and a first DSM based on rough overlap information was calculated. Using this low-resolution imagery assures small processing effort. Based on this rough DSM the actual overlaps were determined and final image pairs incorporated in the matching process were selected. If low-cost consumer grade cameras are used, the signal-to-noise-ratio is rather low. In that case the disparity estimations are comparably noisy. Therefore an efficient algorithm for outlier detection was implemented in which redundantly estimated surface points were checked for geometric consistency.

Figure 15: Pilot starting the UAS platform.

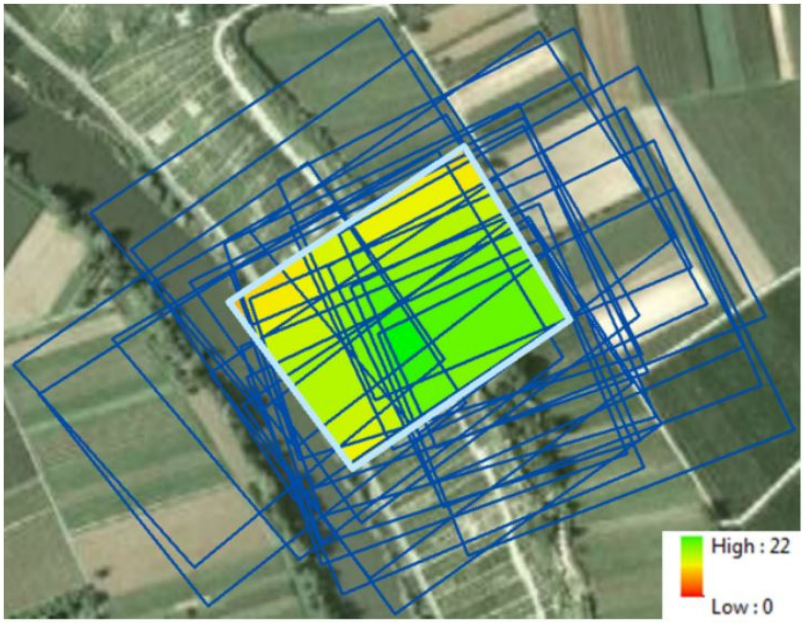

Figure 16: Footprints of exemplary UAS images. The central (coloured) image is matched against up to 22 neighbouring images.

In a last step consistent surface points derived by the single stereo models were fused. The resulting point cloud for the reconstructed surface is shown in Figure 17; the overall processing time was below 20 hours. Precision evaluations of points located in plain surface patches resulted in standard deviations of around 2cm. In our investigations, our implementation of SGM proved to be a robust and easy-to-parameterize matching algorithm. Matching accuracies better than 0.2 pixels at high point densities were feasible even for areas with very little texture. The combination of multiple measurements in triangulation increases the accuracy of the generated 3D point clouds. Even more important, the redundancy available from the combination of stereo matches from different image pairs allows a very efficient elimination of erroneous matches and results in a considerable reliability of the 3D points at vertical accuracies in the centimetre level. Thus, even for aerial imagery of comparatively limited quality a high quality surface reconstruction is feasible. This is especially beneficial for UAS imagery, which is frequently captured using consumer grade digital cameras, but can be collected at high resolutions and large overlaps.

Figure 17: Top view on reconstructed surface points.

Using UAS in National Mapping - the Hessigheim Project

As already mentioned, the unmanned airborne systems (UAS) technology - now often named remotely piloted aircraft systems (RPAS), to illustrate, that there still is a (remote) pilot involved - has matured and is now getting into practice. This became obvious visiting fairs like the Intergeo 2012 or others. For sure, there are not only private companies looking into this technology, also national mapping agencies are interested in this type of geo-data acquisition.

In the year 2012 we started a project together with the Landesamt für Geoinformation und Landentwicklung Baden-Württemberg (LGL), the national mapping agency (NMA) of Baden-Württemberg. Within this project the performance of UAS for the mapping of small areas was evaluated. The LGL here served as a pilot user for all the other national mapping agencies in the federal states of Germany. The goal was to get the 3D surface model and orthophoto of a (quite steep) vineyard area, located at the Neckar River, around 25 km north of Stuttgart. It is the so-called „Hessigheimer Felsengärten“ that have been flown, as the LGL did a land consolidation (Flurbereinigung) in that area recently. This is one of the potential fields of applications where UAS might be used in future in NMAs. Such projects are quite limited in size and request for frequently updated airborne data just to illustrate the land owners how parcels have been changed and what the current status of the whole process is.

In cooperation with the Insitute of Flight Mechanics and Control (iFR) at University of Stuttgart flights were done in that area. The LGL requested to have 3D point clouds, with ground sampling distance (GSD) $<$ 10cm and orthophotos with the same GSD. In order to guarantee an accuracy better than one pixel (i.e. 10 cm) the images were taken with a nominal GSD around 6 cm. As the terrain is very steep, with height changes of about 100 m, the GSD is not constant but varies from 5 - 7 cm. Due to this steepness with some rocks and the almost exclusive land use with vineyards the terrain is photogrammetrically quite demanding. The overall size of the area was 1000 x 400 m^2. Figure 18 shows the planned UAS block geometry overlaid on the perspective terrain visualization.

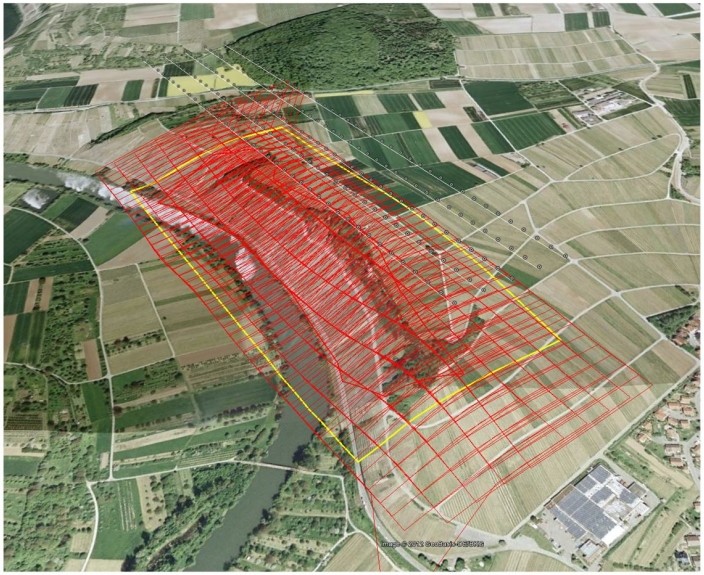

Figure 18: The Hessigheim project area - planned photogrammetric block configuration.

Two different systems have been tested: A Canon Ixus 100 and a Ricoh GXR Mount A12 combined with a Zeiss Biogon 21mm lens. The camera specific parameters can be seen from Figure 19. The given prices of the systems refer to the time of buying. The Canon became available in 2009 already, the Ricoh/Zeiss was ordered in May 2012.

	Canon Ixus 100 IS	Ricoh GXR Mount A12
#Pixel	4000 x 3000	4288 × 2848
Pixelsize	1.54 µm	5.5 µm
Sensorformat	6.16 x 4.62 mm²	23.6 × 15.7 mm²
Optic	3,03-times Zoom	Zeiss Biogon T* 21 mm
Weight (ca.)	180 gr	650 gr
Prize (ca.)	280 EUR	1950 EUR

Figure 19: The parameters of the two consumer cameras used for the UAS flights.

In order to evaluate the performance of both systems tests on their geometric resolution performance were made. This indirectly also reflects their radiometric quality. The tests were made by using Siemens star patterns, that were multiply imaged in terrestrial environments as well as during airborne flights. In Figure 20 two examples are shown, where the left shows the Siemens star (8 m diameter) from the Canon, the right from the Ricoh/Zeiss flight. The images were taken during the flights, the distances between camera and target were slightly different around 175m, which relates to nominal GSD of around 4.5 and 5.0 cm. The results obtained from analysis of point spread functions derived from the Siemens star is given below the Figure. Different measures, referring to image and object space are given. As one can see, the empirical resolution of the Ricoh/Zeiss imagery is always better than the Canon.

It is interesting to see, that when using the Canon and Ricoh/Zeiss images in automatic aerial triangulation (AT) these quality differences are hardly visible, at least, when the final internal and absolute accuracy is investigated. Table 1 compares the results from the ATs for the Canon and Ricoh/Zeiss flights.

GSD nominal: 4.487 cm

	R	G	B
sigma_psf (px)	0.506	0.504	0.468
MTF10 (lines/px)	0.675	0.678	0.729
RP (px/line)	1.480	1.474	1.371
AV_RP (cm)	6.643	6.616	6.154
AV_FWHM (cm)	5.343	5.321	4.950

GSD nominal: 4.942 cm

	R	G	B
sigma_psf (px)	0.397	0.392	0.395
MTF10 (lines/px)	0.861	0.872	0.866
RP (px/line)	1.161	1.147	1.155
AV_RP (cm)	5.738	5.668	5.710
AV_FWHM (cm)	4.615	4.558	4.592

Figure 20: Geometric resolution of Canon Ixus 100 (left) and Ricoh/Zeiss (right).

Camera	σ0 [pix]	Std.Dev. Object Points [m]			RMS from Check Points [m]		
		East	North	Up	East	North	Up
Canon SfM Points	0.7	0.036	0.032	0.141	0.050	0.037	0.095
Canon Match-AAT	0.3	0.008	0.007	0.024	0.030	0.023	0.050
Ricoh/Zeiss SfM Points	0.7	0.034	0.030	0.110	0.031	0.037	0.058
Ricoh/Zeiss AAT	0.3	0.018	0.015	0.049	0.029	0.024	0.043

Table 1: The accuracy from AT for the Canon and Ricoh/Zeiss flight.

Notice, the Canon camera is very low cost (using zoom lenses) and the Ricoh/Zeiss is more expensive and has a high-quality fixed focus lens. Obviously both sensors are nicely controlled when in situ calibration is applied. In both cases the cameras were calibrated from a moveable test pattern, where several images were taken right before take-off. From these images the camera calibration terms were obtained. Camera calibration then was applied before the airborne images were used for the aerial triangulation.

After AT the exterior orientation of each image is available which is the pre-requirement for the generation of 3D point clouds. The determination of dense point clouds is based on the semi-global matching algorithm which was modified and implemented in the ifp SUrface REconstruction (SURE) software package. With that very dense point clouds are derived. The result, the 3D surface model for the whole Hessigheim project area can be seen in Figure 17. Some more details on this surface generation were already discussed in the previous section.

From a technical point of view, the project was very successful. All the products according to the requests from the LGL could be derived. The only problem is the effort, which is needed to get the permission to fly the UAS, even in this quite rural area. It is a time tedious process to get the flight permission from authorities, which to a certain extend limits the flexibility of this technology. Still there is quite some momentum in the regulation of UAS flights going on right now. Different activities in Germany and other countries are on their way, but also in European and international context. It is quite sure, that there will be substantial changes in the flight limitations for UAS within the next 3 years. This will clearly support the flexible use of this technology, even for national mapping applications.

References 2012

Abdel-Wahab, M., Wenzel, K., Fritsch, D.: Efficient Reconstruction of Large Unordered Image Datasets for High Accuracy Photogrammetric Applications. The International Archives of the Photogrammetry, Remote Sensing and Spatial Information Sciences, Volume I, Part 3, 1-6.

Abdel-Wahab, M., Wenzel, K., Fritsch, D.: Automated and Accurate Orientation of Large Unordered Image Datasets for Close-Range Cultural Heritage Data Recording. Photogrammetrie - Fernerkundung - Geoinformation (PFG), Heft 6(2012), 679-690.

Becker, S., Walter, V., Fritsch, D.: Integrated Management of Heterogeneous Geodata with a Hybrid 3D Goeinformation System. The International Archives of the Photogrammetry, Remote Sensing and Spatial Information Sciences, Volume I, Part 2, 87-92.

Cramer, M., Haala, N.: Genauigkeitspotential der photogrammetrischen Bildauswertung für Daten unbemannter Luftfahrzeuge. Tagungsband Vorträge 32. Wissenschaftlich-technische Jahrestagung DGPF, Potsdam, 14.-17. März 2012, Publikationen der Deutschen

Gesellschaft für Photogrammetrie, Fernerkundung und Geoinformation (DGPF) e.V. Band 21, 428-440.

Cramer, M., Kresse, W., Skaloud, J., Haala, N., Nittel, S., Wallgrün, J.: Data Capture and Geosensor Networks. Springer Handbook of Geographic Information.

Fritsch, D.: Vortrag anlässlich der Festveranstaltung „10 Jahre GUC“ an der Universität Ulm, Donnerstag, 12. Juli 2012.

Fritsch, D., Kremer, J., Grimm, A.: A Case Study of Dense Image Matching Using Oblique Imagery - Towards All-in-one Photogrammetry. GIM International 26(4).

Fritsch, D., Abdel-Wahab, M., Cefalu, A., Wenzel, K.: Photogrammetric Point-Cloud Collection with Multi-Camera Systems. In: M. Ioannides, D. Fritsch, J. Leissner, R. Davies, F. Remondino, R. Caffo (Eds.): Progress in Cultural Heritage Preservation. Lecture Notes in Computer Science (LNCS), Springer, Berlin-Heidelberg, 11-20.

Fritsch, D., Mooney, K., Oestman, A.: EduServ - The Education Service of EuroSDR: Sharing Experience for Capacity Building. The International Archives of the Photogrammetry, Remote Sensing and Spatial Information Sciences, Vol. XXXIX, Part B6, 87-90.

Fritsch, D., Pfeifer, N., Franzen, M. (Eds.): High Density Image Matching for DSM Computation. EuroSDR Workshop Proceedings (CD-ROM), EuroSDR, ISBN 9789051797923, ISSN 0257-0505.

Haala, N., Rothermel, M.: Dense Multiple Stereo Matching of Highly Overlapping UAV Imagery. The International Archives of the Photogrammetry, Remote Sensing and Spatial Information Sciences, Vol. XXXIX, Part B1, 387-392.

Haala, N., Rothermel, M.: Dense Multi-Stereo Matching for High Quality Digital Elevation Models. Photogrammetrie - Fernerkundung - Geoinformation (PFG), Heft 4(2012), 331-343.

Haala, N., Fritsch, D., Peter, M., Khosravani, A.: Pedestrian Mobile Mapping System for Indoor Environments Based on MEMS IMU and Range Camera. Archives of Photogrammetry, Cartography and Remote Sensing, Vol. 22, 159-172.

Ioannides, M., Fritsch, D., Leissner, J., Davies, R., Remondino, F., Caffo, R. (Eds.): Progress in Cultural Heritage Preservation. 4th International Conference, EuroMed 2012, Lemessos, Cyprus, October 29 - November 3, 2012, Proceedings Series: Lecture Notes in Computer Science, Vol. 7616, 494p.

Ioannides, M., Fritsch, D., Leissner, J., David, R., Remondino, F., Caffo, R. (Eds.): Short Paper Proceedings. EUROMED 2012, 4th. Int. Conference Progress in Cultural Heritage Preservation, Multi-Science Publishing, Essex, UK, 378p.

Khosravani, A., Lingenfelder, M., Wenzel, K., Fritsch, D.: Co-Registration of Kinect Point Clouds Based on Image and Object Space Observations. Proceedings LCD Workshop, Berlin, December 2012.

Moussa, W., Abdel-Wahab, M., Fritsch, D.: An Automatic Procedure for Combining Digital Images and Laser Scanner Data. The International Archives of the Photogrammetry, Remote Sensing and Spatial Information Sciences, Vol. XXXIX, Part B5, 229-234.

Moussa, W., Abdel-Wahab, M., Fritsch, D.: Automatic Fusion of Digital Images and Laser Scanner Data for Heritage Preservation. Lecture Notes in Computer Science (LNCS), Springer, Berlin-Heidelberg, 76-85.

Peter, M., Fritsch, D., Schäfer, B., Kleusberg, A., Bitsch Link, J.A., Wehrle, K.: Versatile Georeferenced Maps for Indoor Navigation of Pedestrians. In: Proceedings of the 2012 International Conference on Indoor Positioning and Indoor Navigation (IPIN2012), Sydney, Australia, 2012, 4p.

Tang, R.: A Rigorous and Flexible Calibration Method for Digital Airborne Camera Systems. The International Archives of the Photogrammetry, Remote Sensing and Spatial Information Sciences, Vol. XXXIX, Part B1, 153-158.

Tang, R., Fritsch, D., Cramer, M.: A novel family of mathematical self-calibration additional parameters for airborne camera systems. European Calibration and Orientation Workshop (EuroCOW 2012), 7p. on CD-ROM.

Tang, R., Fritsch, D., Cramer, M.: New rigorous and flexible Fourier self-calibration models for airborne camera calibration. ISPRS Journal of Photogrammetry and Remote Sensing 71, 76-85.

Tang, R., Fritsch, D., Cramer, M., Schneider, W.: A Flexible Mathematical Method for Camera Calibration in Digital Aerial Photogrammetry. Photogrammetric Engineering & Remote Sensing (PERS), Vol. 78, No. 10, 1069-1077.

Wenzel, K., Abdel-Wahab, M., Cefalu, A., Fritsch, D.: High-Resolution Surface Reconstruction from Imagery for Close Range Cultural Heritage Applications. The International Archives of the Photogrammetry, Remote Sensing and Spatial Information Sciences, Vol. XXXIX, Part B5, 133-138.

Doctoral Theses

Filippovska, Y.: Evaluierung generalisierter Gebäudegrundrisse in großen Maßstäben. Deutsche Geodätische Kommission, Reihe C, Nr. 658, München 2011, 167p.

Diploma Theses / Master Theses

Gharibi, H.: Extraction and Improvement of Digital Surface Models from Dense Point Cloud. Supervisors: Haala, N., Wenzel, K.

Javaid, M.A.: Automatic Classification of Roof Features from multiple Overlapping Imagery. Supervisor: Haala, N.

Appenzeller, B.: Bildbasierte Georeferenzierung von UAV-Aufnahmen. Supervisor: Haala, N.

Sharakiri, M.N.: Camera Alignment Testing and Calibration. Supervisors: Haala, N., Apel, U. (Robert Bosch GmbH).

Gleffe, G.: Orthophotoerzeugung aus einem UAV-Bildverband. Supervisor: Haala, N.

Schwarz, C.: Entwicklung eines Ansatzes zur Klassifizierung von Pillen in Blistern basierend auf Methoden der Bildverarbeitung. Supervisors: Walter, V., Schöning, S. (IPA Fraunhofer).

Study Theses / Bachelor Theses

Tutzauer, P.: Line Based Object Recognition and Tracking using Sequential Monte Carlo Methods. Supervisor: Cefalu, A.

Zwölfer, T.: Implementation and Evaluation of the DAISY Descriptor for a Semi-Global Matching Framework. Supervisor: Rothermel, M.

Matthias K.: Semi-Global Matching in close-range applications supported by artificial texture from the Microsoft Kinect. Supervisor: Wenzel, K.

Activities in National and International Organizations

Cramer, M.:

President EuroSDR Technical Commission I - Sensors, primary data acquisition and geo-referencing (until October 2012)
Co-Chair ISPRS Working Group I/5 - Integrated Systems for Sensor Georeferencing and Navigation (until August 2012)
Co-Chair ISPRS ICWG III/I: Sensor Modeling for Integrated Orientation and Navigation (since September 2012)

Englich, M.:

Webmaster ISPRS

Fritsch, D.:

Chairman Board of Trustees ‘The ISPRS Foundation’
Member CyberOne Award Commitee
Member Galileo/GMES Award Committee Baden-Württemberg
Member Jury Artur Fischer Invention Award
Member D21 Advisory Board
Member Board of Trustees German University in Cairo (GUC)
Member GUC Academic Advisory Committee
Member Apple’s University Education Forum (UEF)
Member Advisory Board ISPRS
Vice-President Research EuroSDR

Haala, N.:
Chair ISPRS WG I/2 - LiDAR, SAR and Optical Sensors
Vorsitz DGPF Arbeitskreis Sensorik und Plattformen

Walter, V.:
Member of Editorial Advisory Bord of the ISPRS Journal of Photogrammetry and Remote Sensing
Nationaler Berichterstatter für die ISPRS Kommission IV

Education - Lectures/Exercises/Training/Seminars

Bachelor „Geodäsie und Geoinformatik“

Introduction into Geodesy and Geoinformatics (Cramer, Fritsch, Sneeuw, Keller, Kleusberg)	4/2/0/0
Adjustment Theory I (Fritsch, Sneeuw)	1/1/0/0
Adjustment Theory II (Fritsch, Sneeuw)	2/2/0/0
Geoinformatics I (Fritsch, Walter)	2/2/0/0
Geoinformatics II (Walter)	1/1/0/0
Image Processing (Haala)	2/1/0/0
Photogrammetry (Cramer)	2/1/0/0
Signal Processing (Fritsch)	2/1/0/0
Urban Planning (Dvorak)	1/0/0/0

Master Course „Geodäsie und Geoinformatik“

Aerotriangulation (Cramer)	1/1/0/0
Computer Vision for image-based acquisition of Geodata (Haala)	1/1/0/0

Diplomstudiengang „Geodäsie und Geoinformatik“

Advanced Projects in Photogrammetry and GIS (Cramer, Haala, Walter)	1/2/0/0
Animation and Visualisation of Geodata (Haala)	1/1/0/0
Cartography (Urbanke)	1/0/0/0
Close Range Photogrammetry (Fritsch)	2/1/0/0
Databases and Geoinformation Systems (Walter)	2/1/0/0
Geodetic Seminar I, II (Fritsch, Sneeuw, Keller, Kleusberg)	0/0/0/4
Pattern Recognition and Image Based Geodata Collection (Haala)	2/1/0/0

Master Course GEOENGINE

Airborne Data Acquisition (Fritsch, Cramer)	1/1/0/0
Geoinformatics (Fritsch, Walter)	2/1/0/0

Signal Processing (Fritsch)	2/1/0/0
Topology and Optimisation (Fritsch)	2/1/0/0
Integrated Fieldworks (Fritsch, Sneeuw, Keller, Kleusberg)	0/0/4/0

Master Courses „Infrastructure Planning“ and „Water Resource Management“

Introduction to GIS (Walter)	2/0/0/0
Advanced GIS (Walter)	2/0/0/0

Diplomstudiengang Luft- und Raumfahrttechnik

Introduction into Photogrammetry (Cramer)	2/0/0/0